

Supported organic, Nano Metallic and
Enzymatic catalysis
in Microreactors

Supported organic, Nano Metallic and Enzymatic catalysis in Microreactors

Francesca Costantini

Supported organic, Nano Metallic and Enzymatic catalysis in Microreactors 2009

Francesca Costantini

ISBN 978-90-365-2940-2

**SUPPORTED ORGANIC,
NANOMETALLIC, and ENZYMATIC
CATALYSIS IN MICROREACTORS**

This research was supported by NanoNed, a national nanotechnology program coordinated by the Dutch Ministry of the Economic Affairs.

Supported Organic, Nanometallic and Enzymatic Catalysis in Microreactors

Francesca Costantini

Thesis University of Twente, Enschede, The Netherlands

ISBN: 978-90-365-2940-2

Publisher:

Ipskamp Drukkers B.V., Josink Maatweg 43, 7545 PS, Enschede,
The Netherlands, <http://www.ipskampdrukkers.nl>

© Francesca Costantini, Enschede, 2009

Cover graphics by Maria e Marta Mucci, Email: maria.mucci@yahoo.it

Cover Picture: Relativity E.M. Escher 1953.

No part of this work may be reproduced by print, photocopy or any other means without the permission in writing of the author.

**SUPPORTED ORGANIC, NANOMETALLIC,
and ENZYMATIC CATALYSIS IN
MICROREACTORS**

PROEFSCHRIFT

ter verkrijging van
de graad van doctor aan de Universiteit Twente,
op gezag van de rector magnificus,
prof. dr. H. Brinksma,
volgens besluit van het College voor Promoties
in het openbaar te verdedigen
op vrijdag 4 December 2009 om 16:45 uur

door

Francesca Costantini
geboren op 1 Oktober 1977
te Macerata, Italië

Dit proefschrift is goedgekeurd door:

Promotoren: Prof. dr. ir. D. N. Reinhoudt

Prof. dr. ir. J. Huskens

Assistent promotor: Dr. W. Verboom

Dietro ogni problema c'è
un'opportunità

Behind every problem there is an
opportunity

(Galileo Galilei)

Alla mia famiglia ed a mio nonno

CONTENTS

CHAPTER 1	9
GENERAL INTRODUCTION	9
CHAPTER 2	13
MICROREACTORS AS EFFICIENT DEVICES TO PERFORM CATALYZED REACTIONS	13
2.1 INTRODUCTION.....	14
2.2 <i>Reactions Catalyzed by Organic Catalysts</i>	15
2.2.1 <i>Knoevenagel Condensation, Acylation, Dimethyl Acetals Deprotection, and Transesterification Reactions</i>	15
2.3 REACTIONS CATALYZED BY METALLIC AND ORGANOMETALLIC CATALYSTS	21
2.3.1 <i>Kumanda-Corriu Reaction</i>	21
2.3.2 <i>Strecker Reaction</i>	22
3.3 <i>Hydrogenation Reactions</i>	25
2.3.3 <i>Photoreduction</i>	31
2.3.4 <i>Suzuki-Miyaura Coupling and Heck Reactions</i>	32
2.3.5 <i>Alcohol Oxidation</i>	37
2.4 REACTIONS CATALYZED BY ENZYMES.....	41
2.4.1 <i>Glucose Oxidation</i>	41
2.4.2 <i>Synthesis of 2-aminophenoxazin-3-one (APO)</i>	42
2.4.3 <i>Proteolysis</i>	42
2.4.4 <i>Hydroxylation</i>	46
2.4.5 <i>Ester Hydrolysis</i>	47
2.4.6 <i>Lactose Hydrolysis</i>	47
2.5 CONCLUSIONS AND OUTLOOK.....	48
CHAPTER 3	51
SELF-ASSEMBLED MONOLAYERS FOR THE IMMOBILIZATION OF CATALYSTS ON THE INTERIOR OF GLASS MICROREACTORS	51
3.1 INTRODUCTION.....	52
3.2 RESULTS AND DISCUSSION.....	53
3.2.1 <i>Synthesis of Base SAMs on a Flat Surface and their Characterization</i>	53
3.2.2 <i>Synthesis of Propylamine SAM on the Microreactor Interior for the Kinetic study of the Knoevenagel Condensation Reaction</i>	56
3.2.3 <i>Synthesis of TBD and PAMAM SAMs on the Microreactor Interior for the Kinetic study of the Knoevenagel Condensation Reaction</i>	60
3.3 CONCLUSIONS	62
3.4 EXPERIMENTAL	63
CHAPTER 4	68
NANOSTRUCTURE BASED ON POLYMER BRUSHES FOR HETEROGENEOUS CATALYSIS IN MICROREACTORS	68
4.1 INTRODUCTION.....	69
4.2 RESULTS AND DISCUSSION.....	70

4.2.1 <i>Synthesis of Polyglycidylmethacrylate Polymer Brushes and TBD Immobilization on Flat Substrates</i>	70
4.2.2 <i>Synthesis of Polyglycidylmethacrylate Polymer Brushes and TBD Immobilization on Microreactor Channel Wall</i>	72
4.2.3 <i>Kinetic Study of the Knoevenagel Condensation Reaction Performed in the Catalytic Microreactor</i>	73
4.3 CONCLUSIONS	77
4.4 EXPERIMENTAL	77
CHAPTER 5.....	82
HETEROGENEOUS CATALYSIS IN GLASS MICROREACTORS COATED WITH A BRUSH-GEL SILVER NANOPARTICLES HYBRID FILM.....	82
5.1 INTRODUCTION	83
5.2 RESULTS AND DISCUSSION	85
5.2.1 <i>Synthesis of the Hydrogel-Silver Nanoparticles Hybrid Nanostructure on a Flat Surface and its Characterization</i>	85
5.2.2 <i>Synthesis of the Hydrogel-Silver Nanoparticles Hybrid Nanostructure on Microreactor Interior</i>	88
5.2.3 <i>Kinetic Study of the 4-Nitrophenol Reduction Performed in the Microreactor Coated with Brush-gel Silver Nanoparticles</i>	89
5.3 CONCLUSIONS	92
5.4 EXPERIMENTAL.....	92
CHAPTER 6.....	97
HETEROGENEOUS CATALYSIS IN GLASS MICROREACTORS COATED WITH A BRUSH-GEL PALLADIUM NANOPARTICLES HYBRID FILM.....	97
6.1 INTRODUCTION.....	98
6.2 RESULTS AND DISCUSSION.....	99
6.2.1 <i>Synthesis of the Hydrogel-Palladium Nanoparticles Hybrid Nanostructure on a Flat Surface and its Characterization</i>	99
6.2.2 <i>Synthesis of the Hydrogel-Palladium Nanoparticles Hybrid Nanostructure on Microreactor Interior</i>	101
6.2.3 <i>Kinetic Study of the 4-Nitrophenol Reduction Performed in the Microreactor Coated with Brush-gel Palladium Nanoparticles</i>	102
6.2.3 <i>Kinetic Study of the Heck Reaction Performed in the Microreactor Coated with Brush-gel Palladium Nanoparticles</i>	104
6.3 CONCLUSIONS	106
6.4 EXPERIMENTAL	106
CHAPTER 7.....	111
ENZYME IMMOBILIZATION ON A MICROREACTOR CHANNEL WALL USING POLYMETHACRYLIC ACID POLYMER BRUSHES	111
7.1 INTRODUCTION.....	112
7.2 RESULTS AND DISCUSSION.....	114

<i>7.2.1 Synthesis of Polymethacrylic acid Polymer Brushes and Lipase Immobilization on a Flat Surface</i>	114
<i>7.2.2 Synthesis of Polymethacrylic Acid Polymer Brushes and Lipase Immobilization on the Microreactor Channel Wall</i>	116
<i>7.2.3 Kinetic Study of Hydrolysis of 4-Nitrophenyl acetate in the Biocatalytic Microreactor</i>	117
7.3 CONCLUSIONS	120
7.4 EXPERIMENTAL	121
SUMMARY	126
SAMENVATTING	130
ACKNOWLEDGMENTS	134

CHAPTER 1

General Introduction

Over the past decade, the impact of microfluidics technology on the research community has dramatically increased. This has led to a rapid implementation as new products and solutions in different application areas within the biotechnological, diagnostic, medical, and chemical industries have been developed.

The history of microfluidics dates back to the early 1950s, when efforts to dispense small amounts of liquids in the nano-subnanoliter ranges were made for establishing the basis of today's ink-jet technology^[1]. In 1979, a miniaturized gas chromatograph (GC) was realized on a silicon wafer^[2]. The first high-pressure liquid chromatography (HPLC) column device, fabricated using Si-Pyrex technology, was published by Manz *et al.*^[3], initiating a real "microfluidic revolution". At the same time Manz *et al.*^[4] proposed the micro total analysis system (μ -TAS), also known as the lab-on-a-chip concept, opening a new area in the field of analytical chemistry. The main aim of μ -TAS is to fabricate integrated systems ideally able to perform a number of functions in an automated way, in a miniaturized system. Miniaturization has become a dominant trend in the field of

analytical chemistry, as witnessed by the many microfluidic platforms that have been developed during recent years^[5].

Only in the late nineties, microfluidic systems have also been used for chemical synthesis^[6]. A microfluidic system, in which a molecular transformation takes place, is called a microreactor^[7]. Microreactors for conducting organic synthesis offer several advantages over conventional lab-scale equipment. Due to their smaller dimensions, specifically between 10-1000 μm , microreactors require less space, energy, reagents, and catalyst, providing environmental and safety benefits^[8-10]. Moreover, due to the larger surface-to-volume ratio, which directly derives from miniaturization, heat and mass transfer processes occur faster than in standard glassware. This aspect is particularly interesting for heterogeneous catalysis, since it permits to achieve a high interfacial area between the two or three reacting phases^[11]. In addition, continuous flow allows collecting only the desired product(s) at the end of the reactor, thus, the operations of reaction and filtration occur simultaneously^[12]. The main issue for conducting heterogeneous catalysis in microreactors is the implementation of a catalyst in the microfluidic system.

The aim of this thesis is to immobilize catalysts on the inner wall of microreactors in order to provide an efficient and durable catalytic microsystem to conduct organic reactions with a supported catalyst. Ultrathin monolayers and thicker polymer layers are being used as a support for catalyst immobilization to vary and control the catalyst loading. The types of catalysts used in this thesis range from organic, to metallic (in the form of supported nanoparticles), and enzymatic, in order to show the scope of the concept.

Chapter 2 gives an overview of chemical reactions performed in microreactors with supported catalysts, showing the advantages that can be achieved using microfluidic systems. Several approaches for the implementation of catalysts in microreactors are discussed, both regarding microreactor design and catalyst immobilization method.

Chapter 3 deals with the use of self-assembled monolayers (SAMs) to immobilize basic organic catalysts as 1-propylamine, 1,5,7-triazabicyclo[4.4.0]dec-5-ene (TBD), and poly(amidoamine) dendrimer generation 2 (PAMAM G2) on the interior of glass microreactors. The Knoevenagel condensation reaction of benzaldehyde and malononitrile to give 2-benzylidene malononitrile is chosen as a model reaction to investigate the catalytic activity.

In Chapter 4, TBD is anchored on poly(glycidylmethacrylate) (PGMA) polymer brushes grown on the microreactor inner walls. A kinetic study of the above mentioned Knoevenagel condensation reaction is performed in devices with this catalytic coating. The role of the thickness of the polymer brush nanostructure on the amount of immobilized catalyst is investigated as well.

In Chapter 5, a polymer brush-based material is applied for in-situ formation and immobilization of silver nanoparticles (Ag-NPs) as a catalytic coating on the inner wall of a glass microreactor. This catalytic system is applied for the reduction of 4-nitrophenol.

In Chapter 6, catalytic palladium nanoparticles (Pd-NPs) are formed on the glass microreactors applying the same approach as developed in Chapter 5. Microreactors bearing a Pd-NP hybrid layer are employed for the reduction of 4-nitrophenol and for the Heck reaction between ethyl acrylate and iodobenzene to give *trans*-ethyl cinnamate.

In Chapter 7, a brush layer of poly(methacrylic acid) (PMAA) is used to anchor the lipase from *Candida Rugosa* on the inner walls of a silicon-glass microreactor. This microreactor is used for the enzymatic hydrolysis of 4-nitrophenyl acetate as a model reaction to investigate the biocatalytic activity of the enzyme as a result of the immobilization procedure.

References

- [1] H. P. Le, *J. Imaging Sci. Technol.* **1998**, *42*, 49.
- [2] S. C. Terry, J. H. Jerman, J. B. Angell, *Trans. Electron Devices* **1979**, *26*, 1880.
- [3] A. Manz, Y. Miyahara, J. Miura, Y. Watanabe, H. Miyagi, K. Sato, *Sens. Actuators B* **1990**, *1*, 249.
- [4] A. Manz, N. Graber, H. M. Widmer, *Sens. Actuators B* **1990**, *1*, 244.
- [5] S. Haeberle, R. Zengerle, *Lab Chip* **2007**, *7*, 1094.
- [6] T. Jackson, J. H. Clark, D. J. Macquarrie, J. H. Brophy, *Green Chem.* **2004**, *6*, 193.
- [7] R. L. Hartman, K. F. Jensen, *Lab Chip* **2009**, *9*, 2495.
- [8] B. Ahmed-Omer, J. C. Brandt, T. Wirth, *Org. Biomol. Chem.* **2007**, *5*, 733.
- [9] P. Watts, C. Wiles, *Org. Biomol. Chem.* **2007**, *5*, 727.
- [10] P. Watts, C. Wiles, *Chem. Commun.* **2007**, 443.
- [11] J. Kobayashi, Y. Mori, S. Kobayashi, *Chem. Asian. J.* **2006**, *1*, 22.
- [12] G. Jas, A. Kirschning, *Chem. Eur. J.* **2003**, *9*, 5708.

CHAPTER 2

MICROREACTORS AS EFFICIENT DEVICES TO PERFORM CATALYZED REACTIONS

This Chapter gives an overview about catalyzed chemical reactions performed in microreactors. Reactions are described by type together with the corresponding methodology for catalyst incorporation in the device.

2.1 Introduction

The application of microreactor technology for conducting heterogeneous chemical and biochemical reactions offers many advantages to conventional laboratory equipment^[1-6] as already mentioned in Chapter 1. One of the most important features of microchannel reactors is the high surface area to volume ratio. The specific surface areas of microchannel reactors are between 10 000 and 50 000 m⁻¹, whereas traditional reactors are generally about 100 m⁻¹ and in rare cases reach 1000 m⁻¹. This feature creates suitable environments for heterogeneous catalysis since a large interfacial area between different phases, such as gas-liquid and gas-liquid-solid can be achieved. Due to their smaller dimensions molecular diffusion is faster than in conventional batch reactors, allowing rapid mixing and efficient heat transfer. Moreover, most of the catalytic reactions performed in microreactors are performed under addition of continuous flow. Hence, the product is flowing continuously out of the channel minimizing possible side product accumulation, and leaving the catalyst always available to react with fresh reagent solutions. Another important advantage, which is a consequence of miniaturization, is the small amount of catalysts and reagents that are consumed to carry out the reaction, producing less chemical waste and offering safer working conditions.

The incorporation of catalysts in a microreactor is an important goal, since it should ensure sufficient catalyst concentration for reaction efficiency, long time stability and the possibility of catalyst recycling. Packed-bed microreactors, in which a supported catalyst is packed in a microchannel/ capillary reactor, have been widely applied for conducting chemical reactions. Although many material types have been investigated as solid supports for catalysts, most of them clog the devices, causing irreproducibility and a high back-pressure^[4]. This problem has been partially solved using electroosmotic flow, which

permits flow through a wider range of packing materials but is limited only to polar solvents. The use of the inner walls of the microreactor for catalyst immobilization usually solves the problem of the back-pressure, but it necessarily reduces the surface area of the support and thus the amount of catalyst that can be loaded.

Several catalytic reactions have been run in microreactors with organic, metal, and enzymatic catalysts using either the packed-bed technique or with the catalyst immobilized on the channel interior. In the following sections the different catalyzed reactions performed in microreactors will be reviewed by type.

2.2 Reactions Catalyzed by Organic Catalysts

2.2.1 Knoevenagel Condensation, Acylation, Dimethyl Acetals Deprotection, and Transesterification Reactions

3-(1-Piperazino)propyl-functionalized silica gel (**1**), packed into a borosilicate glass capillary (Figure 2.1), was used to catalyze the Knoevenagel condensation reaction (Scheme 1).

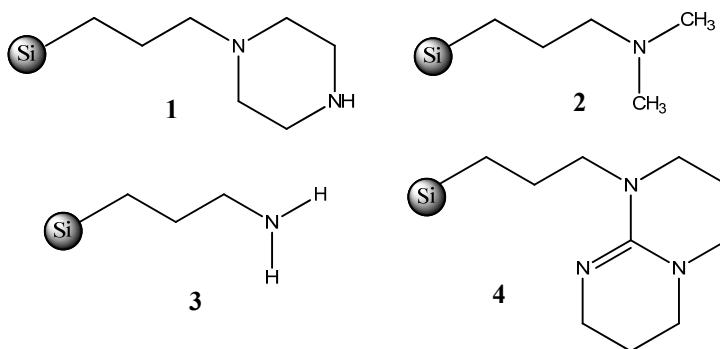


Chart 2.1. Functionalized silica gel: 3-(1-piperazino)propyl (**1**), 3-(dimethylamino)propyl (**2**), 3-aminopropyl (**3**) and 3-(1,3,4,6,7,8-hexahydro-2H-pyrimido[1,2-*a*]pyrimidino)propyl (**4**).

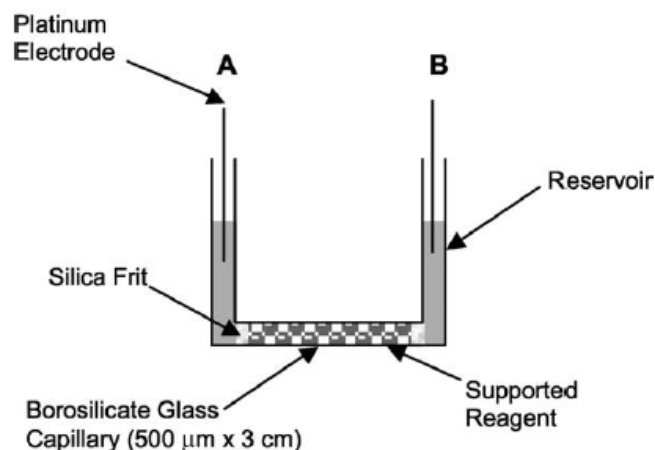
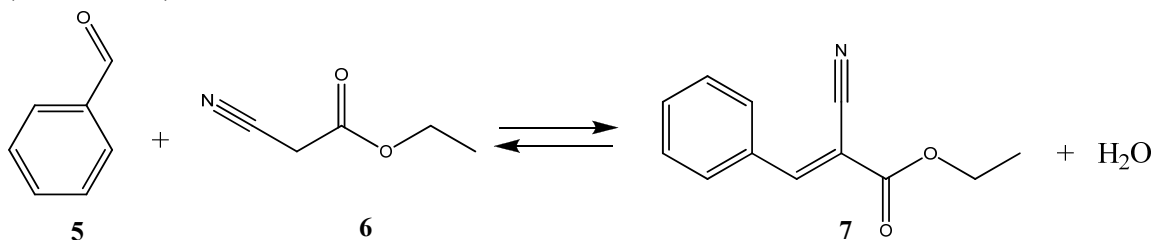


Figure 2.1. Reaction set-up of packed-bed microreactor with incorporated (1-piperazino)propyl-functionalized silica gel (**1**).

Benzaldehyde (**5**) and ethyl cyanoacetate (**6**) were passed through the miniaturized flow reactor, using electroosmotic flow, to give 2-cyano-3-phenyl acrylic acid ethyl ester (**7**)

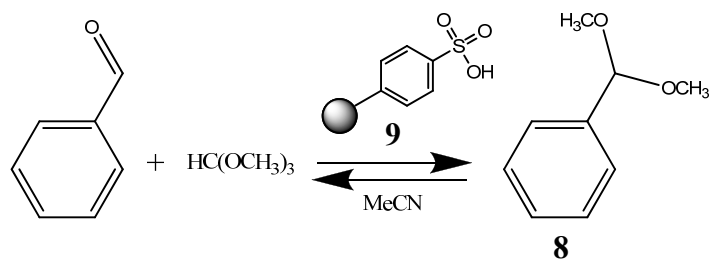
(Scheme 2.1).



Scheme 2.1. Knoevenagel condensation reaction between benzaldehyde (**5**) and ethylcyano acetate (**6**) to give 2-cyano-3-phenyl acrylic acid ethyl ester (**7**).

The same set-up was used for the preparation of several condensation products. Applying different catalytic silica-supported bases (Chart 2.1). In all the synthesis carried out, α,β -unsaturated compounds were obtained in excellent yield and purity.

Solid-supported acid catalyst, Amberlyst-15 (macroreticular sulfonic acid cation exchange resin, **9**), was incorporated in the same glass capillary, and synthesis and deprotection of dimethyl acetals^[7] (Scheme 2.2) were conducted giving full conversion.



Scheme 2.2. Synthesis and deacetalisation of dimethoxymethyl benzene (**8**) catalyzed by Amberlyst-15 (**9**)

Compared to standard batch techniques, the approach described above, has advantages because supported reagents can be recycled without the need of filtration, resulting in more reproducible results. By incorporating both Amberlyst-15 (**10**) and silica supported piperazine (**1**) in the same borosilicate glass capillary reactor (Figure 2.2), Wiles *et al.* evaluated the feasibility of performing multi-step synthesis^[8].

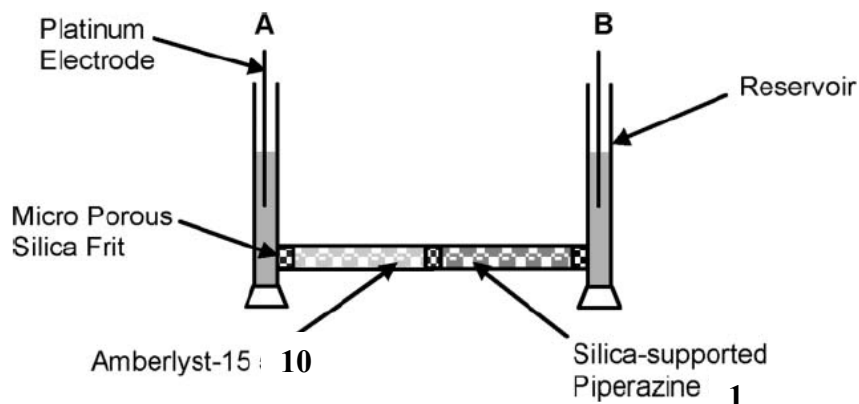
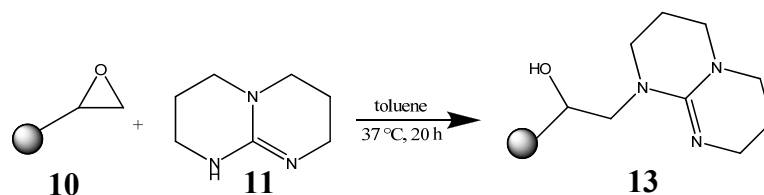


Figure 2.2. Reaction set-up used for the incorporation of Amberlyst-15 -(1-piperazino)propyl-functionalized silica gel (**1**)^[8].

A pre-mixed 1:1 solution of dimethoxymethyl benzene (**9**) and ethyl cyanoacetate (**5**) in MeCN was passed through this reactor using EOF to give the quantitative formation of benzaldehyde (**5**) and subsequently of 2-cyano-3-phenyl acrylic acid ethyl ester (**7**), as monitored by off-line GC-MS. The solid supported catalysts used in these examples could be recycled, and were re-used 203 and 501 times for Amberlyst-15 (**9**) and piperazine (**1**), respectively.

Other types of materials functionalized with organic catalysts have been introduced in a flow reactor to obtain solid supported catalysts^[9]. The methacrylic-based Amberzyme Oxirane resin (**10**, AO-resin), is a macroreticular resin with a large, fixed pore volume and pendant epoxide groups. This catalyst was designed for enzyme immobilization, and employed for anchoring two organic catalysts: 1,5,7-triazabicyclo-[4.4.0]undec-3-ene (**11**, TBD) and 4-dimethylaminopyridine (**12**, DMAP). TBD (**11**) was bound via nucleophilic substitution onto the oxirane ring to give the methacrylic-based Amberzyme Oxirane resin TBD functionalized resin (AO-TBD, **13**) (Scheme 2.3).



Scheme 2.3. Preparation of AO-TBD (**13**) resin.

The functionalized resin (**13**) was packed in a fluorolastomeric tubing (1.6-mm inner diameter and 30 cm length). The packed-bed tubing was then placed in a HPLC column oven set to 60 °C (Figure 2.3).

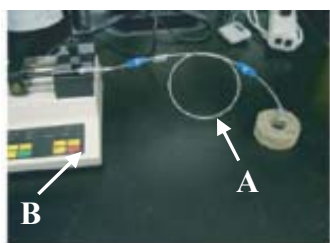
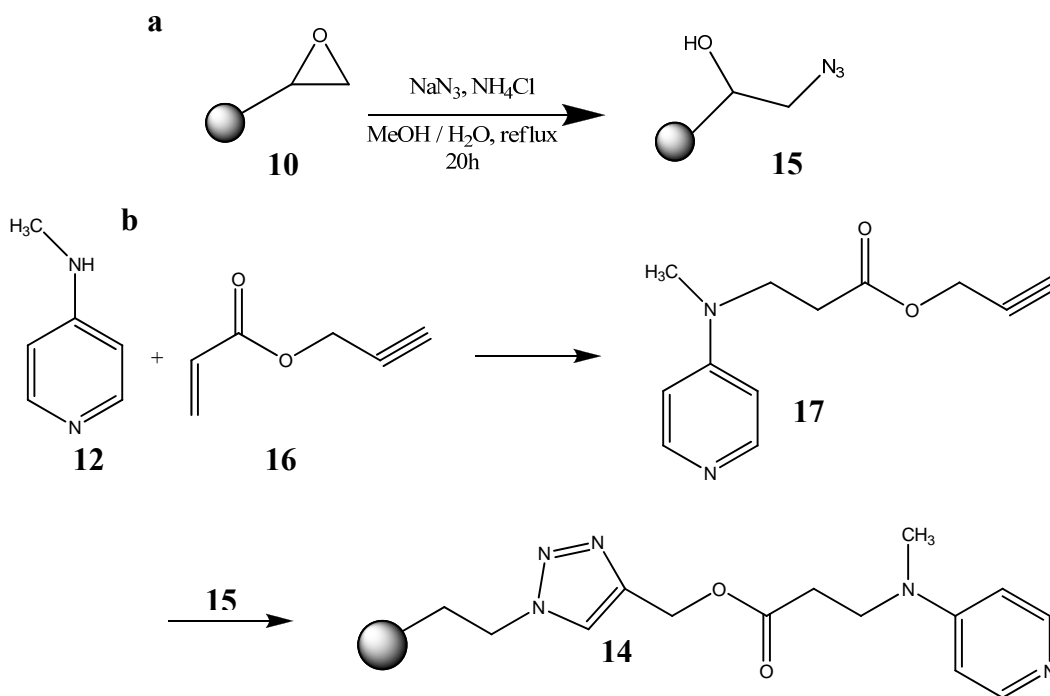


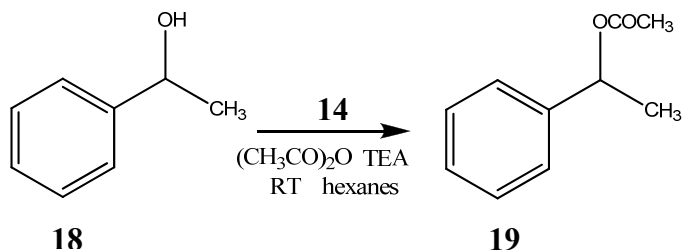
Figure 2.3. Fluorolastomeric tubing (**A**) connected to a syringe pump (**B**)^[9].

Knoevenagel condensation between benzaldehyde (**5**) and ethyl cyanoacetate (**6**) was performed to give **7**. The reagents were flowed through the packed-bed reactor using a syringe-pump (Figure 3). The packed-bed catalytic microreactor gave a yield of 93%, much higher than the yield of 69% on batch-scale under identical reaction conditions.

The AO-resin (**10**) was also functionalized with DMAP (**12**) to give AO-DMAP (**14**). Initially an azide-functionalized resin (AO-N₃, **15**) was prepared by treatment of AO-resin (**10**) with azide (Scheme 2.4a). Subsequently, the DMAP derivative, obtained by Michael addition (Scheme 2.4b) was attached to **15** through a click chemistry approach. The resulting AO-DMAP (**14**) resin was packed in the fluorolastomeric tubing and the acylation of 1-phenylethanol (**18**) (Scheme 2.5) was used as a model reaction to test the catalytic device performance. Full conversion was achieved after about 48 s. Under batch conditions the conversion was marginally lower than using the device. AO-TBD (**13**) and AO-DMAP (**14**) could be re-used 30 and 35 times, respectively.



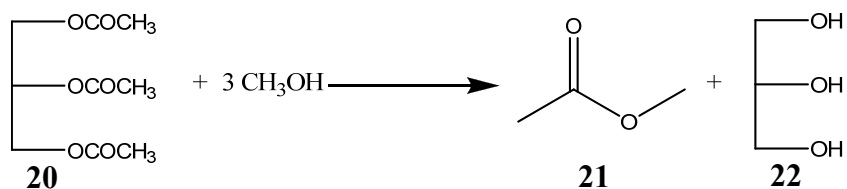
Scheme 2.4. Preparation of (a) AO-N₃ (b) Michael addition derivative and AO-DMAP resin.



Scheme 2.5. The acylation of 1-phenylethanol (**18**). TEA= triethanolamine.

Jackson and co-workers^[10] used silica powder previously functionalized with aminopropyltrimethoxysilane as coating of two etched aluminum plates. Subsequently, the coated plates were assembled to form a flow cell. The flow system was also employed for the Knoevenagel condensation reaction between benzaldehyde (**5**) and ethylcyanoacetate (**6**) (Scheme 1) and the Michael addition reaction between nitroethane and methyl vinyl ketone. The use of this method was advantageous, in terms of yield, for the Knoevenagel condensation reaction compared to batch conditions. However, the catalyst showed short durability and lower conversion was observed upon reuse. This behavior was attributed to the presence of stationary flow areas between the aluminum plates. These areas formed as a consequence of the weak bonding between the two plates.

El Kadib *et al.*^[11] inserted a functionalized inorganic monolith in a polytetrafluoroethylene (PTFE) tube (4 mm inner diameter) for carrying out the Knoevenagel condensation reaction (Scheme 2.1) and the transesterification of triacetine (**20**) by methanol (Scheme 2.6). The monolith MonoSil was functionalized with (3-aminopropyl)triethoxysilane and 2-(4-chlorosulfonylphenyl)ethyltrimethoxysilane to obtain a basic (-NH₂) and an acidic (-HSO₃) MonoSil, respectively.



Scheme 2.6. Transesterification of triacetine (**20**) by methanol.

The performance of MonoSil catalysts was compared with a closed stirred-tank reactor (batch) and a packed-bed microreactor (4.2 mm inner diameter), both containing the same concentration of crushed MonoSil. Batch and flow experiments have been compared in

terms of productivity (Figure 2.4). The reactions with acidic and basic MonoSil microreactors were 18 and 13 times faster, respectively, than the batch reaction.

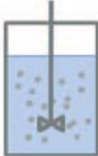
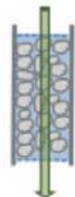

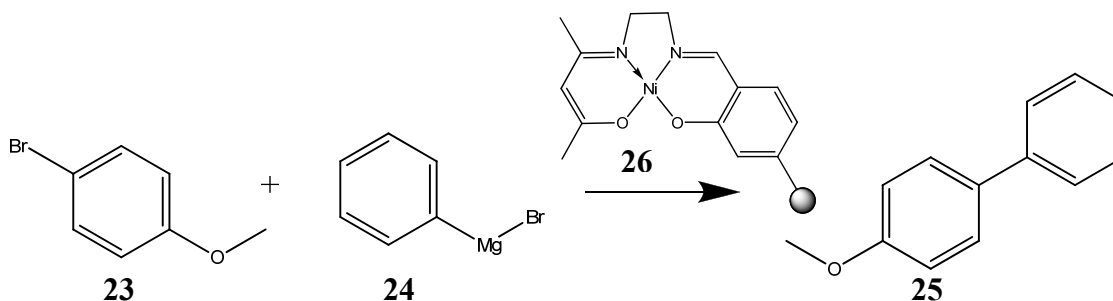
	Reactor		
	Batch	Packed-bed	MonoSil
			
	Productivity [$\text{mol min}^{-1} \text{g}^{-1}$] $\times 10^5$		
Knovenagel	24	108	178
Transesterification	2.5	28	82

Figure 2.4. Productivity of NH_2 - and HSO_3 -MonoSil in batch, packed-bed, and monolith reactors.

2.3 Reactions Catalyzed by Metallic and Organometallic Catalysts

2.3.1 Kumanda-Corriu Reaction

Haswell^[12] and coworkers conducted the Kumanda-Corriu reaction between 4-bromoanisole (**23**) and phenylmagnesium bromide (**24**) to give 4-methoxybiphenyl (**25**) (Scheme 2.7) in polypropylene (inner diameter: 2 mm) or glass tubing (inner diameter: 1 mm) filled with a salen-type nickel complex on Merrifield resin (**26**).



Scheme 2.7. Kumanda-Corriu reaction in a microreactor filled with Merrifield resin functionalized with a nickel catalyst (**15**).

The reaction rates in the flow reactors are over three orders of magnitude higher than those conducted in batch reaction.

2.3.2 Strecker Reaction

A microreactor with polymer-supported (ethylene-diaminetetraacetic acid)ruthenium (III) chloride (PS/RuCl₃)^[13] (**27**) and polymer-bound scandium (III) bis(trifluoromethanesulfonate) [PS-Sc(OTf)₂] (**28**) (Chart 2.2)^[13], was developed by Wiles and Watts with the aim of providing a simple and efficient methodology for the Strecker reaction for the synthesis of α -aminonitriles (Scheme 2.8).

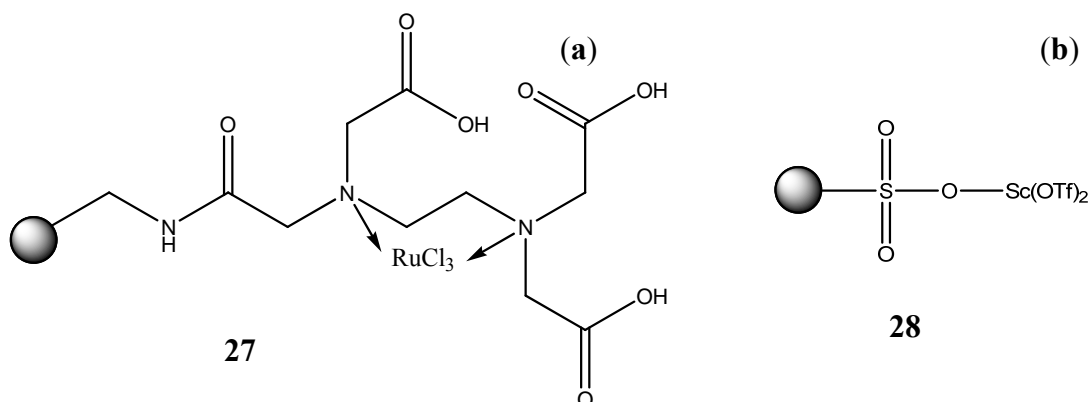
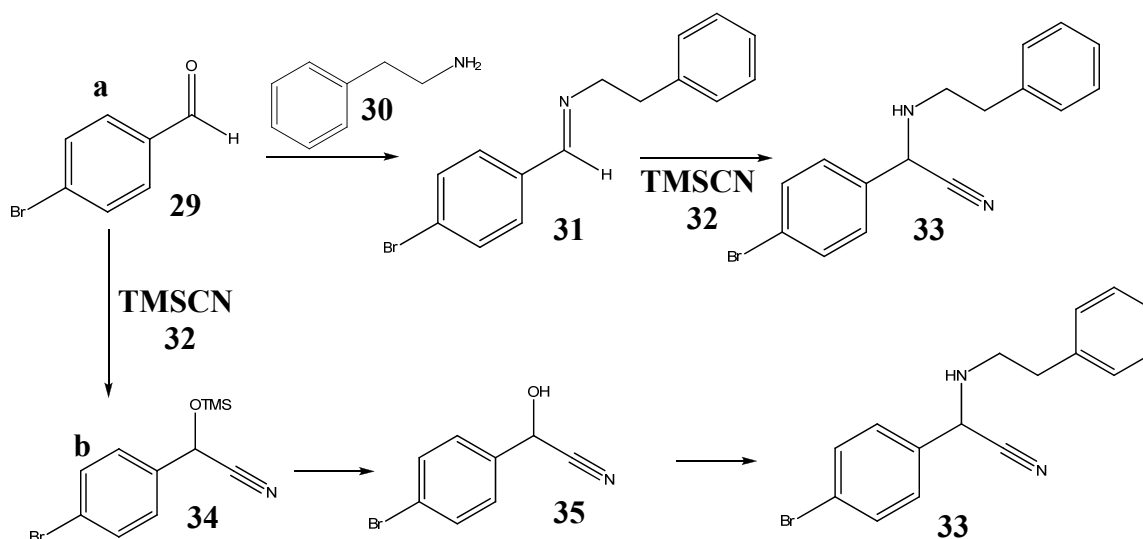


Chart 2.2. Illustration of the two immobilized Lewis acid catalysts polymer-supported (ethylene-diaminetetraacetic acid)ruthenium (III) chloride (PS/RuCl₃) (**27**) and polymer-bound scandium (III) bis(trifluoro-methanesulfonate) [PS-Sc(OTf)₂] (**28**).

A major shortcoming of the multi-component Strecker reaction is the competing cyanohydrin (**35**) formation. When employing aliphatic aldehydes, the respective aldimines (**31**) form rapidly; therefore the possibility of the cyanohydrin (**35**) formation is low, leading to a good/ moderate selectivity for the α -aminonitrile (Scheme 2.8a). On the other hand the aldimines of aromatic aldehydes form slowly, leaving the aldehyde available for reacting with trimethylsilylcyanide (TMSCN, **32**), leading to the O-TMS cyanohydrin formation and the possible hydrolysis to the respective cyanohydrin, resulting in a poor reaction selectivity (Scheme 8b).



Scheme 2.8. a) Strecker reaction between 4-bromobenzaldehyde (**29**) and 2-phenylethylenamine (**30**) to give 2-(4-bromophenyl)-2-(phenylethylamino)-acetonitrile (**33**), b) proposed shortcoming of Strecker reaction.

Watts and Wiles showed that sequential reactants addition can improve the selectivity of the Strecker reaction, and that this reaction is more efficient when performed in continuous flow packed-bed microreactors with catalysts **27** and **28** (Figure 2.5).

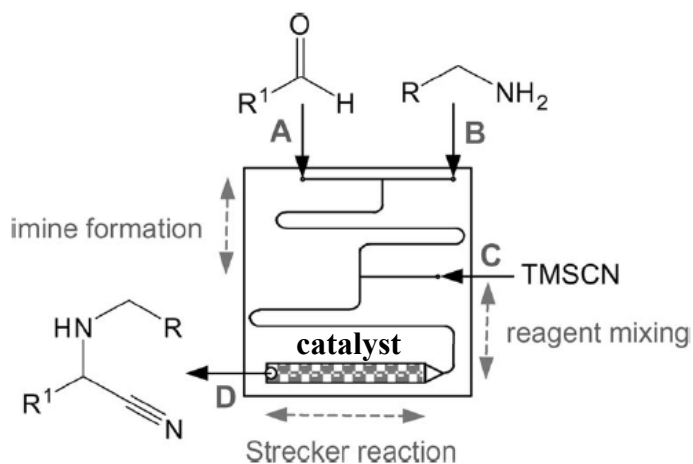
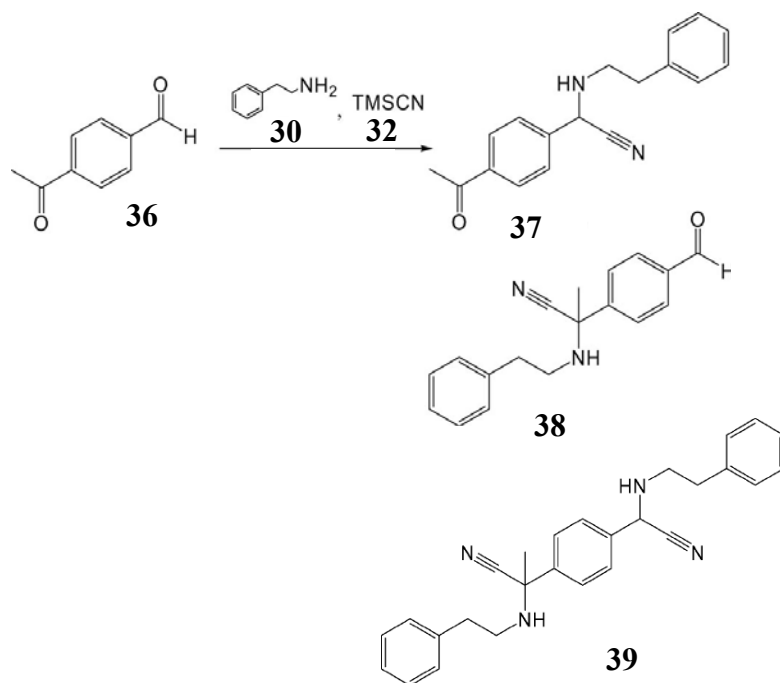


Figure 2.5. Schematic representation of microreactor set-up for performing the Strecker reaction between 4-bromobenzaldehyde (**29**) and 2-phenylethylenamine (**30**) to give 2-(4-bromophenyl)-2-(phenylethylamino)-acetonitrile (**33**) in a packed-bed microreactor.

The synthesis of 2-(4-bromophenyl)-2-(phenylethylamino)-acetonitrile (**33**) was investigated using the following procedure (Figure 2.5). A solution of 4-bromobenzaldehyde (**29**) was introduced from inlet A, followed by 2-phenylethylenamine (**30**) from inlet B and finally TMSCN (**32**) from inlet C, yielding 99.5% of product (**33**) after 5 h. No leaching was observed from the microreactor, on the other hand 440 ppm of Ru was found when the reaction was conducted in the batch system, probably due to catalyst degradation by mechanical stirring while performing the reaction. The technique for performing the Strecker reaction was evaluated reacting other amines with 4-bromobenzaldehyde. The amines were selected to illustrate a range of reactivities. Aniline, benzylamine, and phenylpropylamine showed the same reactivity as 2-phenylethylamine (**30**). However, when an aliphatic amine as pyrrolidine was reacted with 4-bromobenzaldehyde, the reaction proceeded twice as fast due to the formation of an iminium ion as the reactive intermediate. Polymer-bound scandium (III) bis(trifluoromethanesulfonate) [PS-Sc(OTf)₂] (**28**) was shown to be more efficient as the catalyst compared to PS/RuCl₃ (**27**). Having demonstrated the ability to increase the reaction throughput by employing an alternative Lewis acid catalyst, the Strecker reaction was investigated using both aromatic and aliphatic aldehydes with all types of amines mentioned above. In all cases aliphatic aldehydes showed higher reaction rates.

Finally, 4-acetylbenzaldehyde (**36**) (Scheme 2.9) was selected as a reagent for the Strecker reaction. It was demonstrated that when the packed-bed microreactor was employed, upon sequential reactants addition, only 2-(4-acetylphenyl)-2-(phenylethylamino)acetonitrile (**37**) is obtained, while in the batch reaction also 2-(4-formylphenyl)-2-(phenylethylamino)propionitrile (**38**) or bis-adduct (**39**) were formed.



Scheme 2.9. Strecker reaction between 4-acetylbenzaldehyde (**36**) and 2-phenylethylenamine (**30**) to give 2-(4-acetylphenyl)-2-(phenylethylamino)acetonitrile (**37**) and 2-(4-formylphenyl)-2-(phenylethylamino)propionitrile (**38**) or bis-adduct (**39**).

3.3 Hydrogenation Reactions

A new way to perform hydrogenation reactions was developed by Kobayashi^[14] *et al.* They immobilized palladium on the wall of a glass microchannel reactor (width: 200 μm , depth 100 μm , and length 45 cm). The substrate solution and hydrogen were allowed to flow into the channel from the two inlets (Figure 2.6) using pipe flow. The gas was flowed through the center of the channel and the liquid along the inner surface of the channel where the catalyst was anchored.

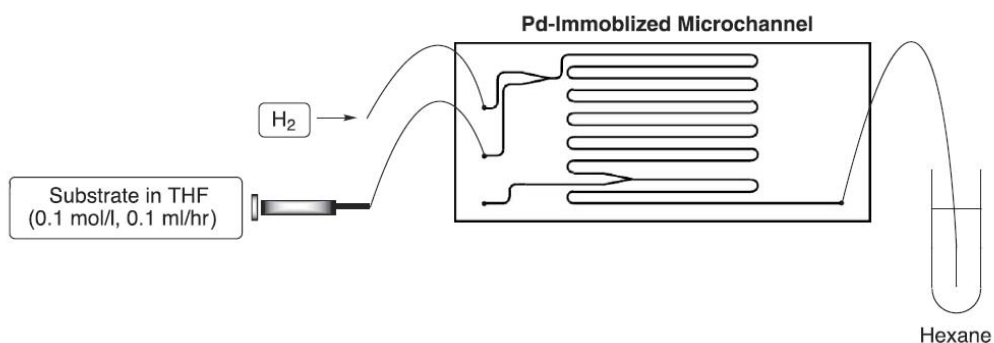
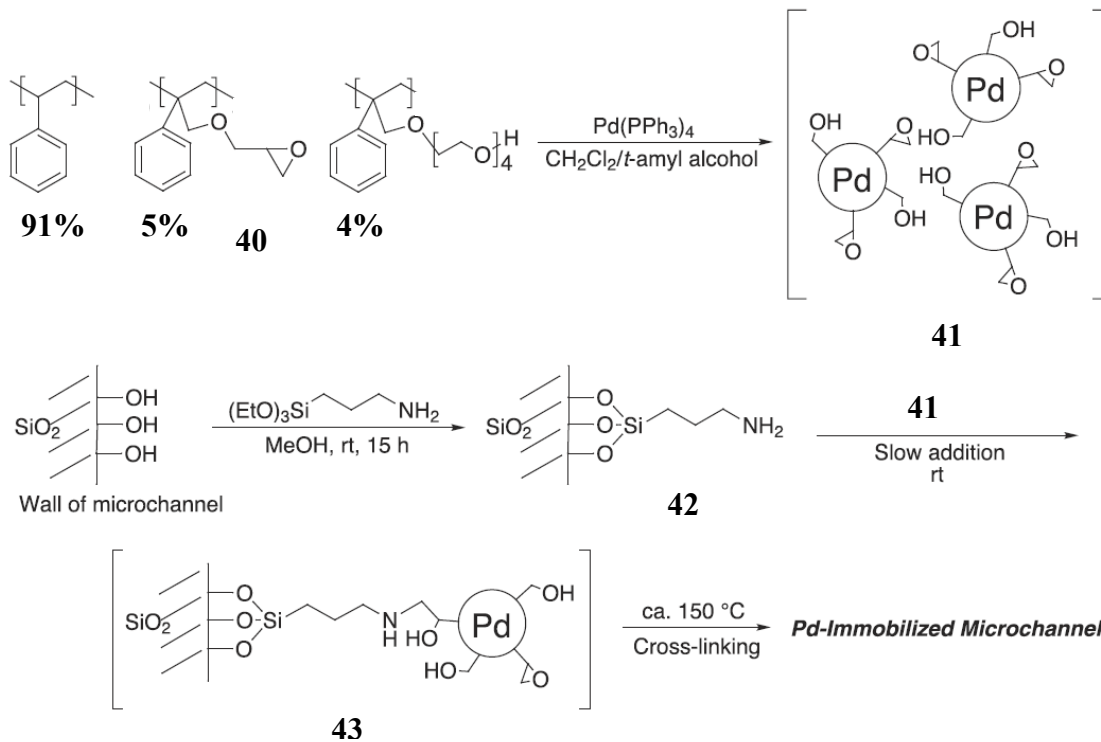


Figure 2.6. Glass microchannel reactor used for the hydrogenation reaction.

This system allows an efficient gas-liquid-solid interaction owing to the large interfacial areas and the short path required for molecular diffusion in the very narrow channel space, which is not attainable in the normal batch reactors.

The immobilization of the palladium (Pd) on the wall was achieved following a procedure which provides catalyst stability and no leaching (Scheme 2.10). First amino groups were introduced onto the surface of the glass channel to form **42**.



Scheme 2.10. General scheme for Pd catalyst encapsulation, and its immobilization on the microchannel interior.

Microencapsulated palladium (MC-Pd, **41**) prepared as shown in Scheme 2.10, was immobilized on a microchannel surface. Microscope observation shows that the inner surface of the channel was covered by polymer containing the palladium catalyst (Figure 2.7).

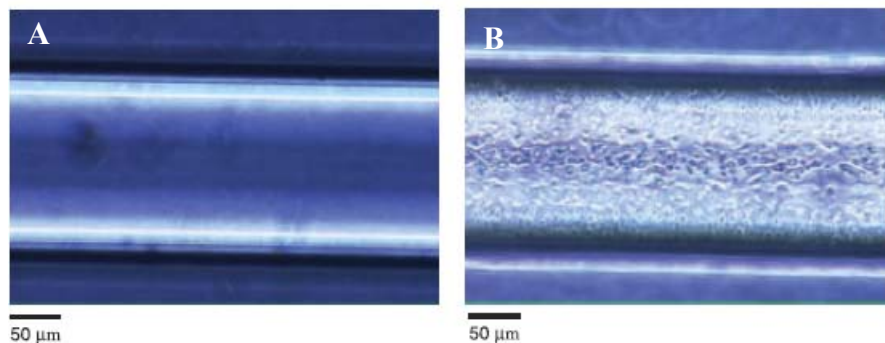
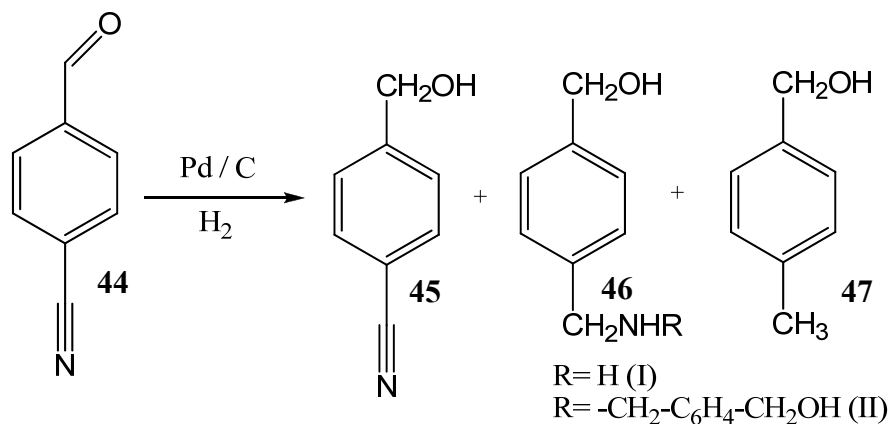


Figure 2.7. Microscope image of the microchannel (A) before and (B) after Pd (MC) immobilization.

Reduction of several olefins and alkynes, and also the cleavage of benzyl ether and carbamate groups were examined. The reaction proceeded smoothly in all cases to afford the corresponding products in quantitative yields (residence time 2 min). Furthermore, chemoselective reduction was successfully carried out, and a triple-bond was reduced without cleavage of a benzyl ether moiety. In all cases the reactions proceeded much faster than in batch reactors, Pd did not leach during the experiments.

Hydrogenation of 4-cyanobenzaldehyde (**44**) in methanol (Scheme 2.11) was reported using a packed-bed microreactor composed by a stainless-steel microflow column (o.d.: 6.3 mm, i.d.: 1.0 mm, length: 25 cm) ^[15]. As 4-cyanobenzaldehyde (**44**) has two functional groups, aldehyde and cyanide, and the former is more easily hydrogenated, the isolated products are 4-cyanobenzyl alcohol (**45**), 4-hydroxymethyl-benzylamine (**46**), bis(4-hydroxymethylbenzyl)amine (**46**), and 4-methylbenzyl alcohol (**47**). The secondary amine seemed to be formed by intramolecular reaction of **46-I** with the imine intermediate.



Scheme 2.11: Hydrogenation reaction of 4-cyanobenzaldehyde (44)

The microflow tube was filled with palladium on carbon (Pd/C) that was kept in the tube by two filters positioned at both ends of the tube (Figure 8). The substrate solution was mixed with hydrogen gas (pressure about 2.5 MPa) in a T-shaped mixer, and in a plug flow fashion (alternate gas and liquid layers) flowed through the tube column. The residence time in the column was only two min. The narrow channels, which are formed between and within Pd/C porous particles (diameter: $20 \pm 10 \mu\text{m}$), give rise to an enhanced mass transfer compared to a batch reactor. As a consequence the hydrogenation reaction was more efficient in the microflow column.

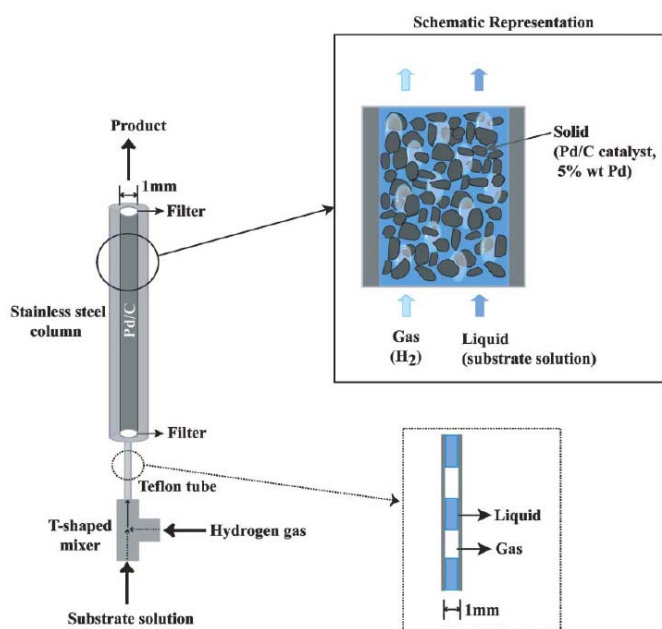
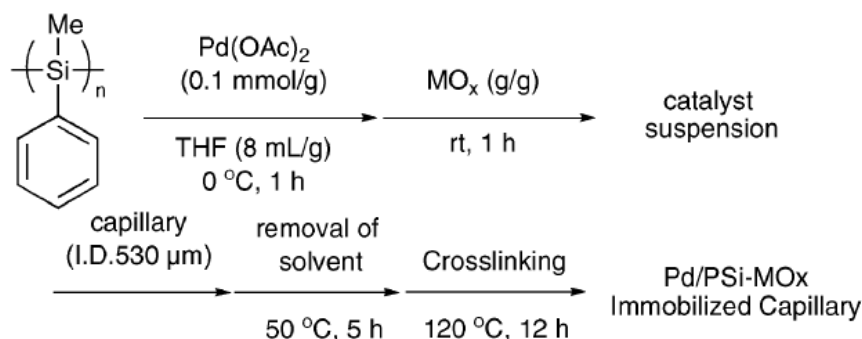


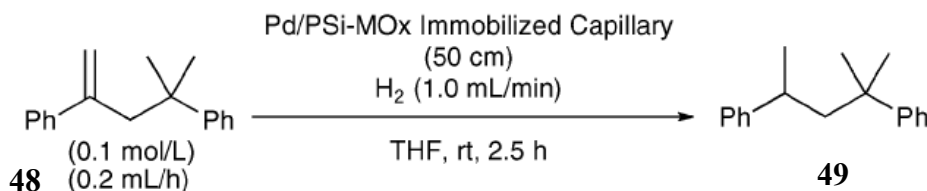
Figure 8. Schematic drawing of the gas-liquid-solid flow reactor^[15].

Ueno^[16] et al. developed a method for performing hydrogenation reactions based on a polysilane-supported palladium catalysts (Pd/PSi) immobilized on the channel wall of a capillary. The Pd/PSi catalyst was prepared in batch. The Pd/PSi immobilized capillary (530 μm i.d.) was obtained as depicted in Scheme 2.12.



Scheme 2.12. Typical procedure for the preparation of Pd/PSi-MO_x immobilized capillaries.

The coated capillary was used first for the hydrogenation of 2,4-diphenyl-4-methyl-1-pentene (**48**) (Scheme 2.13) in order to investigate the best metal oxide additive.



Scheme 2.13. Hydrogenation of 2,4-diphenyl-4-methyl-1-pentene (**48**) in the Pd/PSi coated capillary.

Using titanium oxide as additive, compound **48** was fully converted and no leaching of catalyst was detected. Subsequently, other alkenes were tested for the hydrogenation reaction. In most cases reactions proceeded smoothly to give the corresponding reduced compound. The Pd/PSi-TiO₂ immobilized capillary could be reused for 12 times, but the durability of the catalyst could be improved by varying the cross-linking temperature.

Another method for conducting heterogeneous hydrogenation reactions comprises the use of mesoporous titania nanoparticles^[17]. Nanoparticles doped mesoporous titania thin films were mixed to prepare a Palladium/ Titania sol (Pd/TiO₂) precursor solution which was used to coat the interior surface of a fused silica capillary with an internal diameter of 250 μm and a length of 9 m. The titania sol was withdrawn from the capillary, dried, and calcined in an oven at 300 $^{\circ}\text{C}$, at a residual pressure of 15 mbar in order to obtain the solid catalytic coating (Figure 2.9).

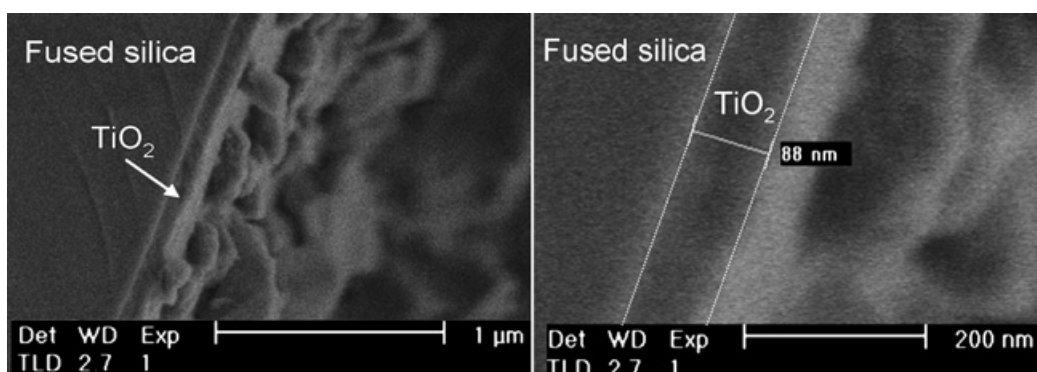


Figure 2.9. Field emission gun scanning electron microscopy (FEG-SEM) images of a cross-section of a coated fused silica capillary with a Pd-doped mesoporous titania film.

The withdrawing rate of the titania solution into the capillary allows control of the coating thickness. The hydrogenation of phenylacetylene in the Pd/TiO₂ coated capillary microchannel was studied in the 30 $^{\circ}\text{C}$ - 50 $^{\circ}\text{C}$ temperature range. The gas and the liquid flows were carefully controlled in order to work under an annular flow regime in all instances. The reaction was tested under different flow and temperature conditions (Table 2.3). It was observed that as the liquid flow rate of the feedstock solution inside the capillary is increased, the conversion of phenylacetylene is reduced, while the selectivity with respect to styrene formation increases. As a result of the increased ratio between the gas and the liquid flow rates, the flowing liquid becomes thinner, which results in higher liquid velocity and consequently a shorter liquid residence time in the reactor. This

improves the selectivity towards the partially hydrogenated product, because at a lower liquid residence time the subsequent hydrogenation of styrene occurs partially.

Table 2.3. Hydrogenation of phenylacetylene in coated Pd/ TiO₂ coated capillary microreactor at different flow rate and temperature conditions.

Temperature	30 °C		40 °C		50 °C	
Flow rate	Conversion	Selectivity ^a	Conversion	Selectivity ^a	Conversion	Selectivity ^a
3 μL min ⁻¹	99.2	64.0	99.5	5.3	99.9	1.6
4 μL min ⁻¹	94.2	85.2	97.5	24.5	99.9	44.8
5 μL min ⁻¹	54.9	94.5	99.8	53.8	99.8	62.8
6 μL min ⁻¹	19.8	94.6	35.2	93.8	50.3	92.8

^aRelative to styrene (semi-hydrogenation product).

These experiments prove that the conversion and the selectivity of the catalytic process can be controlled tuning flow and temperature conditions.

The same type of capillary microreactor with mesoporous titania thin films containing either Pd or bimetallic Pd₂₅Zn₇₅ nanoparticles^[18], was applied to conduct the hydrogenation of 2-methyl-3-butyn-2-ol in methanol. The coated microreactor shows a higher selectivity toward alkenes (90% conversion) than the commercially available Lindlar catalyst (commonly used for this reaction) in a batch reactor.

2.3.3 Photoreduction

Methylene blue was reduced in a microcapillary (length: 5 cm, internal diameter: 530 and 200 μm) coated with TiO₂ as a photocatalyst on the inner wall^[19]. A colloid solution of TiO₂-coated SiO₂ with a core-shell structure was first prepared by using a surfactant to generate a surface charge on the particles (Figure 2.10).

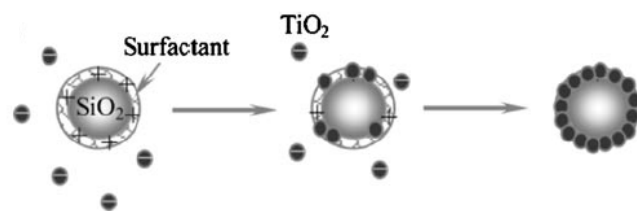
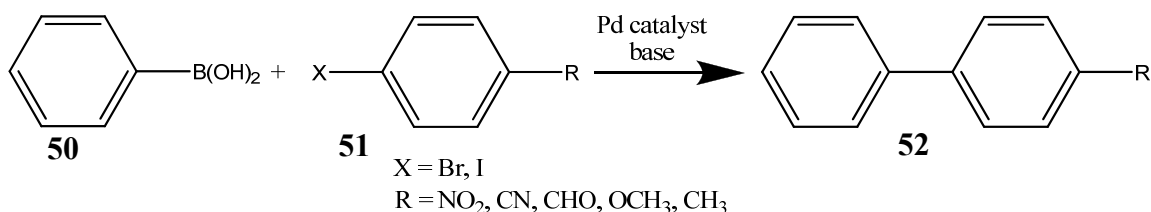


Figure 2.10. Preparation of SiO₂/TiO₂ core-shell particles.

The TiO₂ was introduced and coated on the inner wall of the microcapillary by the self-organization of SiO₂. The reduction of methylene blue was performed in a capillary coated either with TiO₂/SiO₂, with TiO₂ without SiO₂, and in one without any coating. The capillary with the TiO₂/SiO₂ coating gave the best conversion rate. This was attributed not only to a larger surface/volume ratio, but also to the absorption properties of SiO₂ nanoparticles. The corresponding batch reactor gave a lower conversion rate.

2.3.4 Suzuki-Miyaura Coupling and Heck Reactions

The Suzuki cross-coupling reaction between phenylboronic acid (**50**) and 4-bromobenzonitrile (**51**) to give 4-cyanobiphenyl (**52**) (Scheme 2.14) has been carried out in a packed bed microchannel reactor (300 μm wide and 115 μm deep) ^[20].



Scheme 2.14. Suzuki-Miyaura coupling reaction between phenylboronic acid (**50**) and 4-bromobenzonitrile (**51**).

The reagent solutions were transported using electroosmotic flow (EOF) assisted by the incorporation of a microporous silica structure within the microreactor channels, which acted both as a micro-pump and an immobilization technique for the catalyst bed (1.8% palladium on silica), see Figure 2.11.

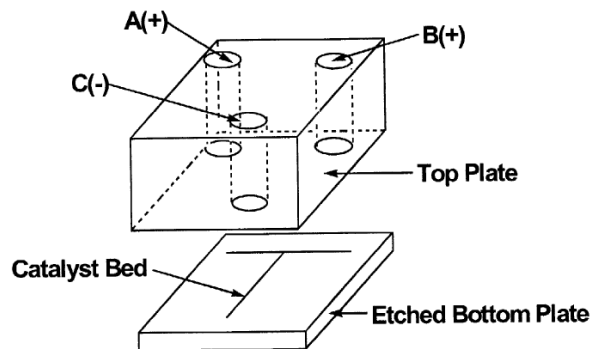


Figure 2.11. Schematic drawing of the microreactor used for the Suzuki-Miyaura reaction (A) and (B) reagent inlets, (C) outlet ^[20].

4-Cyanobiphenyl (**52**) was obtained in a yield of $(67 \pm 7) \%$, with respect to aryl halide (**51**), with a presence of 1.2-1.6 ppb of palladium, due to leaching from the silica bed. Interestingly, the addition of a base was not required. This was attributed to the partial ionization of the aqueous THF which may form a hydroxide species which acts as base in the Suzuki cross-coupling.

The Suzuki cross-coupling reaction of different types of aryl halides (**51**) and phenylboronic acid (**50**) (Scheme 14) to form biaryls, in the presence of potassium carbonate (K_2CO_3), in *N,N*-dimethylformamide (DMF) and water (ratio 3:1), has been performed using a microwave based technique capable of delivering heat locally to a heterogeneous Pd-supported catalyst^[20], located within a microreactor^[21]. Two microreactors designs were used (Figure 2.12).

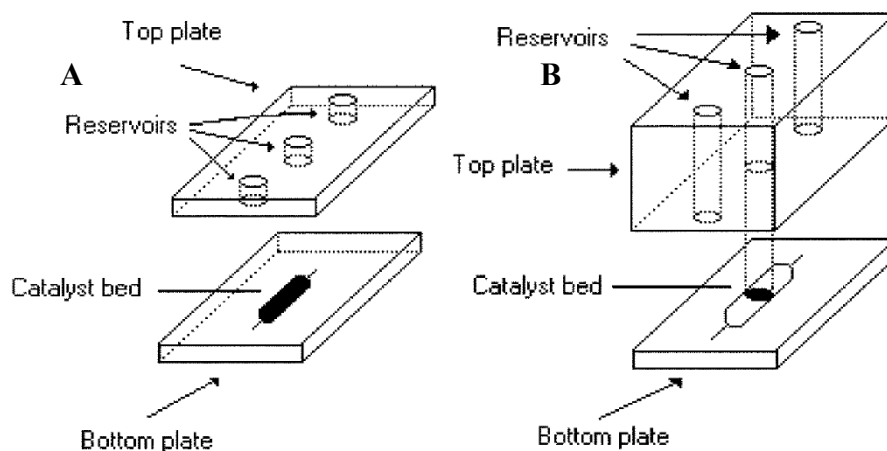


Figure 2.12. Packed-bed microreactors^[21] for Suzuki-Miyaura reactions.

In microreactor **A** the top plate was less thick than in microreactor **B**. Another difference was the amount of catalyst, 1.5 mg and 6 mg of Pd-silica powder, for microreactors **A** and **B**, respectively. A 10-15 cm gold film patch, located on the outside surface of the base of the microreactors, was sufficient to heat the catalyst when irradiated with 55-80 W of microwave power at 2.45 GHz. Using a hydrodynamically pumping system the reagents were brought in contact with the catalyst; the residence time was around 60 s. Product yields, determined by GC, were 98-99% and were similar for the two packing designs. However, inherent to the design, design **A** needed less catalyst and MW energy. This was probably due to the more efficient heat transfer from the gold patches.

Shore^[22] *et al.* reported the deposition of a Pd thin film on the inner surface of capillaries and their use in Suzuki and Heck reactions using microwave irradiation. This set-up was called microwave-assisted continuous-flow organic synthesis (MACOS), since it combines the advantages of microwave-assisted organic synthesis (MAOS) with the benefits offered by continuous flow operation.

Scanning electron microscopy (SEM) applied on the capillary cross section (Figure 2.13) revealed that the film was highly porous and consisted of nanometer size Pd crystallites.

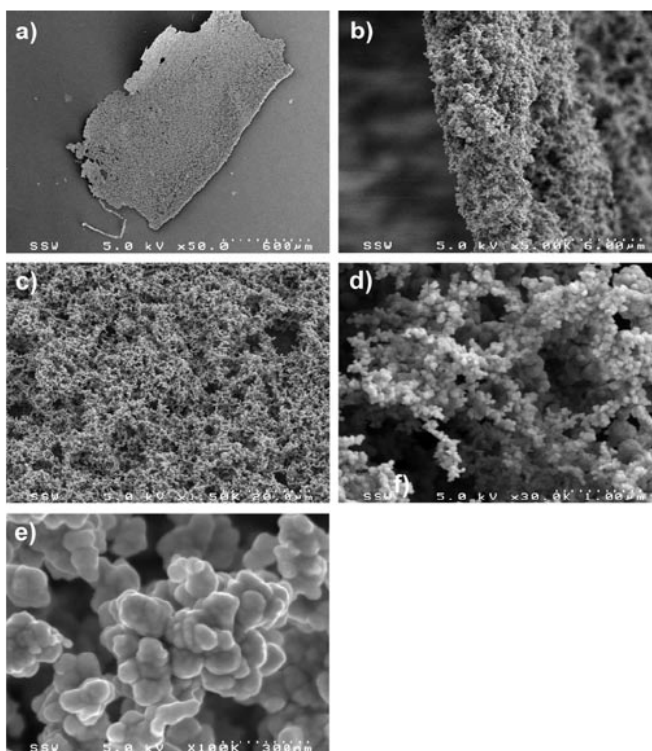
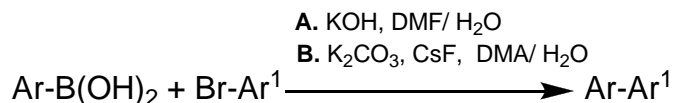


Figure 2.13. a) SEM image of the Pd films prepared inside a glass capillary and removed ($\times 50.0$). b) Cross-section of the edge located on the left-hand side of sample shown in (a) ($\times 5000$). Image taken from the central portion of the sample in (a) at c) $\times 1500$, d) $\times 30\,000$, and e) $\times 100\,000$.

The Pd-coated capillaries were first applied in the Suzuki coupling reaction of different types of aryl halides (Br-Ar^1) and aryl boronic acids (Ar-B(OH)_2) to give biaryls (Scheme 2.15).



Scheme 2.15. Suzuki coupling of aryl boronic acids and bromides using MACOS in Pd coated capillaries.

Premixed solutions of Br-Ar^1 , and Ar-B(OH)_2 , and base were flowed through the metal-coated capillary, while it was subjected to microwave irradiation (power setting $\approx 30\text{ W}$) such that the temperature was kept constantly at $200\text{ }^\circ\text{C}$ (Figure 2.14).

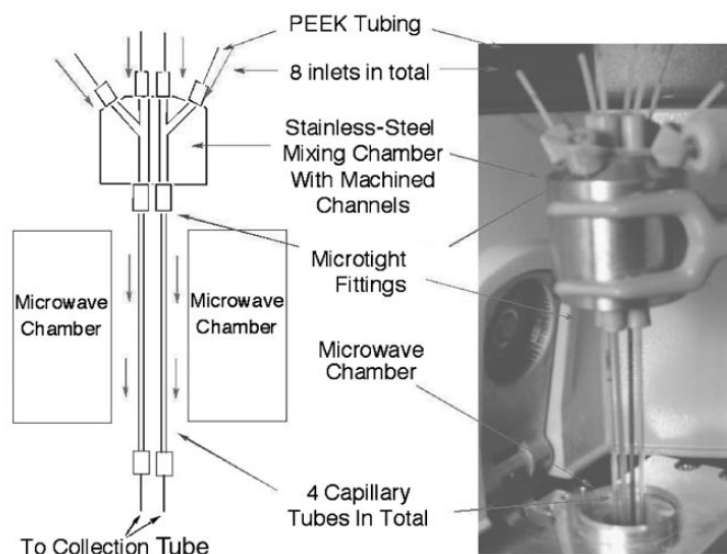
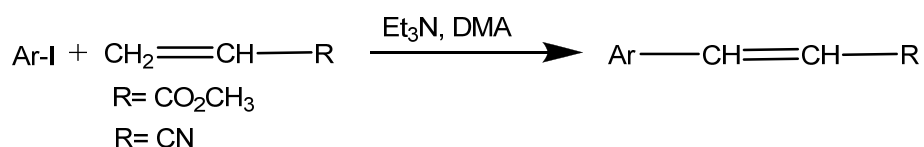


Figure 2.14. Capillary reactor system for the microwave-assisted continuous-flow organic synthesis (MACOS)^[22].

In all cases, including the coupling of both electron-rich and electron-poor aryl halides with electron-poor boronic acids, good to excellent yields were obtained. Pd analysis of the crude cross-coupling product mixtures did show slightly elevated levels of Pd (19.2 ppm) inherent with the reaction mechanism.

The Heck coupling reaction of different aryl iodides (**Ar-I**) with acrolein derivatives was also investigated using MACOS in Pd-coated capillaries (Scheme 2.16). It was found that the Pd film was very efficient at performing this transformation under continuous flow conditions. Conversions obtained indicated that electron-deficient aryl iodides and acrolein derivatives were more reactive. This behavior was attributed to the intrinsic mechanism of the Heck reaction.



Scheme 2.16. Heck coupling of aryl iodides with acrolein derivatives using MACOS in Pd-coated capillaries.

Uozumi^[23] *at al.* reported the introduction of a polymer membrane of a palladium complex inside a microchannel reactor for the Suzuki cross coupling reaction between aryl halides and aryl boronic acids. The poly(acrylamide)-triarylphosphine-palladium (PA-TAP-Pd) membrane (Figure 2.15a) was generated via self assembly complexation of a polymeric phosphine ligand and a palladium complex, at the interface of two laminar layers flowing through the microchannel (100 μm width, 40 μm depth, 140 mm, Figure 2.15b). The Suzuki reaction was successfully carried out in this device with quantitative product formation within 4 s.

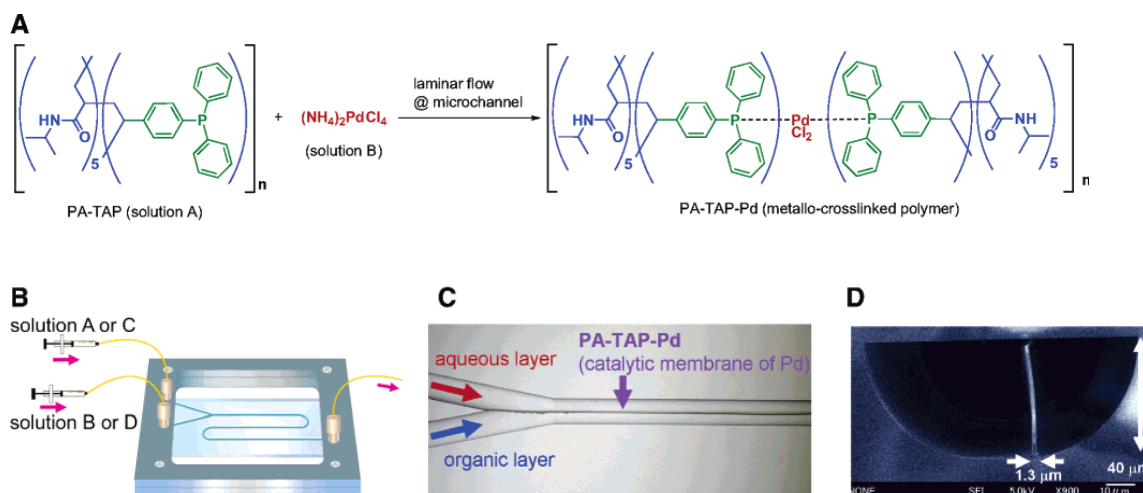


Figure 2.15. Formation of the catalytic membrane inside a microchannel: (A) metallo-cross-linking formation of PA-TAP-Pd polymer, (B) reaction apparatus, (C) microscopic view of the membrane formation (top view), (D) microscopic SEM view of the membrane inside the channel^[23] (cross section).

2.3.5 Alcohol Oxidation

Wang^[24] and coworkers developed a gold-immobilized microchannel reactor for the catalytic oxidation of alcohols with molecular oxygen. A polysiloxane-coated capillary column (Figure 2.16), which contained 50% phenyl and 50% n-cyanopropyl

functionalities (**53**) on silicon atoms with a film thickness of 0.25 μm on the walls, was selected ϵ

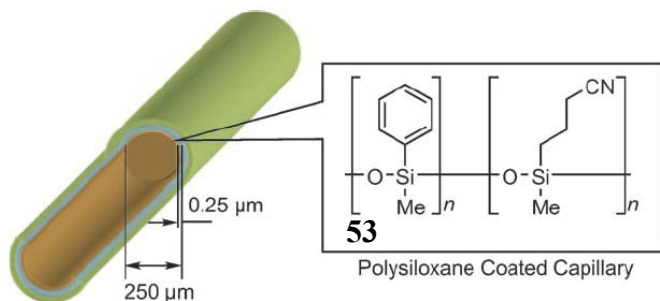
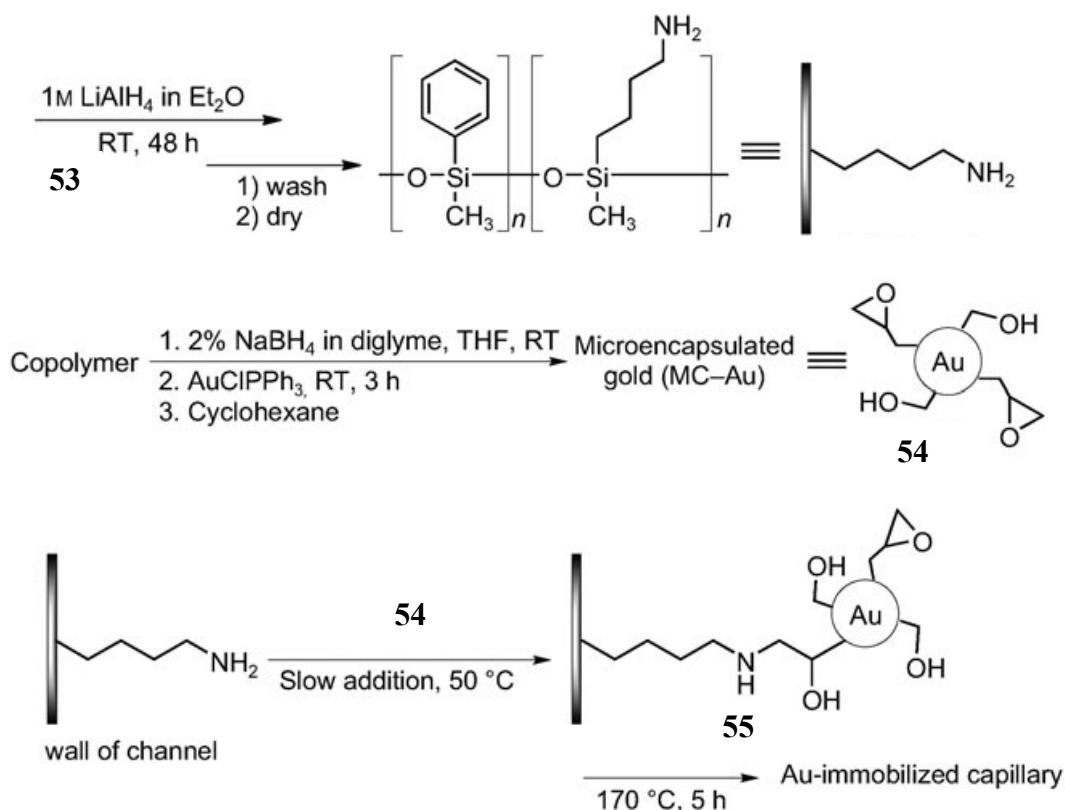


Figure 2.16. Polysiloxane-coated capillary column^[24].

Upon reduction of the cyanopropyl groups, the corresponding amino groups were reacted with microencapsulated gold (MC-Au) (**54**), prepared from chlorotriphenylphosphine gold (AuClPPH_3) and a copolymer. Upon cross-linking of the copolymer the desired gold-immobilized capillary column (**55**) was obtained (Scheme 2.16). The oxidation of 1-phenylethanol was carried out in the catalytic capillary column, using the set-up described in Figure 2.17.



Scheme 2.16. Formation and immobilization of a gold catalyst on the wall of a capillary. a) Reduction of the cyano group to an amine, b) preparation of microencapsulated gold, c) Immobilization of the gold catalyst.

The solution containing the substrate and aqueous K_2CO_3 merged at the T-shaped connector before meeting the oxygen gas at the second T-shaped connector. Subsequently, the reagents mixture was flowed through the capillary with gold immobilized on the wall. 1-Phenylethanol was quantitatively converted into the corresponding ketone. The scope of the aerobic oxidation of alcohols using the capillary with gold immobilized on the wall was studied using benzylic, aliphatic, allylic, and other alcohols. In most cases, the alcohols were successfully oxidized to the corresponding ketones in excellent yield. The oxidation of benzyl alcohol led to a low yield of the expected benzaldehyde, although full conversion was observed. However, when a capillary with gold immobilized on the wall (achieved by combining microencapsulated

gold and palladium^[14]) was used for the reaction, the desired benzaldehyde was obtained in high yield. This shows that the capillary column reactor can accommodate the bimetallic Au/ Pd system.

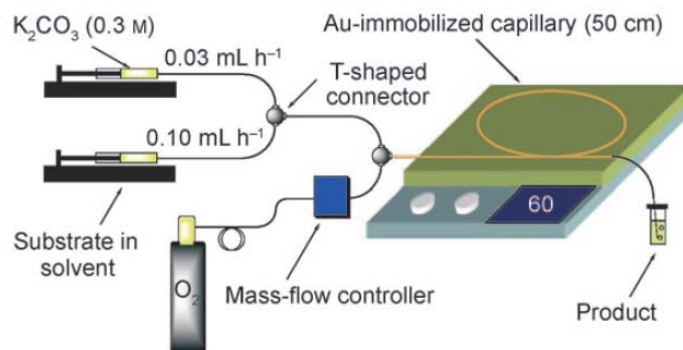


Figure 2.17. Experimental set-up of the gold-catalyzed oxidation reactions^[24].

2.4 Reactions Catalyzed by Enzymes

2.4.1 Glucose Oxidation

Zhang^[25] *et al.* used a poly(dimethylsiloxane) PDMS microchannel for in-situ synthesis of gold nanoparticles to which glucose oxidase enzyme (GOx) was immobilized. The gold nanoparticles are formed by simply flowing an aqueous HAuCl₄ solution through the microchannel. The salt reduction and the concomitant formation of gold nanoparticles were attributed to the residual silicon hydride (Si-H) groups of the PDMS channel surface. The size of the nanoparticles could be adjusted by varying the ratio between the curing agent and the PDMS monomer (η) (Figure 2.18).

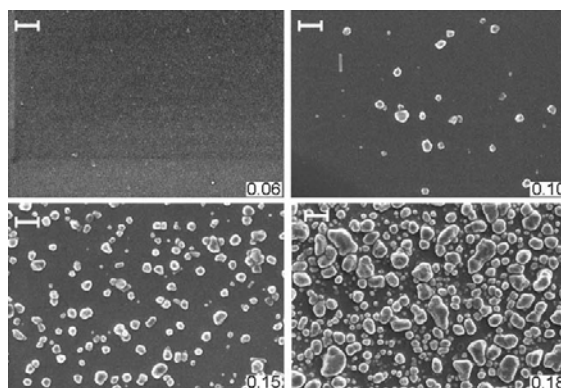


Figure 2.18. SEM images of the PDMS-gold nanoparticles free standing films with different η . Scale bar = 1 μm .

Dithiobissuccinimidyl (DTSP)^[26] was used as a linker to immobilize GOx to the gold nanoparticles. Taking glucose as a substrate, electroosmotic flow as a driving force and amperometry as a detection method, the performance of the reactor was studied. Glucose solutions were added in the sample reservoir and electrokinetically oxidized with dissolved oxygen in the buffer solution forming hydrogen peroxide, which can be detected at the working electrode. The current response increased linearly with the concentration of glucose lower than 10 mM.

2.4.2 Synthesis of 2-aminophenoxazin-3-one (APO)

Silica-immobilized enzymes for multi-step synthesis in microfluidic devices have been reported^[27]. Individual microfluidic chips (40 mm long, 1.5 mm wide, and 0.1 mm deep) containing metallic zinc, silica-immobilized hydroxylaminobenzene mutase and silica-immobilized soybean peroxidase (SBP), respectively, connected in a series to create a chemo-enzymatic system for synthesis (Figure 2.19).

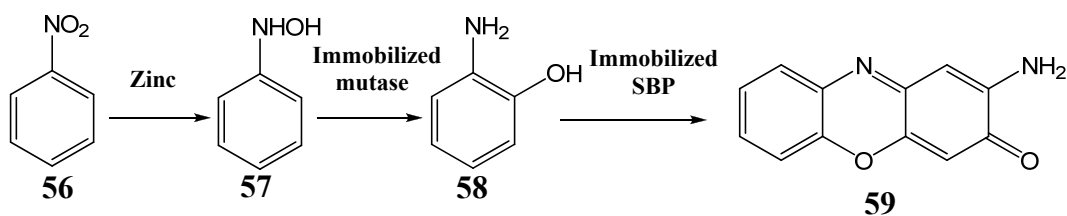


Figure 2.19. Multi-step microfluidic process for the conversion of nitrobenzene (**56**) to 2-aminophenoxazin-3-one (APO) (**59**).

Zinc catalyzes the initial reduction of nitrobenzene (**56**) to hydroxylaminobenzene (**57**).

The zinc chip gave approximately 25% conversion of **58**. At a low flow rate ($2.5 \mu\text{L min}^{-1}$) also aniline was formed as a byproduct of the zinc reduction. The chemoenzymatic system could continuously produce 0.13 mM of APO for over 4 h.

This system is suitable for the synthesis of a complex natural product (APO) from a simple substrate (nitrobenzene) under continuous flow conditions.

2.4.3 Proteolysis

Miyazaki^[28] *et al.* reported a nanostructure based on a multilayer of 3-aminopropyltrimethoxysilane formed on the surface of a silica capillary (320 μm inner diameter) to immobilize a serine protease cucumicin. The amino groups were functionalized with succinic anhydride in order to introduce carboxylic groups which were converted to active esters using 1-ethyl-3-(3-aminopropyl)carbodiimide hydrochloride and *N*-hydroxysuccinimide (NHS-ester). Subsequently, the serine protease

solution was flowed through the capillary and reacted with the NHS-ester groups. The capillary-enzyme efficiency was examined by carrying out the proteolysis of a buffer solution of a polypeptide. After 3.75 s the reaction was completed and after 4 min, 1 mL was produced, while in the batch-wise system, using immobilized enzyme, several hours are required to complete the reaction on a 1 mL scale.

Trypsin was physisorbed on a zeolite nanocrystal surface and these particles were subsequently attached on a PDMS microchannel for carrying out protein digestion^[29]. Two standard proteins with different sizes, cytochrome c and bovine serum albumine, were used as model substrates to evaluate the performance of the nanozeolite-modified enzyme reactor. The generated product was analyzed by MALDI-TOF. The Michaelis-Menten constant (K_M) of 1.5 mM and the maximum velocity (V_{max}) of 7.9 mM s⁻¹ of the tryptic digestion were 1000 times higher than that for free trypsin in a batch reactor. This system was shown to be highly sensitive in the analysis of proteins in low amounts and concentrations. Therefore it was claimed having high potential in automated high-throughput analysis using a parallel-channel microchip platform.

Sakai-kato^[30] and coworkers introduced a trypsin encapsulated sol-gel into a plastic microchip to create a bioreactor that integrates digestion, separation, and detection of proteins. The trypsin encapsulated sol-gel, which was formed from alkoxysilane, was fabricated within a sample reservoir of a poly(methylmethacrylate) (PMMA) microreactor. Substrates as fluorescently labeled arginine ethyl ester dihydrochloride (NBD-ArgOEt), a peptide as NBD-bradikinin, and a protein as casein labeled with a dye were digested in the bioreactor. The substrates were flowed through the bioreactor by electroosmotic flow which was sufficient also to have the separation of the digested fragments subsequently detected by fluorescence microscopy. It was shown that the

tryptic digestion of this system was shorter compared with that reported using standard schemes. Furthermore, the encapsulated trypsin exhibited increased stability, even after continuous use, compared with that in solution.

A water-soluble phospholipids polymer, having an active ester group in the side chain, was used for the immobilization of trypsin on the sample reservoir of a PMMA microreactor^[31]. The covalent immobilization of proteolytic enzyme was achieved by reacting the amino groups of the enzyme with polymer ester moieties. The hydrolysis of fluorescently labeled NBD-ArgOEt to NBD-Arg was achieved in less than 3 min.

α -Chymotrypsin was immobilized on a polymer membrane formed on the inner wall of a microreactor by a cross-linking polymerization method^[32]. Commercially available polytetrafluoroethylene (PFTE) tubing (500 μm inner diameter and 6 cm length) was used as microreactor. Glutaraldehyde (GA) and paraformaldehyde (PA) were employed as bifunctional cross-linker agents to facilitate enzyme-enzyme covalent binding. As shown in Figure 2.20, the α -chymotrypsin and the cross-linker (GA and PA) solutions were separately loaded into a PFTE tube from a syringe at different pumping rates. After a few hours a water insoluble enzyme-membrane was formed on the inner wall surface of the PFTE tube.

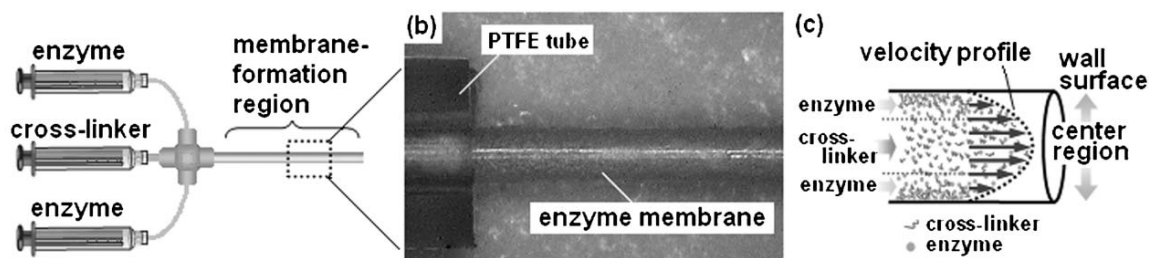


Figure 2.20. Enzyme membrane formed by cross-linking polymerization method^[31].

The α -chymotrypsin enzyme efficiency was evaluated performing the hydrolysis of *N*-glutaryl-L-phenylalanine *p*-nitroanilide. The reaction was carried out in a thermostated

incubator controlled at 37 °C. The constant K_M and the maximum velocity V_{max} were the same as those for the solution phase batch-wise reaction, at the same enzyme/ substrate molar ratio. The enzyme-based catalytic membrane was also used for the digestion of myoglobin and insulin. The technique to obtain the biocatalytic membrane could be extended to other enzymes using poly-L-lysine as cross-linker instead of the aldehydes^[33]. For example, an acylase enzyme-membrane was tested for the hydrolysis of acetyl-D-L-amino acid to give the L-amino acid and the unhydrolyzed acetyl-D-amino acid^[34]. Such enzymatic microreactor was linked to a microextractor which provided a laminar flow of two immiscible solutions (ethyl acetate and water), allowing selective extraction of the products (Figure 2.21).

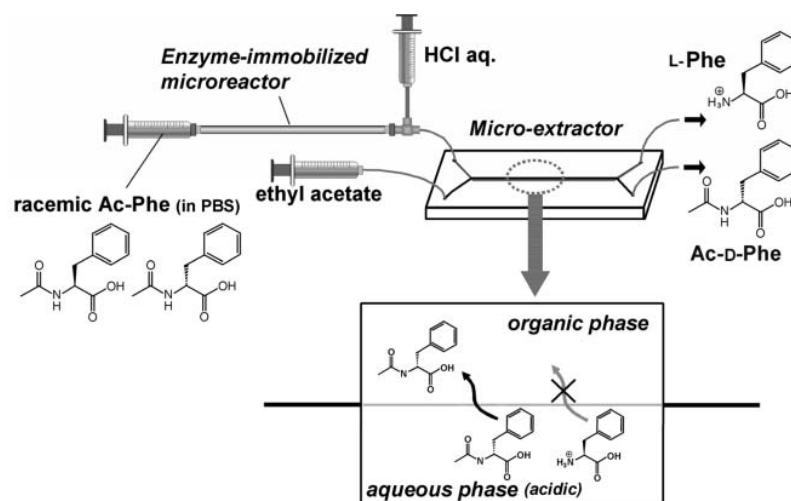
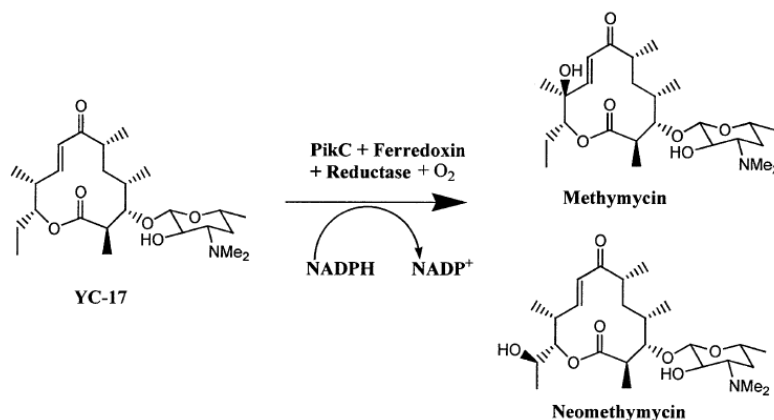


Figure 2.21. Continuous flow system for amino acids formation and for their enantioselective separation^[34].

2.4.4 Hydroxylation

The PikC hydroxylase *Streptomyces venezuelae* was immobilized to agarose beads packed into a PDMS-based microfluidic channel (350 μm wide, 160 μm deep, 30 mm long)^[35]. A Ni-NTA magnetic agarose bead suspension was added to the microchannel inlet reservoir and the beads were packed into the microchannel by applying vacuum to the outlet reservoir until the end of uniform bead packing reached 10 mm (reaction volume 280 nL in the microchannel). The transport of the enzyme and reaction substrate through the microchannel was achieved using a centrifugal force direct flow. To that end, the device was mounted on a Plexiglas platform and the entire platform in a temperature-controlled centrifuge. The fluid flow rate was determined by measuring the amount of liquid collected in the product reservoir at different centrifugal speeds. The enzyme loading was $\sim 6 \mu\text{g}$ per mg of beads resulting in a microchannel loading of 10.7 mg/ mL. This high enzyme loading enabled the rapid hydroxylation of the macrolide YC-17 to methymycin and neomethymycin in about equal amounts with a conversion $> 90\%$ (Scheme 2.17).



Scheme 2.17. PickC catalyzed hydroxylation of YC-17 to methymycin and neomethymicine in the presence of NADPH, ferredoxine, and ferredoxin-NADP⁺ reductase^[35].

The product formation was monitored measuring the collected sample by UV-Vis, following the consumption of NADPH at 340 nm.

2.4.5 Ester Hydrolysis

The methodology to anchor the serine protease cucumicin^[28] was applied to bind lipases, for ester hydrolysis, on the surface of a fused silica capillary-ceramic microreactor^[36], and on silica nanoparticles^[37] immobilized on the channel interior of a microcapillary as discussed in section 2.3.4^[19]. Hydrolysis of 7-acetoxycumarin and umbelliferine acetate gave the products in good yields.

A microreactor containing mesoporous silica as a catalyst support layer to immobilize lipase, without complex chemical modification, was developed by Kataoka and co-workers^[38]. The immobilized lipase showed good enzymatic activity and stability during 24 hours of continuous hydrolysis of 4-nitrophenyl acetate. The reaction followed Michaelis-Menten kinetics, however, the K_M constant was 3 times larger than that calculated from a batch experiment. This was attributed to sterical hindrance induced by the immobilization of the enzyme in mesopores, which limits the accessibility of the reactants.

2.4.6 Lactose Hydrolysis

A multichannel microfluidic element made from vinyl group-containing poly(dimethylsiloxane) (PDMS) with pyrogenic silicic acid as a filler, which provides hydroxy groups for surface chemistry, was developed by Thomsen *et al.*^[39] for the immobilization of a β -glycosidase from *Pyrococcus furiosus*. The microreactor (length: 64 mm width: 350 μ m, height 250 μ m) used for this experiment contained passive mixing

elements to improve the mass transfer to and from the microchannel surface (Figure 2.22).

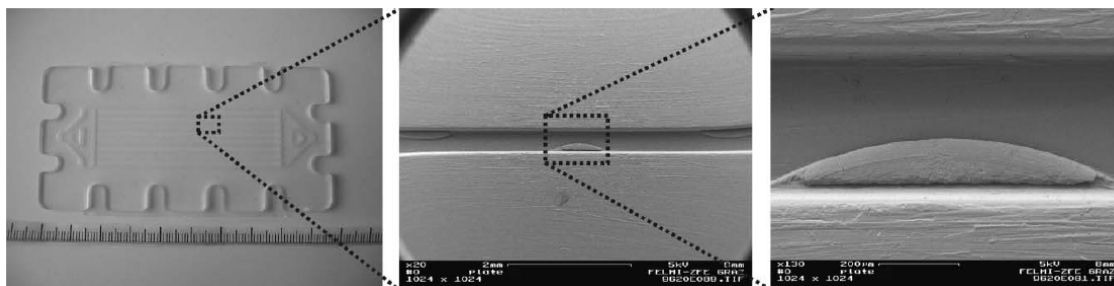


Figure 2.22. Microreactor and mixing elements^[39].

The microchannel surface was silanized with 3-aminopropyltriethoxysilane and subsequently derivatised with glutardialdehyde which was reacted with the enzyme. Hydrolysis of lactose to give glucose and galactose was performed to test the enzyme-microreactor; the conversion was $\geq 60\%$.

2.5 CONCLUSIONS and OUTLOOK

Due to their intrinsic characteristics microreactors often show easier process optimization, higher efficiency in terms of product yield, reaction time, and selectivity when compared to the conventional laboratory glassware equipment.

Both silicon-glass microchannels and silica fused capillaries have been used for creating packed-bed microreactors. Many types of catalysts have been incorporated in such devices demonstrating the wide applicability of the packed-bed microreactor concept. Since the supported catalysts were prepared in batch-scale packed-bed microreactors, it gives the possibility to characterize and quantify the catalyst packed in the device. This also allows to compare the catalytic performance of the device with the lab-scale reaction. On the other hand, the wall of a microchannel which was mainly employed for conducting metal-catalyzed reactions required more sophisticated techniques for

anchoring a catalyst. However, it permits to explore new types of catalytic materials and to use conditions which can not be applied in a standard batch system. Microreactors employed for organic synthesis are mainly made from silicon and glass, while with aqueous solutions, as for enzymatic reactions, PMMA and PDMS devices can be easily fabricated with different types of design.

New methods for catalyst implementation in microreactors are in development resulting in novel catalytic platforms. This type of microreactors may lead to a revolutionary, innovative, and unique environment to conduct heterogeneously catalyzed bio-chemical reactions. The integration of microreactors with immobilized catalysts may also offer the advantage of creating high-speed, high-density information systems and to automatize multi-step synthesis, providing better control and reproducibility.

References:

- [1] B. Ahmed-Omer, J. C. Brandt, T. Wirth, *Org. Biomol. Chem.* **2007**, *5*, 733.
- [2] M. Brivio, W. Verboom, D. N. Reinhoudt, *Lab Chip* **2006**, *6*, 329.
- [3] J. Kobayashi, Y. Mori, S. Kobayashi, *Chem. Asian. J.* **2006**, *1*, 22.
- [4] B. P. Mason, K. E. Price, J. L. Steinbacher, A. R. Bogdan, D. T. McQuade, *Chem. Rev.* **2007**, *107*, 2300.
- [5] P. Watts, C. Wiles, *Org. Biomol. Chem.* **2007**, *5*, 727.
- [6] P. Watts, C. Wiles, *Chem. Commun.* **2007**, 443.
- [7] C. Wiles, P. Watts, S. J. Haswell, *Tetrahedron* **2005**, *61*, 5209.
- [8] C. Wiles, P. Watts, S. J. Haswell, *Lab Chip* **2007**, *7*, 322.
- [9] A. R. Bogdan, B. P. Mason, K. T. Sylvester, D. T. McQuade, *Angew. Chem. Int. Ed.* **2007**, *46*, 1698.
- [10] T. Jackson, J. H. Clark, D. J. Macquarrie, J. H. Brophy, *Green Chem.* **2004**, *6*, 193.
- [11] A. El Kadib, R. Chimenton, A. Sachse, F. Fajula, A. Galarneau, B. Coq, *Angew. Chem. Int. Ed.* **2009**, *48*, 4969.
- [12] S. J. Haswell, B. O'Sullivan, P. Styring, *Lab Chip* **2001**, *1*, 164.
- [13] C. Wiles, P. Watts, *Eur. J. Org. Chem.* **2008**, *12*, 5597.
- [14] J. Kobayashi, Y. Mori, K. Okamoto, R. Akiyama, M. Ueno, T. Kitamori, S. Kobayashi, *Science* **2004**, *304*, 1305.
- [15] N. Yoswathananont, K. Nitta, Y. Nishiuchi, M. Sato, *Chem. Commun.* **2005**, 40.
- [16] M. Ueno, T. Suzuki, T. Naito, H. Oyamada, S. Kobayashi, *Chem. Commun.* **2008**, 1647.

- [17] E. V. Rebrov, A. Berenguer-Murcia, H. E. Skelton, B. F. G. Johnson, A. E. H. Wheatley, J. C. Schouten, *Lab Chip* **2009**, *9*, 503.
- [18] E. V. Rebrov, A. E. Klinger, A. Berenguer-Murcia, E. Sulman, J. C. Schouten, *Org. Process Res. Dev.* **2009**, *13*, 991.
- [19] X. Y. Li, H. Z. Wang, K. Inoue, M. Uehara, H. Nakamura, M. Miyazaki, E. Abe, H. Maeda, *Chem. Commun.* **2003**, 964.
- [20] G. M. Greenway, S. J. Haswell, D. O. Morgan, V. Skelton, P. Styring, *Sens. Actuators B* **2000**, *63*, 153.
- [21] P. He, S. J. Haswell, P. D. I. Fletcher, *Lab Chip* **2004**, *4*, 38.
- [22] G. Shore, S. Morin, M. G. Organ, *Angew. Chem. Int. Ed.* **2006**, *45*, 2761.
- [23] Y. Uozumi, Y. M. A. Yamada, T. Beppu, N. Fukuyama, M. Ueno, T. Kitamori, *J. Am. Chem. Soc.* **2006**, *128*, 15994.
- [24] N. Wang, T. Matsumoto, M. Ueno, H. Miyamura, S. Kobayashi, *Angew. Chem. Int. Ed.* **2009**, 4744.
- [25] Q. Zhang, J. J. Xu, Y. Liu, H. Y. Chen, *Lab Chip* **2008**, *8*, 352.
- [26] M. Darder, K. Takada, F. Pariente, E. Lorenzo, H. D. Abruna, *Anal. Chem.* **1999**, *71*, 5530.
- [27] H. R. Luckarift, B. S. Ku, J. S. Dordick, J. C. Spain, *Biotechnol. Bioeng.* **2007**, *98*, 701.
- [28] M. Miyazaki, J. Kaneno, M. Uehara, M. Fujii, H. Shimizu, H. Maeda, *Chem. Commun.* **2003**, 648.
- [29] Y. H. Zhang, Y. Liu, J. L. Kong, P. Y. Yang, Y. Tang, B. H. Liu, *Small* **2006**, *2*, 1170.
- [30] K. Sakai-Kato, M. Kato, T. Toyo'oka, *Anal. Chem.* **2003**, *75*, 388.
- [31] K. Sakai-Kato, M. Kato, K. Ishihara, T. Toyo'oka, *Lab Chip* **2004**, *4*, 4.
- [32] T. Honda, M. Miyazaki, H. Nakamura, H. Maeda, *Chem. Commun.* **2005**, 5062.
- [33] T. Honda, M. Miyazaki, H. Nakamura, H. Maeda, *Adv. Synth. Catal.* **2006**, *348*, 2163.
- [34] T. Honda, M. Miyazaki, Y. Yamaguchi, H. Nakamura, H. Maeda, *Lab Chip* **2007**, *7*, 366.
- [35] A. Srinivasan, H. Bach, D. H. Sherman, J. S. Dordick, *Biotechnol. Bioeng.* **2004**, *88*, 528.
- [36] J. Kaneno, R. Kohama, M. Miyazaki, M. Uehara, K. Kanno, M. Fujii, H. Shimizu, H. Maeda, *New J. Chem.* **2003**, *27*, 1765.
- [37] H. Nakamura, X. Y. Li, H. Z. Wang, M. Uehara, M. Miyazaki, H. Shimizu, H. Maeda, *Chem. Eng. J.* **2004**, *101*, 261.
- [38] S. Kataoka, A. Endo, M. Oyama, T. Ohmori, *Appl. Catal., A* **2009**, *359*, 108.
- [39] M. S. Thomsen, P. Polt, B. Nidetzky, *Chem. Commun.* **2007**, 2527.

CHAPTER 3

Self-Assembled Monolayers for the Immobilization of Catalysts on the Interior of Glass Microreactors

Self-assembled monolayers (SAMs) are used to immobilize basic organic catalysts as 1-propylamine, 1,5,7-triazabicyclo[4.4.0]dec-5-ene (TBD), and poly(amidoamine) dendrimer generation 2 (PAMAM G2), on the interior of glass microreactors. The Knoevenagel condensation reaction of benzaldehyde (**1**) and malononitrile (**2**) was carried out in these catalytic devices as a model reaction to investigate the catalytic activity.

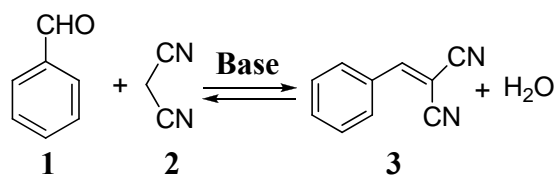
3.1 Introduction

As discussed in Chapter 2, one of the most striking features of microreactors is the high surface-to-volume ratio resulting from downsizing^[1-3]. The large active surface area available within microchannels has proven to be beneficial for heterogeneous catalysis, in which a catalyst is either immobilized on the channel surface^[4] or introduced into the channel on a solid support^[5-7]. Although immobilization of metal catalysts and enzymes to microreactor channel walls has been described, there is only one example^[8] in literature, where an organic catalyst has been anchored onto the microchannel interior.

In addition, microreactors, due to their small dimensions, need low amounts of reagents and catalyst, offering the possibility to screen different conditions for performing catalytic reactions in a fast and economic way.

In this chapter we describe the use of self-assembled monolayers (SAMs) for covalently anchoring organic catalysts to the inner wall of a glass microreactor. SAMs on a silicon oxide and a glass surface are commonly applied in many fields like (bio)chemical sensing and nanotechnology; they offer a wide range of chemical functionalities for further derivatization. Another advantage of using SAMs for binding a catalyst to the wall is the relatively easy procedure which ensures an in situ functionalization by a simple flow of solutions through the channel without purification steps, and/ or complicated immobilization techniques.

To study our approach, 1-propylamine^[8] and 1,5,7-triazabicyclo[4.4.0]dec-5-ene (TBD)^[9] were immobilized on the interior of a silicon glass microreactor, and the base-catalyzed Knoevenagel condensation reaction between benzaldehyde (**1**) and malononitrile (**2**) to give 2-benzylidene malononitrile (**3**) (Scheme 3.1) was chosen as a model reaction to study the performance of these catalytic devices.



Scheme 3.1. Knoevenagel condensation reaction between benzaldehyde (1) and malononitrile (2) in acetonitrile at 65 °C.

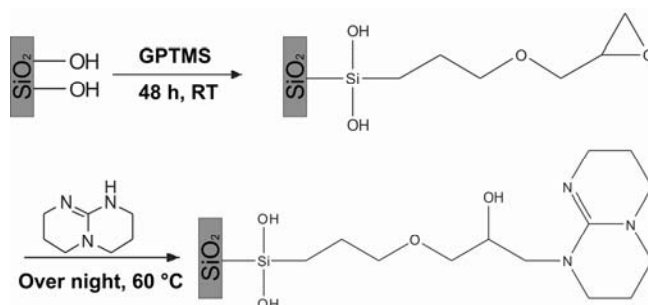
To increase the number of the catalytic units on the surface, also poly(amidoamine) dendrimer generation 2 (PAMAM G2) was anchored on the microchannel interior.

3.2 Results and Discussion

3.2.1 Synthesis of Base SAMs on a Flat Surface and their Characterization

Propylamine SAMs, made by reaction of aminopropyltriethoxysilane (APTES) on a silicon oxide surface, have been made and characterized extensively before, and were therefore not further studied here.

TBD catalyst immobilization was studied first on a silicon oxide and a glass surface, following a two-step procedure (Scheme 3.2). First an epoxide monolayer of (3-glycidylpropoxy)trimethoxysilane (GPTMS) was grown on silicon oxide and a glass surface. Subsequently, TBD was anchored via a nucleophilic substitution reaction.



Scheme 3.2. General scheme for epoxide monolayer formation and TBD catalyst immobilization on a silicon oxide surface and the microreactor interior.

The monolayer formation was monitored with a variety of techniques, including contact angle goniometry, ellipsometry, and X-ray photoelectron spectroscopy (XPS), see Table 3.1.

Table 3.1. Advancing (θ_a) and receding (θ_r) water contact angles, ellipsometric thickness, and selected XPS data of SAMs depicted in Schemes 3 and 4.

SAM	θ_a (°)	θ_r (°)	Ell. Thickness (nm)	C/N (XPS)	C/N (Calc.)
EPOXIDE	57 ± 5	39 ± 5	1.3 ± 0.1	-	-
TBD	42 ± 2	36 ± 3	0.80 ± 0.05	4.3 ± 0.3	4.6
PAMAM G2	44 ± 2	28 ± 5	1.7 ± 0.2	5.4 ± 0.5	2.5

SAMs formed from (3-glycidylpropoxy)trimethoxysilane^[12] (epoxide SAMs) had an advancing contact angle of 57° and an ellipsometric thickness of 1.3 nm, consistent with previously reported values^[12].

TBD SAMs were obtained incubating the epoxide SAMs in a solution of TBD in ethanol at 60 °C over night. Upon reaction the measured advancing contact angle was 42°, showing that the surfaces became more hydrophilic compared to the epoxide SAMs, indicating that TBD was immobilized. Analysis of the TBD SAMs by ellipsometric thickness measurements displays a layer of 0.8 nm. This decrease of the thickness, after TBD immobilization, may be attributed to the oxirane ring opening as a result of the nucleophilic substitution reaction with TBD. To test this hypothesis, we performed XPS on TBD SAMs, which gave a carbon to nitrogen ratio of 4.3, close to the theoretical value of 4.6. This indicates not only that TBD was anchored, but also that almost 100% of the oxirane groups reacted with TBD.

PAMAM G2 dendrimer (Figure 3.1) SAMs on a silicon oxide and a glass surface were obtained incubating substrates having epoxide SAMs in a solution of PAMAM dendrimer

G2 in methanol at 60 °C (Scheme 3.3). After incubation, the advancing contact angle was 44° (Table 3.1), therefore a more hydrophilic surface compared to the epoxide SAMs was achieved, suggesting the successful fabrication of the PAMAM G2 SAMs. The ellipsometric thickness, of the PAMAM G2 SAMs was 1.7 nm. The substrates were also analyzed with XPS displaying a carbon to nitrogen ratio of 5.4. This value is about half of the theoretical value of 2.5. Assuming that all oxirane functional groups reacted with PAMAM, this indicates that, on average, two oxirane rings react with one PAMAM G2 entity.

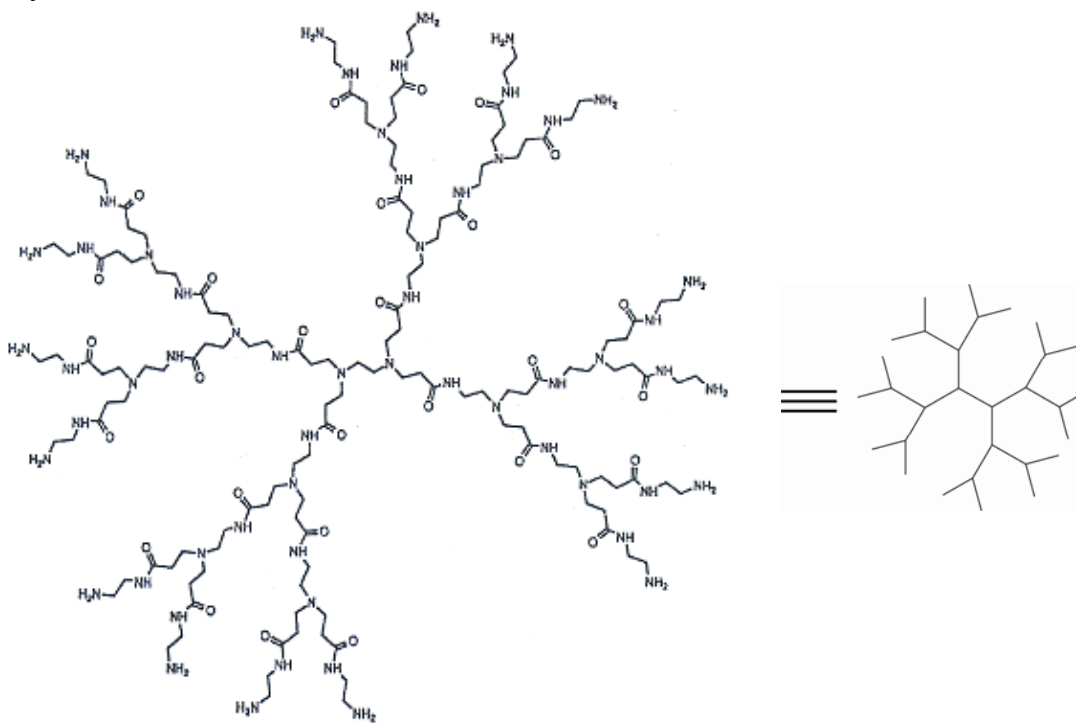
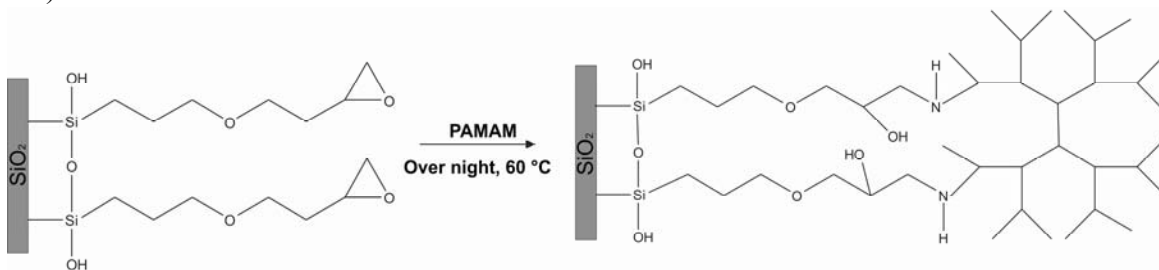


Figure 3.1. Molecular structure of a second generation PAMAM dendrimer (PAMAM G2).



Scheme 3.3. General scheme of PAMAM dendrimer G2 catalyst immobilization on a silicon oxide and the microreactor interior.

3.2.2 Synthesis of Propylamine SAM on the Microreactor Interior for the Kinetic Study of the Knoevenagel Condensation Reaction

The inner walls of several glass microreactors, see Figure 3.2, were coated with 1-propylamine, flowing a solution of aminopropyltrimethoxysilane^[10] (APTES) through the microreactor at a flow rate of 0.1 $\mu\text{L}/\text{min}$ (Scheme 3.4).

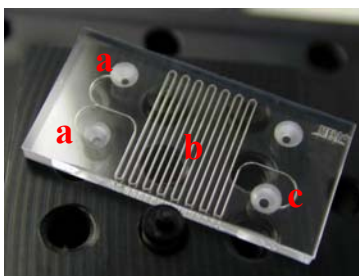
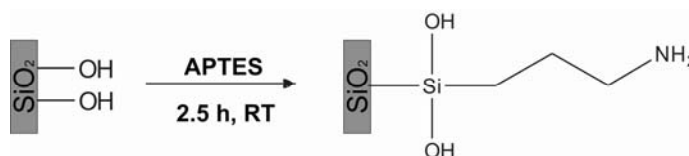


Figure 3.2. Glass microreactor: **a)** inlets, **b)** reaction zone and **c)** outlet.



Scheme 3.4. General scheme for 1-propylamine catalyst immobilization on the microreactor interior.

The Knoevenagel condensation reaction between benzaldehyde (**1**) and malononitrile (**2**) in acetonitrile was carried out in this catalytic microreactor, in continuous flow (0.1-0.02 $\mu\text{L}/\text{min}$). To perform the experiments, the microreactor was placed in a home-built chip holder design for fitting fused silica fibers into the inlet/outlet chip reservoirs (Figure 3.3a-b).

Initially, the Knoevenagel condensation was carried out both at room temperature and 65 °C. The temperature of the microreactor was controlled by interfacing a thermoelectric module with a heat sink and a copper plate to the chip (Figure 3.3d).

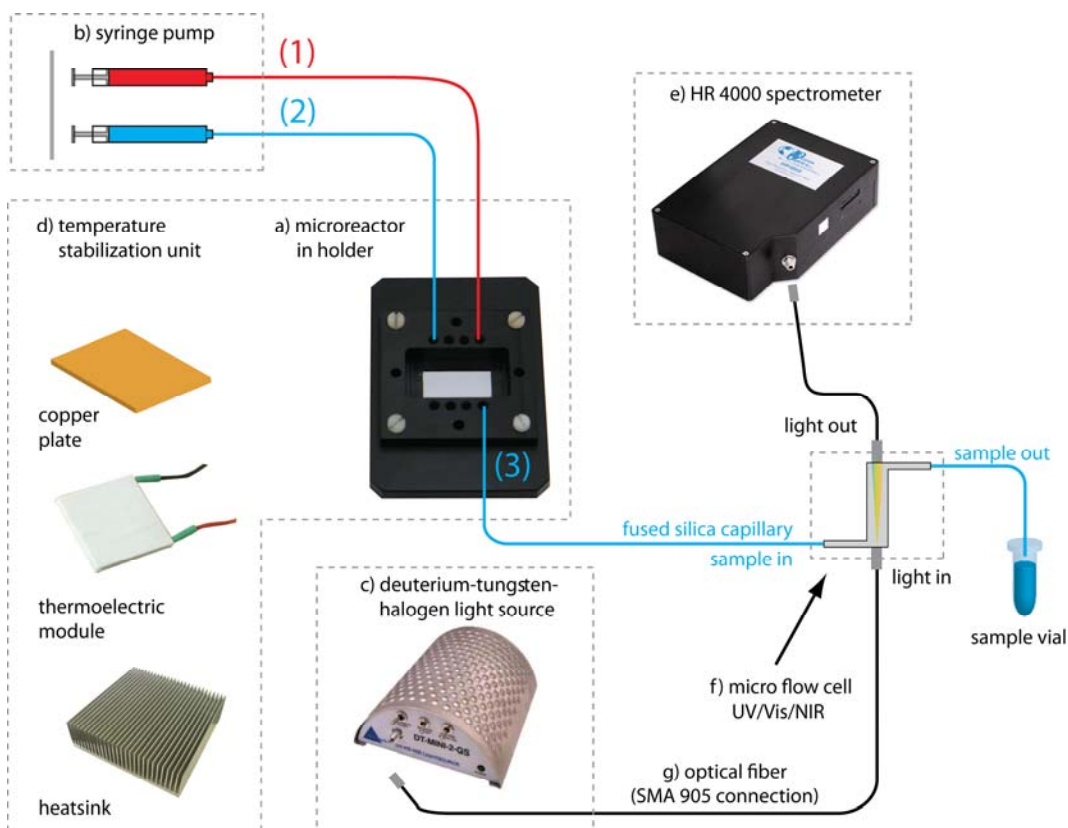


Figure 3.3: The microreactor set-up: a) glass microreactor assembled in a home-built holder, b) syringe pump, c) deuterium-tungsten-halogen light source, d) temperature stabilization unit, e) high-resolution spectrometer, f) micro-flow cell (internal volume 1 μL), g) solarisation-resistant optical fibers.

2-Benzylidene malononitrile (**3**) as the reaction product was collected over night and analyzed by UV-vis off-line (Figure 3.4). In each step the catalytic layer was rinsed with a solution of triethylamine in order to reactivate the catalytic layer. The reaction was also carried out at lab-scale applying the same reagents and catalyst concentrations used in the microreactor (Figure 3.4).

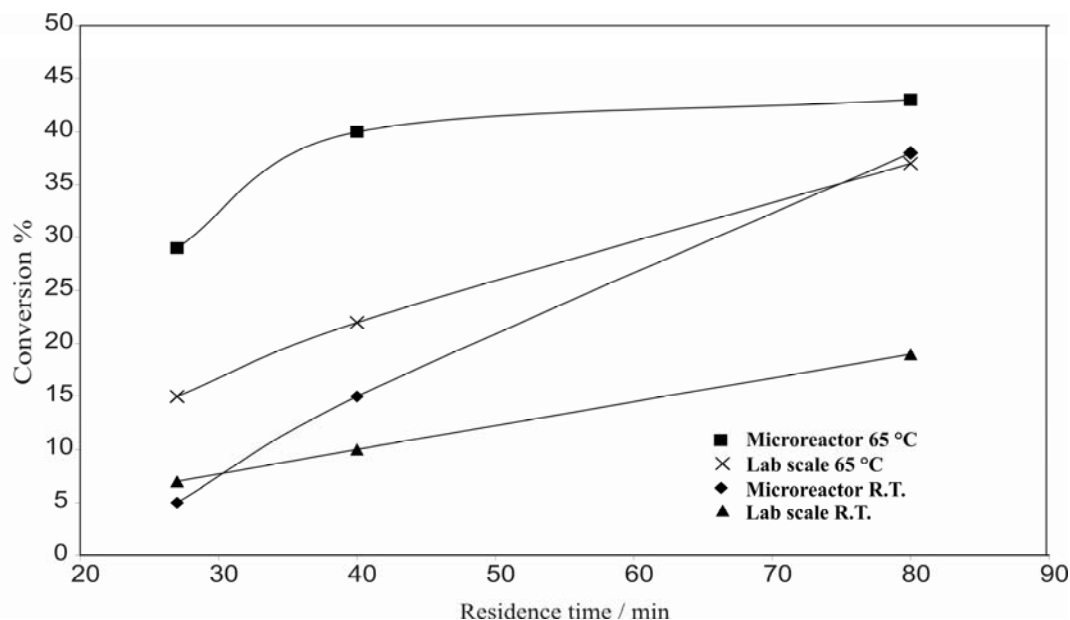


Figure 3.4. Formation of 2-benzylidene malononitrile (**3**) (followed off-line) catalyzed by 1-propylamine immobilized on the microreactor interior and interior and by 1-propylamine at lab-scale, [1] = 0.01 M and [2] = 0.01 M.

The concentration of the 1-propylamine catalyst of 0.5×10^{-3} M employed in the lab-scale experiment correspond to the number of reacting SiOH groups, contained on the internal silica surface area of the microchannel per square centimeter^[11], assuming that each hydroxyl group reacted with one molecule of aminopropyltriethoxysilane. It turned out that the conversion obtained performing the reaction in the microreactor was higher than that observed in the lab-scale experiment. However, it may be that the reaction partially occurred in the vial while collecting the sample for analysis, since some 2-benzylidene malononitrile (**3**) formation was observed when benzaldehyde (**1**) and malononitrile (**2**) were mixed together in acetonitrile over night, as also witnessed by the room temperature reactions (Figure 3.3).

In order to follow the reaction in real time the formation of the condensation product 2-benzylidene malononitrile (**3**) was monitored by an in-line UV-vis detection set-up. The outlet of the microreactor was joined to a micro-flow cell, connected to a lamp and to a

high resolution spectrometer via optical fibers, where the sample passes through (Figure 3.3f-g). The conversion of the reaction was measured following the increase of the 2-benzylidene malononitrile (**3**) absorption peak at 305 nm. UV-vis detection spectroscopy is a suitable detection technique for this type of reaction, since no by-products are formed. In case of not UV-vis active reactant or reaction products, the catalytic microreactors can easily be connected to a $^1\text{H-NMR}$ microprobe.

A kinetic study was performed under pseudo-first order conditions, using an excess of malononitrile (**2**) (0.05 M), while the benzaldehyde (**1**) concentration was 50 μM . The second-order rate constant of $(1.7 \pm 0.2) \times 10^{-3} \text{ s}^{-1} \text{ M}^{-1}$ was calculated using the initial rate method (Figure 3.5), since after 60 min, the coated device showed decrease of activity. No reaction was observed when the reagents were flowed through the microreactor in absence of the APTES monolayer, proving that immobilized 1-propylamine was the catalytic species.

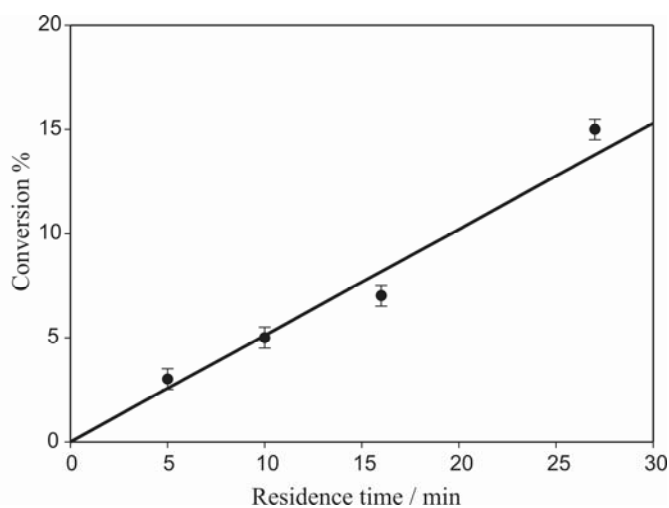


Figure 3.5. Formation of 2-benzylidene malononitrile (**3**) catalyzed by 1-propylamine immobilized on the microreactor interior, [**1**] = 50 μM and [**2**] = 0.05 M.

3.2.3 Synthesis of TBD and PAMAM SAMs on the Microreactor Interior for the Kinetic Study of the Knoevenagel Condensation Reaction

TBD SAMs were grown on microreactor channel walls following the same procedure applied for silicon oxide surfaces (Scheme 3.2). First a solution of (3-glycidylpropoxy)trimethoxysilane in toluene and subsequently a solution of TBD in ethanol were flowed through the microchannel at a flow rate of 0.1 $\mu\text{L}/\text{min}$. The Knoevenagel condensation reaction between **1** and **2** was carried out using the same conditions applied for microreactors coated with 1-propylamine. The second-order rate constant of $(2.0 \pm 0.2) \times 10^{-3} \text{ s}^{-1} \text{ M}^{-1}$ was calculated using the initial rate method (Figure 3.6), since after 60 min the coated device showed decrease of activity. The rate constant is almost similar to that determined with 1-propylamine. No conversion was observed when the microreactor was only coated with (3-glycidylpropoxy)trimethoxysilane.

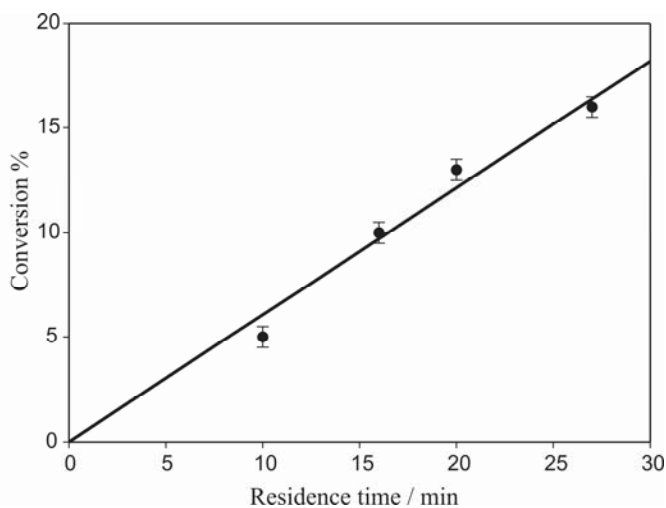


Figure 3.6. Formation of 2-benzylidene malononitrile (**3**) catalyzed by TBD immobilized on the microreactor interior, $[\mathbf{1}] = 50 \mu\text{M}$ and $[\mathbf{2}] = 0.05 \text{ M}$.

PAMAM dendrimer G2 was immobilized on microreactor channel walls using the same procedure applied for silicon oxide and glass surfaces (Scheme 3.3). The aim of using

PAMAM G2 was used to improve the catalytic SAM stability and consequently the conversion of the Knoevenagel reaction. To obtain the catalytic SAMs first a solution of (3-glycidylpropoxy)trimethoxysilane in toluene and subsequently a solution of PAMAM dendrimer G2 in methanol were flowed through the microchannel at a flow rate of 0.1 $\mu\text{L}/\text{min}$. The Knoevenagel condensation reaction between **1** and **2** was carried out using the same conditions applied for microreactors coated with propylamine or TBD. The second-order rate constant value of $(1.7 \pm 0.2) \times 10^{-3} \text{ s}^{-1} \text{ M}^{-1}$ was calculated using the initial rate method (Figure 3.7), since also in this case after 60 min the coated device showed decrease of activity.

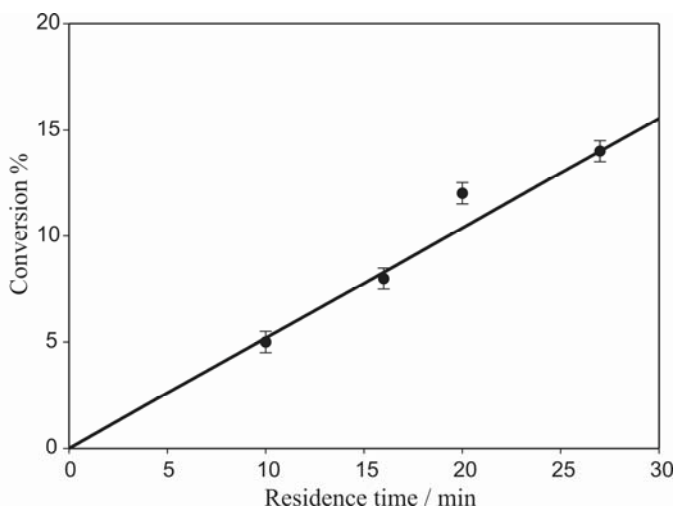


Figure 3.7. Formation of 2-benzylidene malononitrile (**3**) catalyzed by PAMAM G2 immobilized on the microreactor interior, $[\mathbf{1}] = 50 \mu\text{M}$ and $[\mathbf{2}] = 0.05 \text{ M}$.

Although PAMAM G2 dendrimer has a larger number of amino functional groups, an improvement of the catalytic activity was not observed. This may be due to the low solubility of PAMAM G2 dendrimer in acetonitrile. As a consequence, the PAMAM G2 SAM may behave as an impenetrable layer which does not allow the reagents to get in contact with all amino groups. Steric hindrance between dendrimer chains may be another cause of limited accessibility of the reagents to reach all catalytic species.

3.3 Conclusions

In this chapter three different types of catalytic SAMs, 1-propylamine, TBD, and PAMAM dendrimer G2, were successfully immobilized on the microchannel interior of glass microreactors. The Knoevenagel condensation reaction of benzaldehyde (**1**) and malononitrile (**2**) was conducted in such catalytic devices and a kinetic study was carried out. It turned out that the three catalysts had almost the same catalytic activity. This is in contrast with other literature results, where it was shown that for the Knoevenagel condensation reaction, a primary amine has a higher turnover frequency compared to a tertiary amine due to a different catalytic mechanism^[13]. This incongruence may be related to the intrinsic morphology of the catalytic SAMs. It could be that 1-propylamine and PAMAM SAMs have less accessible catalytic sites and therefore they do not exhibit a higher catalytic activity as expected.

SAMs together with microreactor technology provide an easy and fast method to investigate the activity of a catalyst towards a chemical reaction. However, this type of coating did not provide long time stability, probably due to the hydrolysis of the silane layer on the surface. In addition, the amount of catalyst that can be immobilized on the microchannel interior using SAMs is not sufficient to have full product formation. To have an efficient catalysis the number of catalytic groups anchored on the channel interior must be increased creating a porous structure in which all catalytic sites are active in the catalysis.

3.4 Experimental

Materials and Equipment. All commercial reagents were purchased from Aldrich Chemicals. PAMAM dendrimer G2 was purchased from Dendritech, Inc. Benzaldehyde was distilled under vacuum before use. The other chemicals were used without further purification. Methanol, ethanol, (VWR, analytical reagent grade), and acetonitrile (analytical reagent grade, Acros) were used without further purification. Toluene (VWR, analytical reagent grade) was distilled over sodium.

Contact Angle Goniometry. Contact angles were measured with Millipore water on a Krüss G10 contact angle measuring instrument, equipped with a CCD camera. Advancing and receding contact angles were determined automatically during growth and shrinkage of the droplet by a drop shape analysis routine.

Ellipsometry. Ellipsometric layer thickness measurements were performed on a Plasmon Ellipsometer ($\lambda = 632.8$ nm) assuming a refractive index of 1.500 for the monolayers and 1.457 for the underlying native oxide. The thickness of the SiO₂ layer was measured separately on an unmodified part of the same wafer and subtracted from the total layer thickness determined for the monolayer covered silicon substrate.

XPS. XPS spectra were obtained on a Quantera Scanning X-ray Multiprobe instrument, equipped with a monochromatic Al_{K α} X-ray source producing approximately 25 W of X-Ray power. Spectra were referenced to the main C 1s peak set at 284.0 eV. XPS-data were collected from a surface area of 1000 $\mu\text{m} \times 300 \mu\text{m}$ with a pass energy of 224 eV and a step energy of 0.8 eV for survey scans and 0.4 eV for high resolution scans. For quantitative analysis, the sensitivity factors used to correct the number of counts under each peak were: C 1s, 1.00; N 1s, 1.59.

Microreactor Fabrication. The microfluidic devices (microreactors) used in this work were made of borosilicate glass (Borofloat 33, Schott Technical Glasses, Germany). Borosilicate glass substrates (100 mm diameter, thickness 1.1 mm) were ultrasonically cleaned in isopropanol (15 min), and fuming 100% nitric acid (15 min), followed by quick dump rinsing in de-mineralized water and dry spinning. Subsequently, the topside of the substrates was sputter-coated with a gold-chromium layer (200 nm Au, 15 nm Cr). This metal thin-film was patterned using photo-resist (standard UV-lithography), Au-etchant and Cr-etchant, and the stack of photo-resist/Au/Cr acted as a mask-layer during isotropic etching of serpentine-shaped microchannels (depth 50 μm , width 110 μm , length 300 mm) with 25% hydrofluoric acid. After etching, the substrates were ultrasonically rinsed with flushing DI-water (5 min), followed by removal of the photoresist layer and the Au/Cr thin-film. To the topside of other substrates photosensitive foil was attached. In this foil access holes were defined using lithography, and powderblasting was used to make accesses through the substrates. After removal of the foil, ultrasonic cleaning with demineralized water and rinsing with 100% nitric acid, substrates with microchannels and substrates with access holes were aligned and prebonded. The glass-glass bond was finalized by annealing in air (600 $^{\circ}\text{C}$, 1 h), followed by dicing of the waferstack in individual chips of 20 \times 10 mm.

Setup of the Microfluidic Device. In all experiments sample solutions were mobilized by means of a PHD 22/2000 series syringe pump (Harvard Apparatus, United Kingdom) equipped with 250 μL flat tip syringes (Hamilton). Syringes were connected to fused silica capillaries (100 μm i.d.) by means of Upchurch NanoportTM assembly parts (i.e. NanoTightTM unions and fittings, Upchurch Scientific Inc. USA).

During the experiments the microreactor was placed in a home-built chip holder designed for fitting fused silica fibers into the inlet/outlet chip reservoirs by means of commercially available Upchurch Nanoport™ assembly parts.

The temperature in the microreactor was controlled by interfacing a thermoelectric module with a heat sink to the microreactor. The temperature variation on the glass surface of the microreactor measured with a thermocouple was less than ± 0.1 °C.

On-line UV-vis Detection. The formation of 2-benzylidene malononitrile (**3**) was followed using a micro HPLC flow-through cell (ZEUTEK opto-elektronik, Germany), with a spectral UV/VIS/NIR range of 250-2500 nm, an optical path length of 5 mm, and an internal volume of 1 μ L. The flow cell is connected, via 2 optical fibers (SR 600 nm, Ocean optics Inc., The Netherlands), to a miniature deuterium halogen light source (DT-Mini-2-GS, Mikropack GmbH, Germany) and to a high-resolution miniature fiber optic spectrometer (HR4000, Ocean optics Inc., The Netherlands).

Preparation of the Catalytic SAMs. Microchannels, silicon wafers and glass surface were first cleaned with a Piranha solution ($\text{H}_2\text{SO}_4:\text{H}_2\text{O}_2$ 3:1) and then copiously rinsed with water and dried with a stream of nitrogen. Caution: Piranha solution is a very strong oxidant and reacts violently with many organic materials.

1-Propylamine monolayer: silicon oxide substrates were immersed in a 2.5% solution of aminopropyltriethoxysilane in dry toluene for 2.5 h, under argon. For the preparation in the device the same solution was flowed through the microchannel at 0.1 μ L/ min. Silicon oxide substrates and microchannel were subsequently rinsed with dried toluene and ethanol. Subsequently, they were dried with a stream of nitrogen.

TBD monolayer: silicon oxide substrates were immersed in a 2.5% solution of (3-glycidylpropoxy)trimethoxysilane in dry toluene for 48 h, under argon. For the

preparation in the device the same solution was flowed through the microchannel at 0.1 $\mu\text{L}/\text{min}$. Silicon oxide substrates and microchannel were subsequently rinsed with dried toluene and ethanol. Subsequently, they were dried with a stream of nitrogen. Afterwards the substrates were immersed in a 0.1 M solution of TBD in ethanol. For the preparation in the device the same solution was flowed through the microchannel at 0.1 $\mu\text{L}/\text{min}$, at 60 $^{\circ}\text{C}$, over night. Silicon oxide substrates and microchannel were subsequently rinsed with ethanol and dried with a stream of nitrogen.

PAMAM G2 SAMs: Silicon substrates having epoxide SAMs were immersed in a 0.1 M solution of PAMAM G2 in methanol, at 60 $^{\circ}\text{C}$ over night. For the preparation in the device the same solution was flowed through the microchannel, bearing previously immobilized epoxide layer, at 0.1 $\mu\text{L}/\text{min}$, at 60 $^{\circ}\text{C}$ over night. Silicon oxide substrates and microchannel were subsequently rinsed with ethanol and dried with a stream of nitrogen.

Kinetic Study. The Knoevenagel condensation reaction of benzaldehyde (**1**) (50 μM) and malononitrile (**2**) (0.05 M) was performed in acetonitrile at 65 $^{\circ}\text{C}$. The molar absorptivity of 2-benzylidene malononitrile (**3**) is $\epsilon_{305} = 20630 \text{ M}^{-1} \text{ cm}^{-1}$.

The k values were calculated, using the initial rate method, by fitting the experimental data with the following equation: $[\mathbf{3}] = k \cdot t$. The experimental error in these measurements is $\pm 10\%$.

References

- [1] B. Ahmed-Omer, J. C. Brandt, T. Wirth, *Org. Biomol. Chem.* **2007**, *5*, 733.
- [2] M. Brivio, W. Verboom, D. N. Reinhoudt, *Lab Chip* **2006**, *6*, 329.
- [3] K. Jahnisch, V. Hessel, H. Lowe, M. Baerns, *Angew. Chem. Int. Ed.* **2004**, *43*, 406.
- [4] J. Kobayashi, Y. Mori, K. Okamoto, R. Akiyama, M. Ueno, T. Kitamori, S. Kobayashi, *Science* **2004**, *304*, 1305.
- [5] J. Kobayashi, Y. Mori, S. Kobayashi, *Chem. Asian. J.* **2006**, *1*, 22.

- [6] P. Watts, C. Wiles, *Org. Biomol. Chem.* **2007**, *5*, 727.
- [7] P. Watts, C. Wiles, *Chem. Commun.* **2007**, 443.
- [8] T. Jackson, J. H. Clark, D. J. Macquarrie, J. H. Brophy, *Green Chem.* **2004**, *6*, 193.
- [9] Y. V. S. Rao, D. E. De Vos, P. A. Jacobs, *Angew. Chem. Int. Ed. Engl.* **1997**, *36*, 2661.
- [10] P. Mela, S. Onclin, M. H. Goedbloed, S. Levi, M. F. Garcia-Parajo, N. F. van Hulst, B. J. Ravoo, D. N. Reinhoudt, A. van den Berg, *Lab Chip* **2005**, *5*, 163.
- [11] S. R. Wasserman, Y. T. Tao, G. M. Whitesides, *Langmuir* **1989**, *5*, 1074.
- [12] M. Wanunu, S. Livne, A. Vaskevich, I. Rubinstein, *Langmuir* **2006**, *22*, 2130.
- [13] D. Brunel, *Micropor. Mesopor. Mat.* **1999**, *27*, 329.

CHAPTER 4

Nanostructure Based on Polymer Brushes for Heterogeneous Catalysis in Microreactors

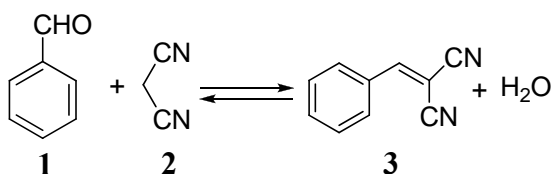
In this chapter, polyglycidylmethacrylate (PGMA) polymer brushes are applied to form a polymeric nanostructure, as a new method for the covalent immobilization of an organic catalyst, 1,5,7-triazabicyclo[4.4.0]dec-5-ene (TBD), to the inner wall of silicon-glass microreactors. The Knoevenagel condensation reaction of benzaldehyde (**1**) with malononitrile (**2**) was chosen as a model reaction to study the performance of these catalytic devices. The nanostructure turned out to be very efficient in the catalysis. In addition, the amount of catalyst could be tuned varying the thickness of the polymer brush nanostructure.

Parts of this Chapter have been published: F. Costantini, W.P. Bula, R. Salvio, J. Huskens, H.J.G.E. Gardeniers, D.N. Reinhoudt, W. Verboom *J. Am. Chem. Soc.* **2009**, *131*, 1650-1651.

4.1 Introduction

In chapter 3 it was shown that self assembled monolayers (SAMs) can be used to anchor organic catalysts on the interior of microreactors to perform heterogeneous catalysis. However, the reaction conversion was low. While SAMs afford a high degree of molecular control over surface composition and architecture, they can only provide a limited density of functional groups on a substrate. To overcome this problem, several research groups developed grafting chemistry to attach polymeric films to surfaces and increase the areal density of the functional groups^[1]. Polymer brushes obtained by atom transfer radical polymerization (ATRP)^[2] is a “living” polymerization technique which allows to have a dense functional film directly grown from a surface by grafting end-functionalized polymer chains onto a SAMs coated substrate. The living controlled/character of ATRP process results in polymers with relatively low polydispersity and permits a better control over the polymer thickness. In this Chapter it is displayed that using polyglycidylmethacrylate (PGMA) polymer brushes it is possible to increase the number of catalytic sites forming a polymeric nanostructure to covalently attach an organic catalyst to the inner wall of a silicon-glass microreactor. PGMA brushes^[3] contain a large number of epoxy groups that can be used for linkage of an organic catalyst via nucleophilic attack. By varying the polymerization time and consequently the nanostructure thickness, the amount of catalyst can be easily tuned. PGMA polymer brushes do not swell in water^[4] protecting the silane layer from hydrolysis, as a result the catalytic nanostructure would display longer stability. Herein, 1,5,7-triazabicyclo[4.4.0]dec-5-ene (TBD)^[5] was attached to the PGMA polymer brushes. The Knoevenagel condensation reaction between benzaldehyde (**1**) and

malononitrile (2) to give 2-benzylidene malononitrile (3) (Scheme 4.1) was chosen as a model reaction to study the performance of these catalytic devices.

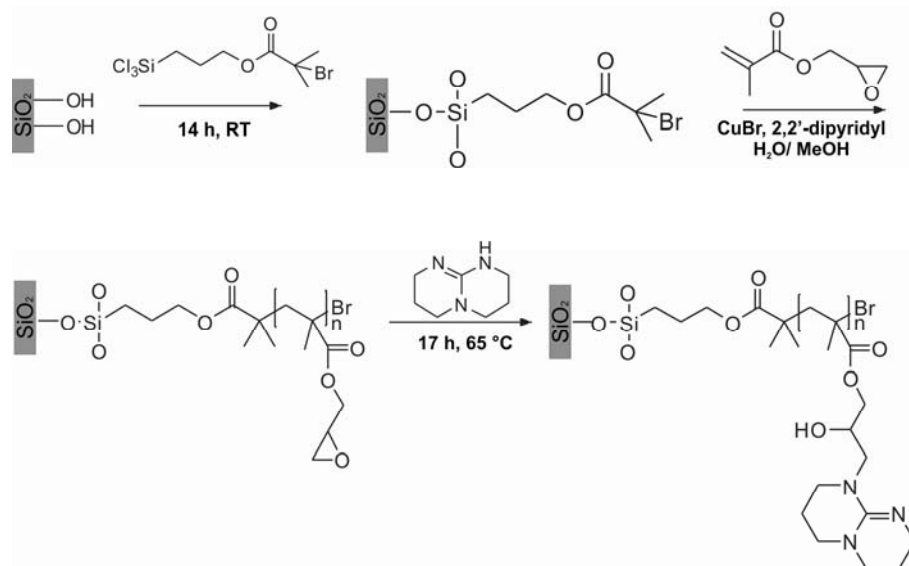


Scheme 4.1. Knoevenagel condensation reaction between benzaldehyde (1) and malononitrile (2) in acetonitrile at 65 °C.

4.2 Results and Discussion

4.2.1 Synthesis of Polyglycidylmethacrylate Polymer Brushes and TBD Immobilization on Flat Substrates

The fabrication of the catalytic nanostructure based on polymer brushes was first studied on a flat silicon oxide surface. PGMA polymer brushes^[3] were synthesized according to the procedure summarized in Scheme 4.2. Subsequently, the polymer coated surfaces were reacted in a 0.1 M solution of TBD in ethanol at 65 °C for 17 h (Scheme 2). Upon reaction of the oxirane groups of the polymer with TBD, the thickness of the layer increased from 180 nm (obtained after 2 h of polymerization) to about 230 nm as measured by ellipsometry and atomic force microscopy (AFM) (Figure 4.1) This thickness increase suggests that the reaction between the oxirane groups and the TBD occurred.



Scheme 4.2. General scheme for initiator immobilization, surface-initiated polymerization of GMA, and reaction with TBD.

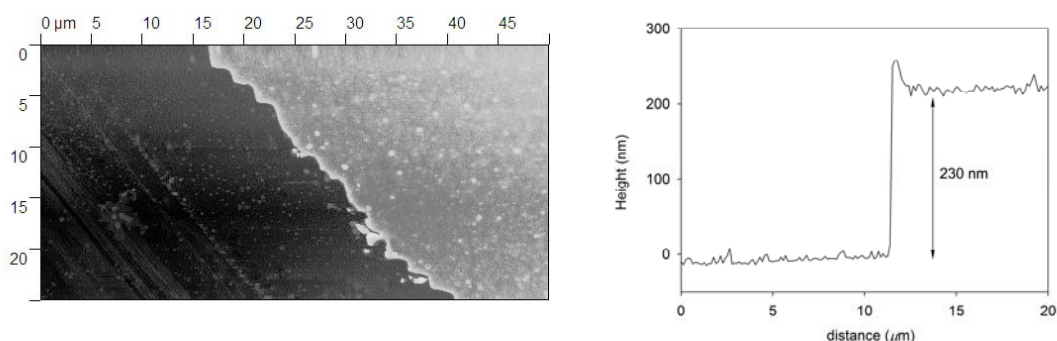


Figure 4.1. AFM image of the catalytic nanostructure on a silicon oxidized surface.

Analysis of the surfaces by transmission FTIR spectroscopy, before and after the reaction with TBD, showed the complete disappearance of the epoxide stretching band at 910 cm^{-1} indicating that all oxirane units reacted with TBD (Figure 4.2). Furthermore, the intensity of the C-H stretching at 2857 cm^{-1} increases, due to the presence of more C-H bonds as result of the presence of TBD, and the absorptions of the O-H stretching at 3400 cm^{-1} and the guanidine stretching at 1592 cm^{-1} appear.

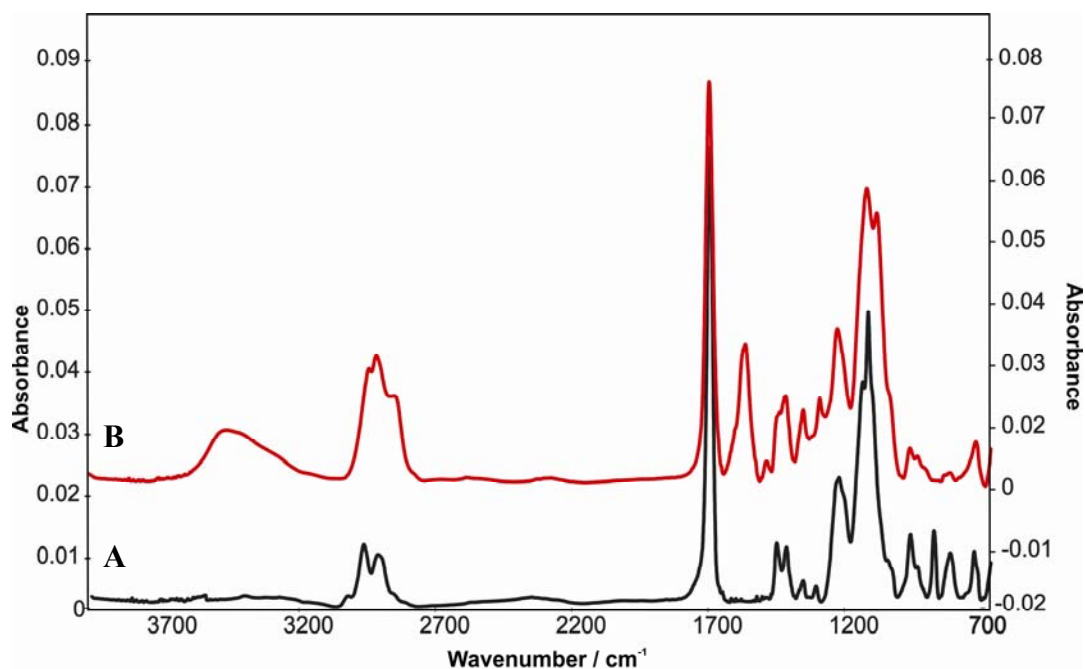


Figure 4.2. Transmission FT-IR spectra of PGMA brushes before (A) and after (B) TBD immobilization.

4.2.2 Synthesis of Polyglycidylmethacrylate Polymer Brushes and TBD Immobilization on Microreactor Channel Wall

The inner walls of several microreactors (Figure 4.3), were coated with PGMA polymer brushes by filling the channel with a solution of glycidyl methacrylate (GMA) monomer in MeOH:H₂O 4:1 in the presence of CuBr and 2-2'-bipyridyl and leaving the solution inside for 20-120 min.

To obtain different polymer thicknesses and consequently different numbers of catalytic units, we varied the reaction time. Afterward, a 0.1 M solution of TBD in EtOH was flowed through the channel at 65 °C for 17 h.

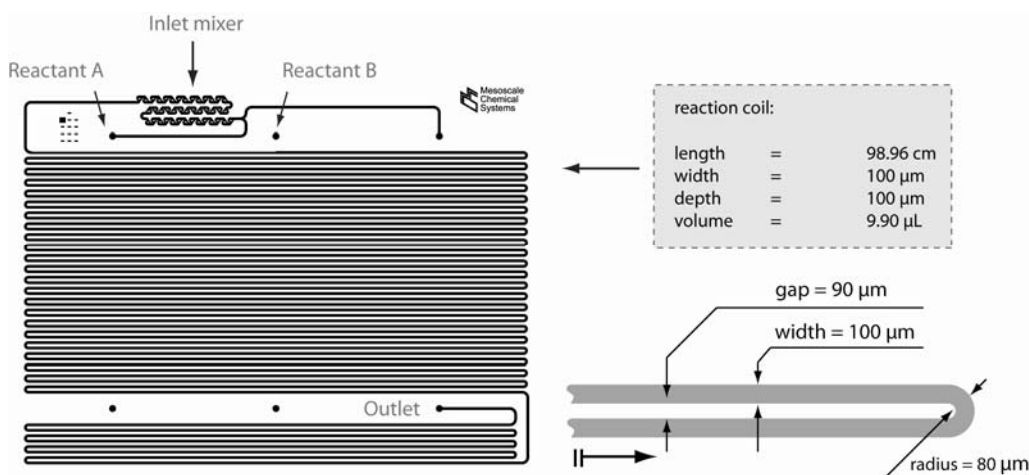


Figure 4.3. Schematic representation of silicon-glass microreactor.

The Knoevenagel condensation reaction between **1** and **2** in acetonitrile was carried out in these catalytic microreactors at 65 °C, in continuous flow. The formation of the condensation product **3** was monitored in real time by in-line UV-vis detection described in chapter 3. The reaction times were varied by changing the flow rates from 20 to 0.2 $\mu\text{L}/\text{min}$.

4.2.3 Kinetic Study of the Knoevenagel Condensation Reaction Performed in the Catalytic Microreactor

To perform a kinetic analysis of the Knoevenagel condensation reaction, an excess of malononitrile **2** was used to achieve pseudo-first-order conditions. The polymeric coating turned out to be highly effective in the catalysis. In all experiments carried out in the presence of the catalytic coating the reaction was complete in a few minutes. No reaction was observed when the reagents were flowed into a microreactor coated with unmodified PGMA brushes for 2 h. This proved that TBD is the catalytically active species.

The experimental data were fitted to a first-order rate equation. Measurements at different concentrations of **1** were carried out in a microreactor with a layer thickness of 150 nm, keeping constant the concentration of **2** (Figure 4.4); hourly output at 75 μM of **1** is 1.2

mM of **3**. The values of the rate constants at different benzaldehyde **1** concentrations were the same, within experimental error. The value of the pseudo-first-order rate constant is $(1.3 \pm 0.1) \times 10^{-2} \text{ s}^{-1}$ ($[\mathbf{2}] = 125 \text{ mM}$).

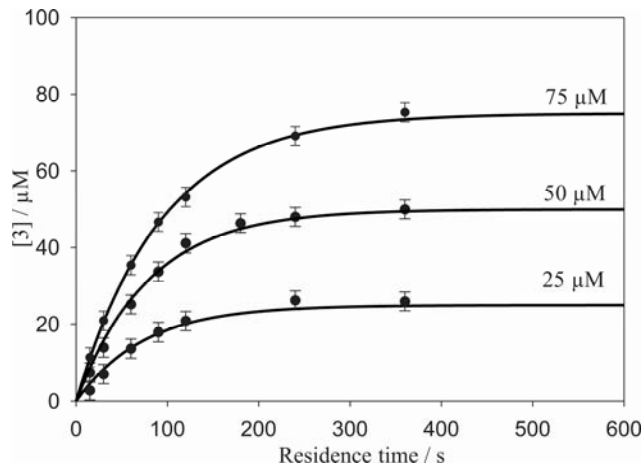


Figure 4.4. Formation of **3** catalyzed by the polymeric coating (150 nm) in the microreactor at different concentrations of **1** ($[\mathbf{2}] = 125 \text{ mM}$, $65 \text{ }^\circ\text{C}$).

Also the malonitrile **2** concentrations were varied in the range 31-125 mM. The rate constants are proportional to the concentration of **2**, as expected for a pseudo-first-order reaction (Figure 4.5). The second-order rate constant is $0.10 \pm 0.01 \text{ s}^{-1} \text{ M}^{-1}$.

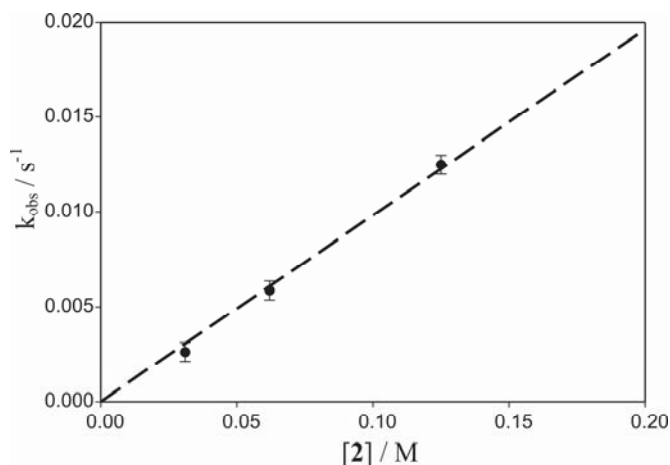


Figure 4.5. Pseudo-first-order rate constants for the formation of **3** vs the concentration of malonitrile (**2**); $k_2 = 9.8 \cdot 10^{-2} \text{ M}^{-1} \text{ s}^{-1}$.

After each experiment the catalytic nanostructure was regenerated by flushing a 0.1 M solution of triethylamine^[6] through the microchannel in order to avoid diminished catalyst activity due to its possible protonation. The PGMA-TBD coated devices showed no decreasing of the catalytic activity or leaching after being used for 25 times. With the catalytic device, stored under nitrogen, the results of the experiments were reproducible also when repeated, after 30 days.

Experiments carried out with microreactors bearing coatings with different thicknesses showed a relation with the catalytic activity. The thicknesses (θ) of the polymeric coatings were measured by high resolution scanning electron microscopy (HR-SEM). These analyses were carried out on the channel cross section after breaking the device (Figure 4.6).

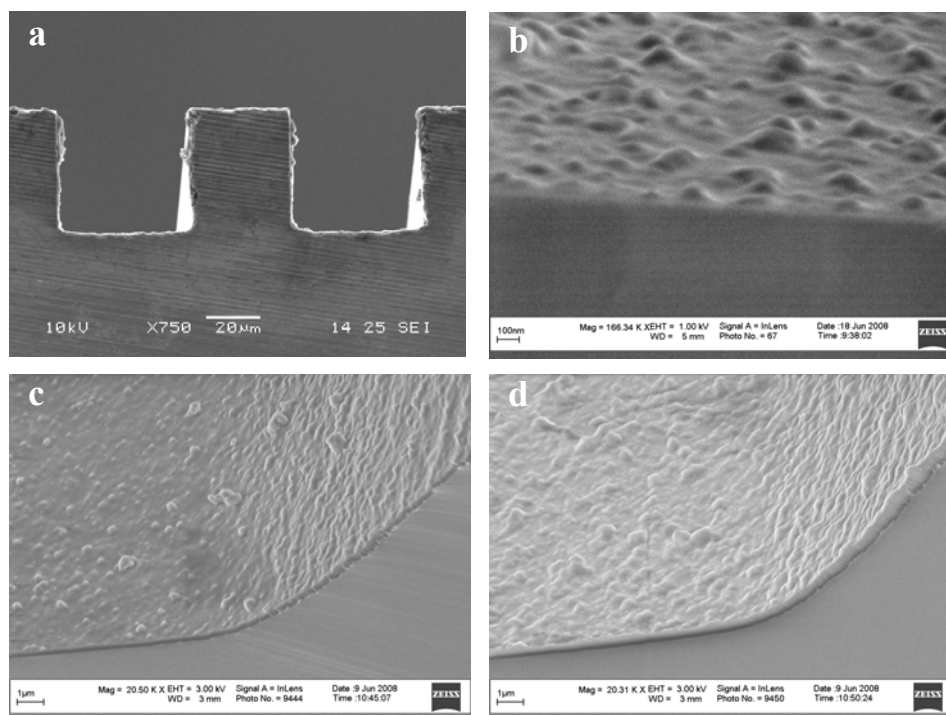


Figure 4.6. (a) HR-SEM picture of the channel cross section before polymer immobilization. The channel surface shows some roughness as a consequence of the etching procedure. Channel cross-section of a device bearing TBD-PGMA polymer brushes formed with a polymerization time of 20 min (b), 60 min (c), and 120 min (d).

A linear dependence was found between θ and the pseudo-first-order rate constant k_{obs} (Figure 4.7). For PGMA-TBD thicknesses of 50 and 400 nm, the k_{obs} values are $(6.9 \pm 0.7) \times 10^{-3}$ and $(3.7 \pm 0.4) \times 10^{-2} \text{ s}^{-1}$, respectively ($[\mathbf{2}] = 125 \text{ mM}$; $[\mathbf{1}] = 50 \mu\text{M}$).

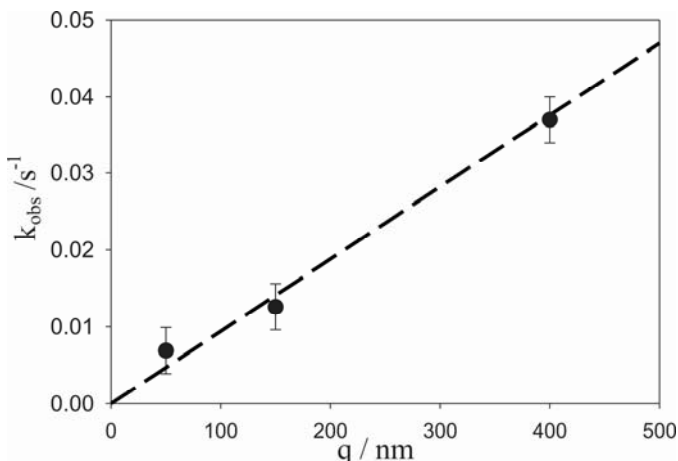


Figure 4.7. Rate constants for reaction of **1** with **2** in microreactors with different polymer coating thicknesses.

On the basis of this result, we conclude that the whole nanostructure is involved in the catalysis and that reaction does not occur only at the interface, but the reagents diffuse throughout the coating to reach all catalytic units. This also proves the complete swelling of the PGMA polymer brushes in acetonitrile. Other solvents have not been studied here, since the rate of the Knoevenagel condensation reaction is solvent dependent^[7]. Although batch reactions appeared to be faster in DMF and EtOH, acetonitrile constitutes a good compromise as PGMA brushes are known to swell in this solvent.^[4] In addition, changing the solvent will also influence the swelling of the PGMA polymer brushes, resulting in less accessible catalytic sites. This makes a comparison of the effect of different solvents very complicated.

To estimate the number of TBD units in the polymer, we applied Gisin's acid-base titration procedure.^[7] The amount of catalyst is 2, 4, and 9 μg of TBD for the devices with thicknesses of 50, 150, and 400 nm, respectively.

4.3 Conclusions

In conclusion, we have reported the fabrication and application of a catalytic nanostructure based on polymer brushes as support for the catalytic coating of the inner wall of microreactors. The second-order rate constant of $0.30 \pm 0.03 \text{ s}^{-1} \text{ M}^{-1}$, calculated for the device having a layer of 400 nm PGMA-TBD, shows that the reaction proceeds up to 150 times faster than in the case of a monolayer coating of TBD. This has to be attributed to the higher number of catalytic groups that can be anchored due to the intrinsic characteristic of polymer brushes. In addition, the hydrophobicity of PGMA ensures a longer stability of the catalytic structure. We have also shown that the amount of catalyst can be tuned by variation of the polymerization times. An advantage of PGMA polymer brushes is the versatility offered by the oxirane groups for the anchoring of a variety of catalysts via a nucleophilic substitution reaction.

4.4 Experimental

Materials and Equipment. All commercial reagents were purchased from Aldrich Chemicals. Benzaldehyde was distilled under vacuum before use. The other chemicals were used without further purification. 3-(Trichlorosilyl)propyl 2-bromo-2-methylpropanoate was synthesized following a reported procedure.^[8] CuBr (99.999%) was stored in a vacuum desiccator. Methanol, ethanol, dichloromethane, acetone (VWR, analytical reagent grade), and acetonitrile (analytical reagent grade, Acros), were used without further purification. Toluene (VWR, analytical reagent grade) was distilled over sodium. Water was purified with the Milli-Q plus (MILLIPORE, R=18.2 M Ω ·cm) ultra pure water system.

Ellipsometry. See Chapter 3.

Atomic Force Microscope (AFM). Samples were measured using an atomic force microscope (AFM) Nanoscope III (Veeco digital instrument, USA) in tapping mode, equipped with a Si₃N₄ tip with a J scanner at a scan rate of 0.6 Hz.

FT-IR. FT-IR spectra were recorded using a BioRad FTS-60A spectrometer. Spectra of brushes were taken in transmission mode using a bare silicon wafer as background.

Scanning Electron Microscopy (HR-SEM). Polymer brushes in microreactors were analyzed by HR-SEM. All HR-SEM images were taken with a HR-LEO 1550 FEF SEM.

UV-vis Spectrophotometer. The UV measurements for Gisin's acid-base titration were performed with a standard Varian Cary 300 spectrophotometer.

Microreactor Fabrication. The silicon-glass microreactor was fabricated by a standard microfabrication process.^[9] The channels were formed in 4 inch (100) silicon wafers by deep reactive ion etching (BOSCH-type process) using a mask of photoresist. Inlet holes were fabricated using powder-blasting. The silicon wafer was anodically bonded to Pyrex glass ($T = 400\text{ }^{\circ}\text{C}$, $U_{\text{max}} = 1000\text{ V}$, $t = 20\text{ min}$) and the silicon-glass stack was diced into separate chips. The use of only (oxidized) silicon and glass makes the chip compatible with a wide range of organic solvents and reaction temperatures. Channel dimensions are $100\text{ }\mu\text{m} \times 100\text{ }\mu\text{m}$ (width x depth), length 98.96 cm.

Setup of the Microfluidic Device. The same set-up was used as described in Chapter 3.

On-line UV-vis Detection. The same set-up was used as described in Chapter 3.

Synthesis of the Catalytic Polymer Coating. Trichlorosilane initiator immobilization and the polymer brushes synthesis on the silicon oxide surface were carried out following a published procedure.^[3] Microchannels and silicon wafers were first cleaned with a Piranha solution (H₂SO₄:H₂O₂ 3:1) and then copiously rinsed with water and dried with a

stream of nitrogen. Caution: Piranha solution is a very strong oxidant and reacts violently with many organic materials. The cleaned silicon wafers were soaked in a solution of 20 μL of 3-(trichlorosilyl)propyl 2-bromo-2-methylpropanoate in dry toluene (10 mL) for 14 h under argon. For the synthesis in the device the same solution was flowed for 14 h at a flow rate of 0.1 $\mu\text{L}/\text{min}$. Silicon wafers and microchannel were rinsed with dry toluene, ethanol, and acetone and dried with a stream of nitrogen. A solution of glycidyl methacrylate (5 mL, 5.21 g, 36.7 mmol) in methanol (4 mL) and water (1 mL) was degassed using the freeze-pump-thaw method (the solution in a sealed Schlenk vessel is frozen by immersion in liquid nitrogen. When the solvent is completely frozen the flask is kept under high vacuum for 5 min, with the flask still immersed in the liquid nitrogen. The flask is then closed and warmed until the solvent has completely melted. This process is repeated 3 times and after the last cycle the flask is filled with argon). CuBr (36.4 mg, 0.368 mmol) and 2,2'-bipyridyl (141 mg, 0.904 mmol) were added to this solution. To dissolve all solid material, the mixture was stirred for 5 min under continuous argon bubbling. Afterwards an initiator coated silicon wafer was placed in a Schlenk tube and the flask sealed with a septum. The tube was filled with argon and the monomer solution syringed inside. For the polymerization in the device the same solution was syringed through the microchannel till the device was completely filled. The solution was kept in contact with the silicon wafer and with the microchannel for 20-120 min. After the polymerization, the silicon wafer and the microchannel were rinsed with methanol, water, and dichloromethane and dried with a stream of nitrogen. In the next step the silicon wafers were soaked in a 0.1 M solution of 1,5,7-triazabicyclo[4.4.0]dec-5-ene (TBD) in ethanol at 65 °C. The same solution was flowed at a flow rate of 0.1 $\mu\text{L}/\text{min}$ through the microreactor. After 17 h they were rinsed with ethanol and dried with

a stream of nitrogen. The microreactor was also rinsed extensively with acetonitrile at 65 °C before use, to make sure the complete removal of the ethanol that can interfere in the kinetic study.

Kinetic Study. The Knoevenagel condensation reaction of benzaldehyde (**1**) (25-75 μM) and malononitrile (**2**) (0.0312-0.125 M) was performed in acetonitrile at 65 °C. The molar absorptivity of 2-benzylidene malononitrile (**3**) is $\epsilon_{305} = 20630 \text{ M}^{-1} \text{ cm}^{-1}$.

The k_{obs} values were calculated by fitting (least-squares method) the experimental data with the following equation: $[\mathbf{3}] = [\mathbf{1}]_0 * (1 - \exp(-k_{obs} * t))$. The experimental error in these measurements is $\pm 10\%$.

Titration with Picric Acid. The number of catalytic sites was estimated using Gisin's acid-base titration procedure^[9]. The microreactor channel was rinsed for 6 min with a solution of 5% diisopropylethylamine in dichloromethane and washed with dichloromethane for 6 min. Then a 0.1 M solution of picric acid in dichloromethane was flowed for 6 min and afterwards the microreactor was washed with dichloromethane for 10 min. The picric acid was eluted with a solution of 5% diisopropylethylamine in dichloromethane and collected in a volumetric flask. The solution was analyzed spectrophotometrically ($\epsilon_{355} = 26000 \text{ M}^{-1} \text{ cm}^{-1}$).

References

- [1] S. Edmondson, V. L. Osborne, W. T. S. Huck, *Chem. Soc. Rev.* **2004**, *33*, 14.
- [2] W. Huang, J. B. Kim, M. L. Bruening, G. L. Baker, *Macromolecules* **2002**, *35*, 1175.
- [3] S. Edmondson, W. T. S. Huck, *J. Mater. Chem.* **2004**, *14*, 730.
- [4] T. Fukuda, N. Kohara, Y. Onogi, H. Inagaki, *J. Appl. Poly. Sci.* **1991**, *43*, 2201.
- [5] Y. V. S. Rao, D. E. De Vos, P. A. Jacobs, *Angew. Chem. Int. Ed. Engl.* **1997**, *36*, 2661.
- [6] A. R. Bogdan, B. P. Mason, K. T. Sylvester, D. T. McQuade, *Angew. Chem. Int. Ed.* **2007**, *46*, 1698.
- [7] A. Corma, S. Iborra, I. Rodriguez, F. Sanchez, *J. Catal.* **2002**, *211*, 208.
- [8] B. F. Gisin, *Anal. Chim. Acta* **1972**, *58*, 248.
- [9] M. Husseman, E. E. Malmstrom, M. McNamara, M. Mate, D. Mecerreyes, D. G. Benoit, J. L. Hedrick, P. Mansky, E. Huang, T. P. Russell, C. J. Hawker, *Macromolecules* **1999**, *32*, 1424.
- [10] W. P. Bula, W. Verboom, D. N. Reinhoudt, H. J. G. E. Gardeniers, *Lab Chip* **2007**, *7*, 1717.

CHAPTER 5

Heterogeneous Catalysis in Glass Microreactors Coated with a Brush-Gel Silver Nanoparticles Hybrid Film

A polymer brush based material was applied for the formation and in-situ immobilization of silver nanoparticles, as catalytic coating on the inner wall of a glass microreactor. The brush film was grown directly on the microchannel interior via ATRP, which allows control over the polymer film thickness and therefore permits to tune the number of nanoparticles formed on the channel walls. After introducing carboxylic acid groups by reacting the poly(hydroxyethylmethacrylate) (PHEMA) with succinic anhydride, silver nitrate was used to form carboxylate-silver complexes. The particles were formed by reduction with sodium borohydride. The applicability of the catalytic system was demonstrated using the reduction of 4-nitrophenol (**1**) to give 4-aminophenol (**2**) as a model reaction.

5.1 Introduction

Recently, much attention has been focused on metal nanoparticles as gold, silver, platinum, and palladium because their properties may differ from those of the respective bulk metals. As noble metals are reduced in size to tens of nanometers, a new very strong absorption is observed resulting from the collective oscillation of the electrons in the conduction band from one surface of the particle to the other. This oscillation has a frequency that absorbs the visible light. This is called the surface plasmon absorption. This strong absorption, giving rise to a vivid characteristic color, has been observed and used, but not understood, since the 17th century. The gold particles, giving rise to a brilliant rose color, have been used throughout Europe in stained glass windows of cathedrals and by the Chinese in coloring vases and other ornaments^[1].

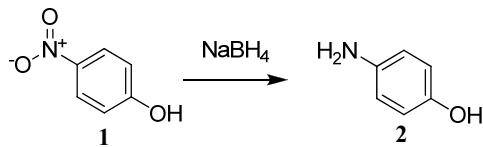
Self-assembly of these nanoparticles by different techniques, either from the bottom-up techniques (assembling particles synthesized in solution) or from the top-down techniques (different lithographic methods), is being explored. Although many future applications will make use of the properties of the individual nanoparticles (sensors, medical diagnostics, etc.), there are other important applications that would require self-assembled nanoparticles, as nanoelectronics, optoelectronics, photonics, and heterogeneous catalysis^[2].

Due to the nanometer size, metal nanoparticles are characterized by a high surface-to-volume ratio, which make them particular attractive in the field of heterogeneous catalysis. However, being so small could make the surface of metal nanoparticles unstable due to the high surface energy and the large surface curvature, as a consequence the immobilization of metal nanoparticles in a solid matrix has raised a lot of interest in fabricating practical heterogeneous catalysts^[3, 4]. The reduction of metal ions in the

presence of a stabilizer like polymers^[5], dendrimers^[3], microgels^[6], surfactants^[7], and colloids^[8], which prevents the nanoparticles aggregation and serves as carrier has been described. The incorporation of catalytic metal nanoparticles in a microreactor offers the possibility to join the intrinsic advantages of the two systems to perform heterogeneous catalysis. Literature shows different methodologies for the implementation of metal nanoparticles in microreactors and among all, their immobilization on the inner wall of microreactors gives several benefits (see Chapter 2). Examples have been reported by Kobayashi^[9, 10] *et al.* mainly using encapsulated palladium and gold nanoparticles, and by Rebrov^[11, 12] *et al.*, using mesoporous materials. In both methods, the metal nanoparticles are prepared in batch and subsequently flowed through a microreactor to form a catalytic film on the channel wall. The main disadvantage in these approaches is the probability to clog the microchannel^[13], due to its small dimensions, while introducing the nanoparticles.

To our best knowledge, in this type of systems varying the number of metal nanoparticles to study the effect on a catalytic reaction has not been studied.

Herein we describe a brush-gel polymer film, grown on the inner wall of a glass microreactor, for in-situ formation and immobilization of silver nanoparticles. To investigate the coated microreactor performance, the reduction of 4-nitrophenol (**1**) to give 4-aminophenol^[3] (**2**) was carried out as model reaction (Scheme 5.1). In addition, it is demonstrated that changing the polymerization time, and therefore the polymer thickness, the number of silver nanoparticles formed within the polymer film can be tuned, influencing the reaction rate.



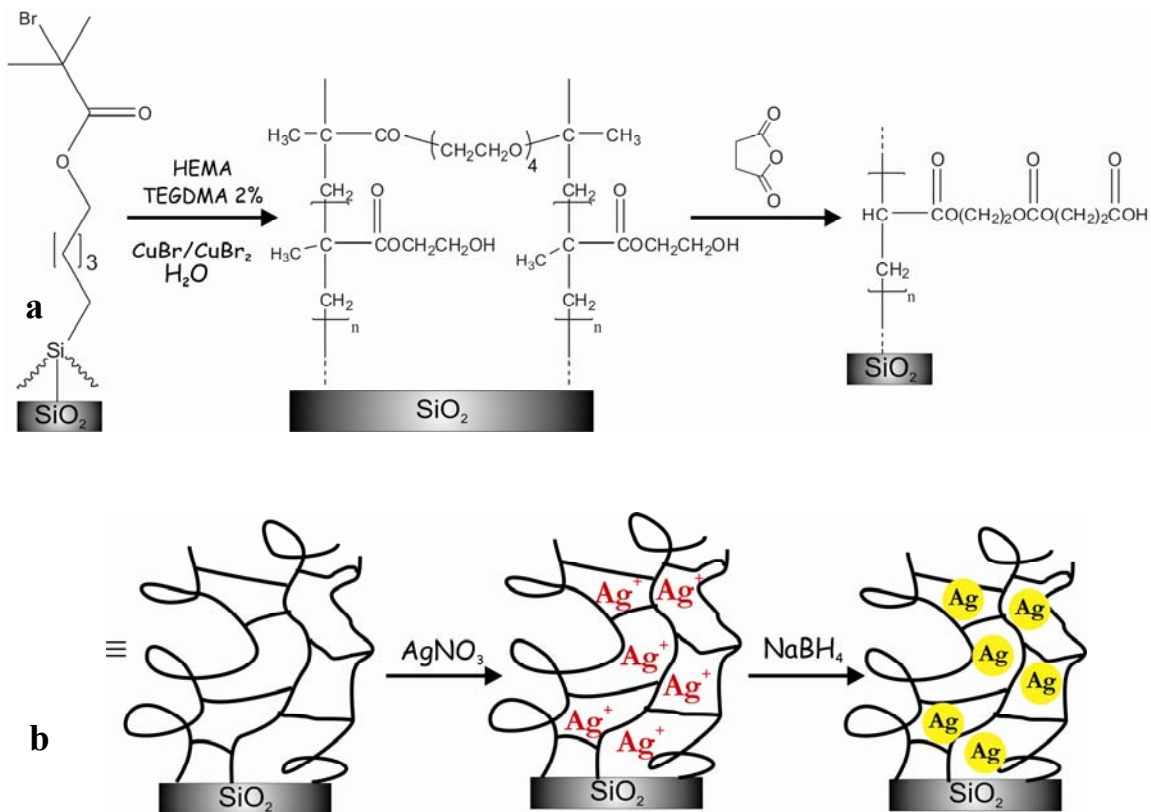
Scheme 5.1. Reduction of 4-nitrophenol (**1**) to 4-aminophenol (**2**) in water at room temperature.

5.2 Results and Discussion

5.2.1 Synthesis of the Hydrogel-Silver Nanoparticles Hybrid Nanostructure on a Flat Surface and its Characterization

First a monolayer of atom transfer polymerization (ATRP) initiator was grown on silicon oxide substrates^[14]. Subsequently, a solution of 2-hydroxyethyl methacrylate (HEMA) with 2% tetraethylene glycol dimethacrylate (TEGDMA) in water in the presence of 2-2'-bipyridyl, CuBr and CuBr₂, was used to grow the brush-gel (PHEMA-PEG) via ATRP (Scheme 2a). After 5 min polymerization time the hydrogel thickness is 31 nm as measured by ellipsometric thickness and confirmed by atomic force microscopy (AFM).

In order to introduce carboxylic groups, the PHEMA-PEG layers were reacted with a 0.1 M solution of succinic anhydride in dry pyridine for 24 h (Scheme 5.2a).



Scheme 5.2. a) Preparation of the brush-gel (PHEMA-PEG) via ATRP and post-functionalization of the PHEMA-brush based layers by reaction with succinic anhydride, b) carboxylate-silver complexes and silver nanoparticles (Ag-NPs) formation.

After reaction with succinic anhydride, an increase of the thickness to 52 nm, measured by AFM and ellipsometric thickness, was observed, suggesting all alcohol groups reacted with succinic anhydride.

Also FT-IR spectroscopy was used to prove the presence of the carboxylic groups inside the brush-gel architecture. As can be seen in Figure 5.1, after the PHEMA-PEG layers reacted with succinic anhydride, the $-OH$ band completely disappears, and a clear signal related to the stretching of COO^- moieties appears at 1580 cm^{-1} [14].

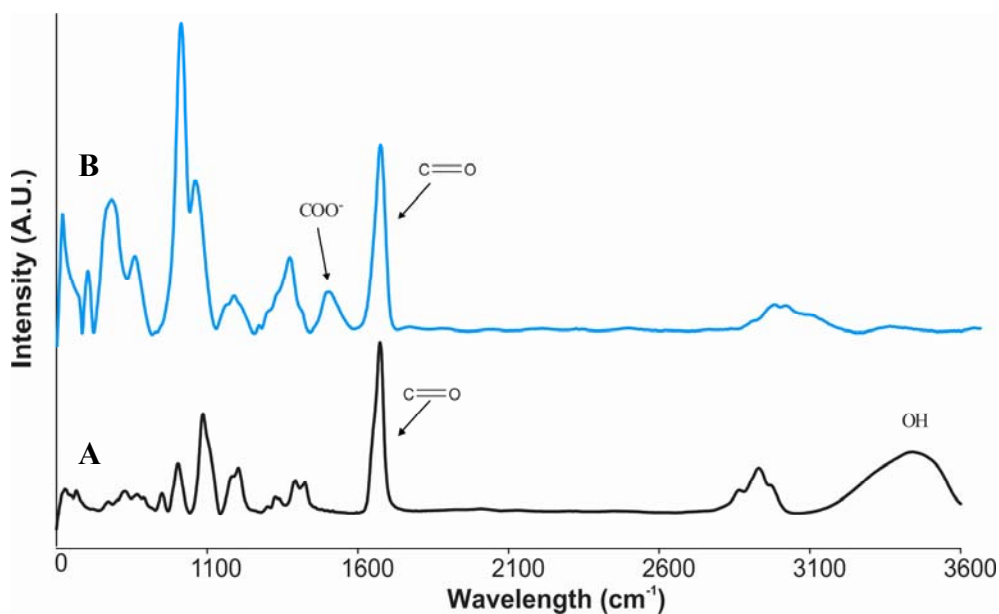


Figure 5.1. Transmission FT-IR spectra of **A)** PHEMA-PEG brush-gel, **B)** brush-gel after reaction with succinic anhydride.

Subsequent incubation of the substrate in a 0.05 M solution of silver nitrate in water, over night, led to the formation of the carboxylate-silver complexes. Then, the material was treated with a 1.3 mM solution of sodium borohydride^[4] (NaBH_4) in water for 10 seconds, to give the silver nanoparticles (Ag-NPs) (Scheme 5.2b). From AFM analysis (Figure 5.2a-b) of the brush-gel silver nanoparticles hybrid layer (brush-NPs), the size distribution of the NPs was calculated and an average diameter of 20 nm was found for Ag-NPs (Figure 5.2).

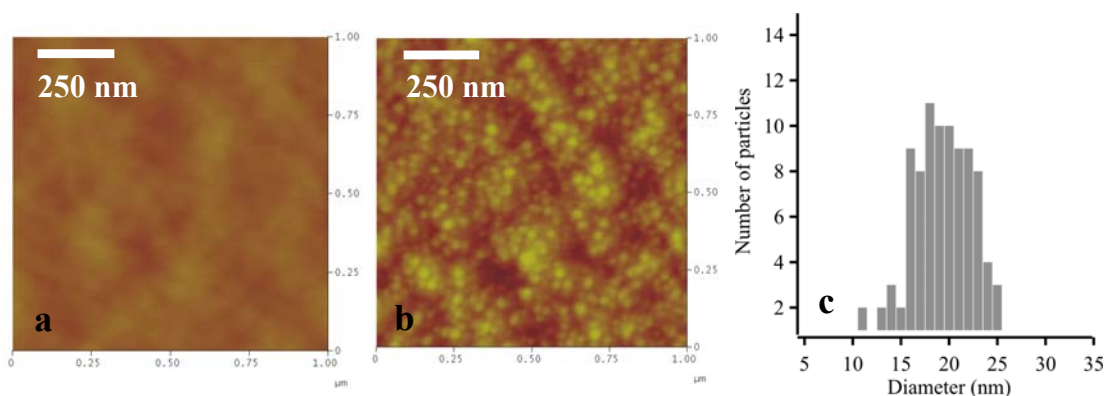


Figure 5.2. **a)** AFM image of hybrid polymer film treated with AgNO_3 . **b)** AFM image of hybrid polymer film after reduction with NaBH_4 . **c)** Silver nanoparticles size distribution.

FT-IR spectra of the brush-gel hybrid material recorded before and after the formation of the Ag-NPs, (Figure 5.3) show that after incubation of the brush-gel with AgNO₃, the stretching signal related to the carboxylate at 1550 cm⁻¹ appears, confirming the formation of the carboxylate/Ag(I) complex. Upon reaction with NaBH₄ this band disappears^[14] due to the re-protonation of the carboxylate groups and the concomitant reduction of the Ag(I) to form Ag-NPs.

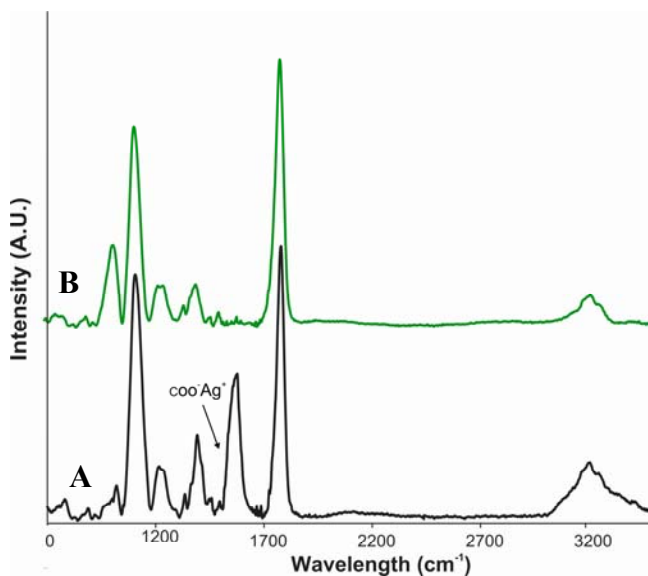


Figure 5.3. Transmission FT-IR spectra of film hybrid layer **A)** after incubation with AgNO₃, **B)** after formation of Ag-NPs.

5.2.2 Synthesis of the Hydrogel-Silver Nanoparticles Hybrid Nanostructure on the Microreactor Interior

The same procedure used for the silicon oxide substrates (Scheme 5.2), was followed to fabricate brush-NPs hybrid layers on the channel interior of glass microreactors (see Chapter 3). The brush-NPs hybrid layer was grown on the microchannel interior in stop flow, varying the polymerization time between 1.5-10 min in order to obtain different polymer layer thicknesses, and consequently a different number of functional groups. PHEMA-PEG was then reacted with a solution of succinic anhydride in continuous flow

(0.1 $\mu\text{L}/\text{min}$). Afterwards an aqueous solution of silver nitrate was flowed through the microchannels over night (0.1 $\mu\text{L}/\text{min}$). Upon salt reduction within the polymer matrix, the microchannel turned yellow indicating the formation of Ag-NPs (Figure 5.4).

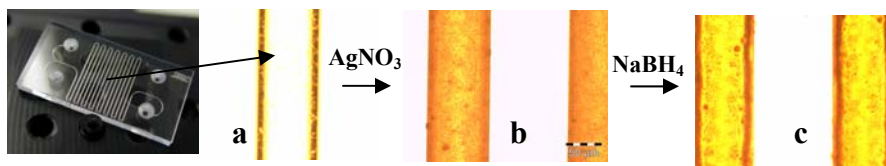


Figure 5.4. Microscope microchannel pictures of microreactor coated with brush-gel **a**) reacted with succinic anhydride, **b**) after incubation in AgNO_3 , and **c**) after reaction with NaBH_4 to form Ag-NPs.

5.2.3 Kinetic Study of the 4-Nitrophenol Reduction Performed in the Microreactor Coated with Brush-gel Silver Nanoparticles

Microreactors, bearing in-situ formed silver nanoparticles, were used for the reduction of 4-nitrophenol^[3] (**1**) to 4-aminophenol (**2**) in the presence of NaBH_4 at room temperature, in water (Scheme 5.1).

The brush-NPs hybrid layer turned out to be very efficient in the catalysis. In all experiments performed in the presence of the catalytic coating, the reaction was complete within a few seconds. No reaction was observed when the reagents were flowed through microreactors only coated with PHEMA-PEG, proving that the silver nanoparticles were the catalytically active species.

The reaction times were varied by changing the flow rates from 20 to 0.1 $\mu\text{L}/\text{min}$ and the formation of the product was monitored measuring the extinction of the solution at 400 nm. A kinetic analysis of the reduction of **1** was carried out using an excess of NaBH_4 . Measurements at different concentrations of **1** ($4\text{-}8 \times 10^{-5}$ M) were carried out in microreactors with a coating of 47 nm obtained after 10 min polymerization time, keeping the excess concentration of NaBH_4 constant (Figure 5.5).

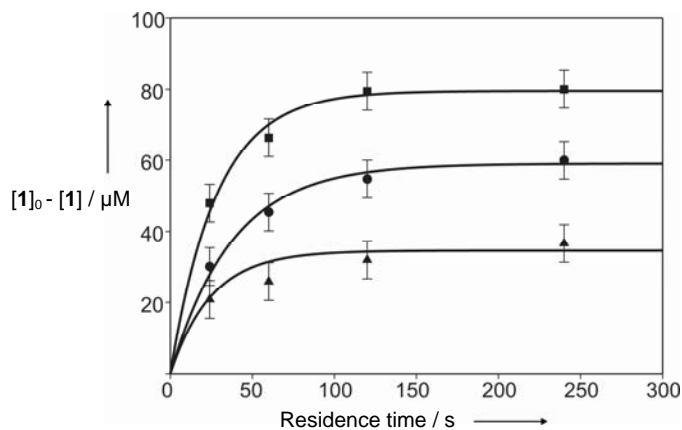


Figure 5.5. Conversion of **1** catalyzed by silver nanoparticles in a microreactor at different initial 4-nitrophenol ($[1]_0$) concentrations: (■) = 8×10^{-5} M, (●) = 6×10^{-5} M, (▲) = 4×10^{-5} M ($[NaBH_4] = 2.5 \times 10^{-3}$ M); hydrogel thickness 47 nm.

The $NaBH_4$ concentration was varied in the range $2.5-5 \times 10^{-3}$ M. The pseudo-first-order rate constants were proportional to the concentration of $NaBH_4$, indicating a first-order dependence of $NaBH_4$. The resulting second-order rate constant is $13 \pm 1 \text{ s}^{-1} \text{ M}^{-1}$.

The thickness of the PHEMA-PEG layers, grown on the microchannel interior, was measured by high resolution scanning electron microscopy (HR-SEM). These analyses were carried out on the microchannel cross section after breaking the device (Figure 5.6a). The thicknesses were 47 nm (Figure 6b) and 100 nm (see Chapter 6) after 10 and 20 min polymerization time, respectively^[15].

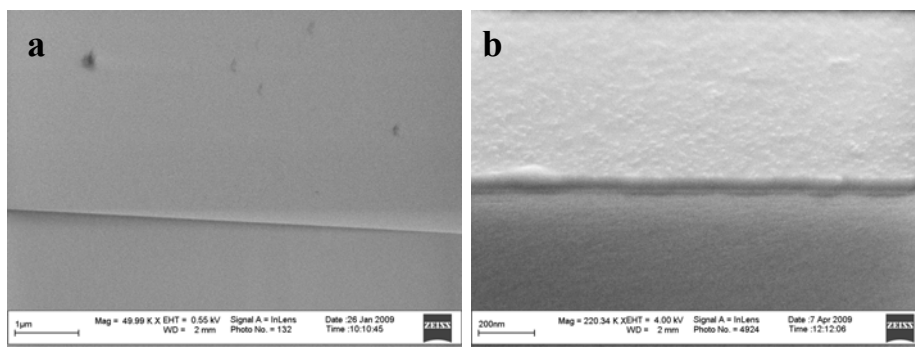


Figure 5.6. HR-SEM **a)** zoom of microchannel cross section without polymer, **b)** zoom microchannel cross section of polymer film with Ag-NPs (10 min polymerization time, thickness 47 nm).

Experiments carried out in microreactors, having different brush-NPs thicknesses showed a correlation with the catalytic activity (Figure 5.7a). A linear dependence was found between the polymerization time and the pseudo-first-order rate constants k_{obs} (Figure 5.7b). This result indicates that, since PHEMA-PEG is completely swollen at pH 9^[14], the pH of the reaction mixture, the entire brush-gel structure is involved in the catalysis, and consequently that the nanoparticles are formed within the whole polymer matrix.

From AFM analysis, the number of Ag nanoparticles formed within the polymer film with a thickness of 47 nm was estimated to be $9.4 \times 10^2 \mu\text{m}^{-2}$. This value was close to the value ($8.0 \times 10^2 \mu\text{m}^{-2}$) estimated assuming full loading of all carboxylate groups by Ag^+ ions and subsequent reduction to Ag particles of 20 nm (see Experimental).

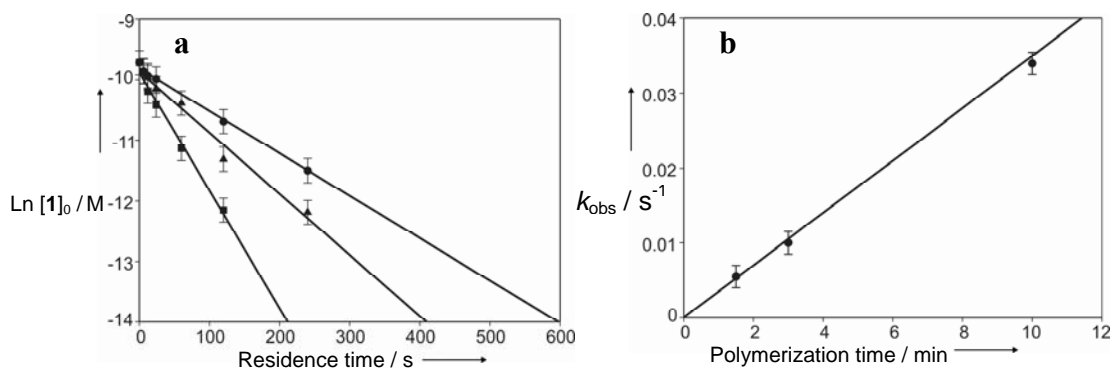


Figure 5.7. (a) Conversion of **1** catalyzed by silver nanoparticles in microreactors coated with polymer layers created with different polymerization times: (■) = 10 min, (▲) = 3.5 min, (●) = 1.5 min, ($[\text{NaBH}_4] = 2.5 \times 10^{-3} \text{ M}$, $[1]_0 = 6 \times 10^{-5} \text{ M}$), (b) Dependence of observed pseudo-first-order rate constant k_{obs} as a function of polymerization time, for the reduction of **p-NP** catalyzed by silver nanoparticles.

The catalytic devices coated with Ag-NPs exhibited no leaching and could be re-used for at least 4 months, without showing a decrease of catalytic activity, when stored under nitrogen.

5.3 Conclusions

In conclusion, we have reported the fabrication of a hydrogel-silver nanoparticles hybrid nanostructure on a microchannel interior, as a novel method for performing heterogeneous catalysis in microreactors. The number of nanoparticles synthesized within the nanostructure can easily be tuned by changing the polymerization time. The Ag-NPs were formed within the complete brush-gel and the whole hybrid brush-gel nanostructure was involved in the catalysis. This procedure for immobilizing Ag-NPs allows having efficient catalysis for 4-nitrophenol reduction and forming a thin film with a large surface area, which is the main issue when the microreactor interior is used to deposit a catalytic layer^[11]. The devices exhibit long term stability.

5.4 Experimental

Materials and Equipment. All commercial reagents were purchased from Aldrich Chemicals. All chemicals were used without purification unless specified. 3-(5'-Trichlorosilylpentyl) 2-bromo-2-methylpropionate was synthesized following a literature procedure^[16]. CuBr (99.999%) was stored in a vacuum desiccator. Methanol and ethanol (VWR, analytical reagent grade) were used without further purification. Toluene (VWR, analytical reagent grade) was distilled over sodium. Pyridine was distilled over calcium hydride prior to use. Water was purified with the Milli-Q plus (MILLIPORE, R=18.2 M Ω :cm) ultra pure water system.

Ellipsometry, Atom Force Microscopy (AFM), FT-IR, Scanning Electron Microscopy (HR-SEM), UV-vis Spectrometer See Chapter 4.

Microreactor Fabrication. See Chapter 3.

Synthesis of the Catalytic Polymer Coating. For the trichlorosilane initiator immobilization see Chapter 4. A solution of 2-hydroxyethyl methacrylate (HEMA) (5 mL, 5.36 g, 41 mmol) with 2% tetraethylene glycol dimethacrylate (TEGDMA) in water (4 mL) was degassed using the freeze-pump-thaw method (see Chapter 4). CuBr (53 mg, 0.37 mmol), CuBr₂ (6 mg, 0.02 mmol) and 2,2'-bipyridyl (0.350 g, 2.24 mmol) were added to this solution. To dissolve all solid materials, the mixture was stirred for 30 min under a continuous flow of argon. Afterwards an initiator coated silicon wafer was placed in a Schlenk tube and the flask sealed with a septum. The tube was filled with argon and the monomer solution syringed inside. For the polymerization in the device the same solution was syringed through the microchannel till the device was completely filled. The solution was kept in contact with the silicon wafer and with the microchannel for 1.5-10 min. After the polymerization, the silicon wafer and the microchannel were rinsed with methanol and water and dried with a stream of nitrogen. In the next step the silicon wafers were soaked in a 0.1 M solution of succinic anhydride for 24 h. The same solution was flowed at a flow rate of 0.1 $\mu\text{L}/\text{min}$ through the microreactor. After 24 h they were rinsed with methanol and water and subsequently dried with a stream of nitrogen.

For the preparation of silver nanoparticles/brush film hybrid layers all the samples were first incubated overnight in a 0.5 M aqueous solution of AgNO₃. The same solutions were flowed at a flow rate of 0.1 $\mu\text{L}/\text{min}$ through the microreactor. Subsequently, the silicon wafer and microchannel were rinsed with milliQ water. Then the material was treated with a 1.3 mM solution of sodium borohydride (NaBH₄) for 10 s for the formation of silver nanoparticles.

Kinetic Study. The reduction of 4-nitrophenol (**1**) ($4\text{-}8 \times 10^{-5}$ M) to 4-aminophenol (**2**) was performed using an excess of NaBH₄ ($2.5\text{-}5 \times 10^{-3}$ M) in water at room temperature.

The formation of the product was followed using UV-Vis detection, measuring the extinction at 400 nm. The molar absorptivity of 4-nitrophenol (**1**) in an aqueous solution at pH = 9, is $\epsilon_{400} = 18200 \text{ cm}^{-1} \text{ M}^{-1}$.

The k_{obs} values were calculated by fitting (least-squares method) the experimental data with the following equation: $[2] = [1]_0(1-\exp(-k_{obs}t))$ or $\ln [1] = -kt + \ln [1]_0$. The experimental error in these measurements is $\pm 10\%$.

Concentration of Silver Nanoparticles in the Microreactor:

Assuming that all carboxylate protons were replaced by silver cations, with the following calculation the number of nanoparticles within the polymer film was determined.

$$\alpha = d_{PHEMA} \times \theta = 4.23 \times 10^{-6} \text{ g cm}^{-2} \quad (1)$$

Where α is the number of grams of polymer per cm^2 , $d_{PHEMA} = 1.5 \text{ g cm}^{-3}$ is the density of PHEMA, and $\theta = 28.2 \text{ nm}$ is the thickness of the polymer after 10 min polymerization time, before reaction with succinic anhydride.

$$\alpha_{mol} = \frac{\alpha}{MW_{(HEMA)}} = 3.25 \times 10^{-8} \text{ mol cm}^{-2} \quad (2)$$

Where α_{mol} is the number of moles of HEMA monomer units per cm^2 and $MW = 130.14 \text{ g mol}^{-1}$ is the molecular weight of HEMA.

$$m = V \times d_{Ag} = 4.39 \times 10^{-17} \text{ g} \quad (3)$$

Where m is the mass of one nanoparticles, $V = 4.19 \times 10^{-18} \text{ cm}^3$ is the volume of one nanoparticle considering it as a sphere, having a diameter of 20 nm, and $d_{Ag} = 10.49 \text{ g cm}^{-3}$ is the density of the silver.

$$M_{mol, Ag} = \frac{m}{AW_{Ag}} = 4.07 \times 10^{-19} \text{ mol} \quad (4)$$

Where $M_{mol, Ag}$ is the number of moles of silver atoms in one nanoparticle, and $AW_{Ag} = 108 \text{ g mol}^{-1}$ is the atomic weight of silver.

$$N = \frac{\alpha_{mol}}{M_{mol, Ag}} = 798 \text{ nanoparticles per } \mu\text{m}^2 \quad (5)$$

Where N is the number of nanoparticles per μm^2 . Multiplying N with the internal area of the microchannel $A_I = 1.08 \times 10^8 \mu\text{m}^2$, the total number of nanoparticles N_T is:

$$N_T = N \times A_I = 8.61 \times 10^{10} \text{ nanoparticles} \quad (6)$$

Dividing N_T by Avogadro number, N_{AV} , and the microchannel volume, V_m , the molar concentration of nanoparticles, N_M , immobilized on the microchannel interior is:

$$N_M = \frac{N_T}{V_m \times N_{AV}} = 8.42 \times 10^{-8} M \quad (7)$$

And the active particle area is:

$$A_{Ag} = N_M \times S_{Ag} \times N_{AV} = 63.68 \text{ m}^2 \text{ L}^{-1} \quad (8)$$

Where $S_{Ag} = 12.56 \times 10^{-16} \text{ m}^2$ is the surface area of one silver nanoparticle.

AFM analysis of the hybrid film showed on average the presence of 400 nanoparticles per μm^2 , considering that the polymer film thickness, after 10 min polymerization time, is 47 nm and that the diameter of one nanoparticle is 20 nm. In the microreactor with an internal area of $A_I = 1.08 \times 10^8 \mu\text{m}^2$ there are 10.15×10^{10} nanoparticles. This value is close to the one obtained in equation (6).

References

- [1] C. Burda, X. Chen, R. Narayanan, M. A. El-Sayed, *Chem. Rev.* **2005**, *105*, 1025.
- [2] J. M. Campelo, D. Luna, R. Luque, J. M. Marinas, A. A. Romero, *ChemSusChem* **2009**, *18*.
- [3] K. Esumi, R. Isono, T. Yoshimura, *Langmuir* **2004**, *20*, 237.
- [4] Y. Mei, Y. Lu, F. Polzer, M. Ballauff, M. Drechsler, *Chem. Mater.* **2007**, *19*, 1062.

- [5] Y. Li, E. Boone, M. A. El-Sayed, *Langmuir* **2002**, *18*, 4921.
- [6] J. Zhang, S. Xu, E. Kumacheva, *J. Am. Chem. Soc.* **2004**, *126*, 7908.
- [7] W. Bonnemann, A. Brijoux, T. Schulze, K. Siepen, *Top. Catal.* **1997**, *4*, 217.
- [8] Z. Liang, A. Susa, F. Caruso, *Chem. Mater.* **2003**, *15*, 3176.
- [9] J. Kobayashi, Y. Mori, K. Okamoto, R. Akiyama, M. Ueno, T. Kitamori, S. Kobayashi, *Science* **2004**, *304*, 1305.
- [10] N. Wang, T. Matsumoto, M. Ueno, H. Miyamura, S. Kobayashi, *Angew. Chem.* **2009**, *4838*; *Angew. Chem. Int. Ed.* **2009**, 4744.
- [11] E. V. Rebrov, A. Berenguer-Murcia, H. E. Skelton, B. F. G. Johnson, A. E. H. Wheatley, J. C. Schouten, *Lab Chip* **2009**, *9*, 503.
- [12] E. V. Rebrov, A.E. Klinger, A. Berenguer-Murcia, E. M. Sulman, J. C. Schouten, *Org. Process Res. Dev.* **2009**, *13*, 991.
- [13] A. R. Bogdan, B. P. Mason, K. T. Sylvester, D. T. McQuade, *Angew. Chem. Int. Ed.* **2007**, *46*, 1698.
- [14] E. M. Benetti, X. F. Sui, S. Zapotoczny, G. J. Vancso, *Submitted*.
- [15] Devices with a brush-gel thickness obtained with a polymerization time < 3.5 min, could not be accurately measured by HR-SEM.
- [16] M. Husseman, E. E. Malmstrom, M. McNamara, M. Mate, D. Mecerreyes, D. G. Benoit, J. L. Hedrick, P. Mansky, E. Huang, T. P. Russell, C. J. Hawker, *Macromolecules* **1999**, *32*, 1424.

CHAPTER 6

Heterogeneous Catalysis in Glass Microreactors Coated with a Brush-Gel Palladium Nanoparticles Hybrid Film

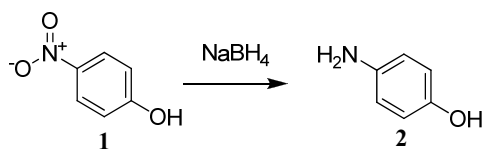
The brush-gel polymer film was used to form and immobilize palladium nanoparticles (Pd-NPs) on the microreactor channel walls. The activity of the catalytic device was tested performing the reduction of 4-nitrophenol (**1**) to give 4-aminophenol (**2**). The catalytic microreactors were also used for carrying out the Heck reaction between ethyl acrylate (**3**) and iodobenzene (**4**) to give *trans*-ethyl cinnamate (**5**) showing the versatility of the brush-gel hybrid material for conducting metal-catalyzed chemical reactions in microreactors.

6.1 Introduction

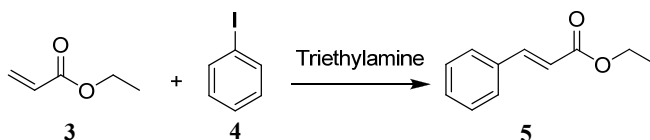
Palladium catalysis is often used in organic synthesis^[1], and its applicability is known for coupling reactions as Heck, Suzuki, Sonogashira, and Stille reactions^[2], but also for hydrogenation reactions.

To demonstrate the wide applicability of the method described in Chapter 5, for the implementation of metal nanoparticles on the inner wall of a microreactor, palladium nanoparticles (Pd-NPs) were selected in this Chapter to be formed within the brush-gel architecture. Palladium nanoparticles have been packed in microchannel/capillary reactors but also anchored as catalytic film on the wall of microreactors as described in Chapter 2^[3-10].

Microreactors coated with Pd-NPs, were first used for 4-nitrophenol (**1**) reduction to give 4-aminophenol^[11] (**2**) (Scheme 6.1), subsequently, they were applied for carrying-out the Heck reaction between ethyl acrylate (**3**) and iodobenzene (**4**) to give *trans*-ethyl cinnamate (**5**) (Scheme 6.2).



Scheme 6.1. Reduction of 4-nitrophenol (**1**) to 4-aminophenol (**2**) in water at room temperature.

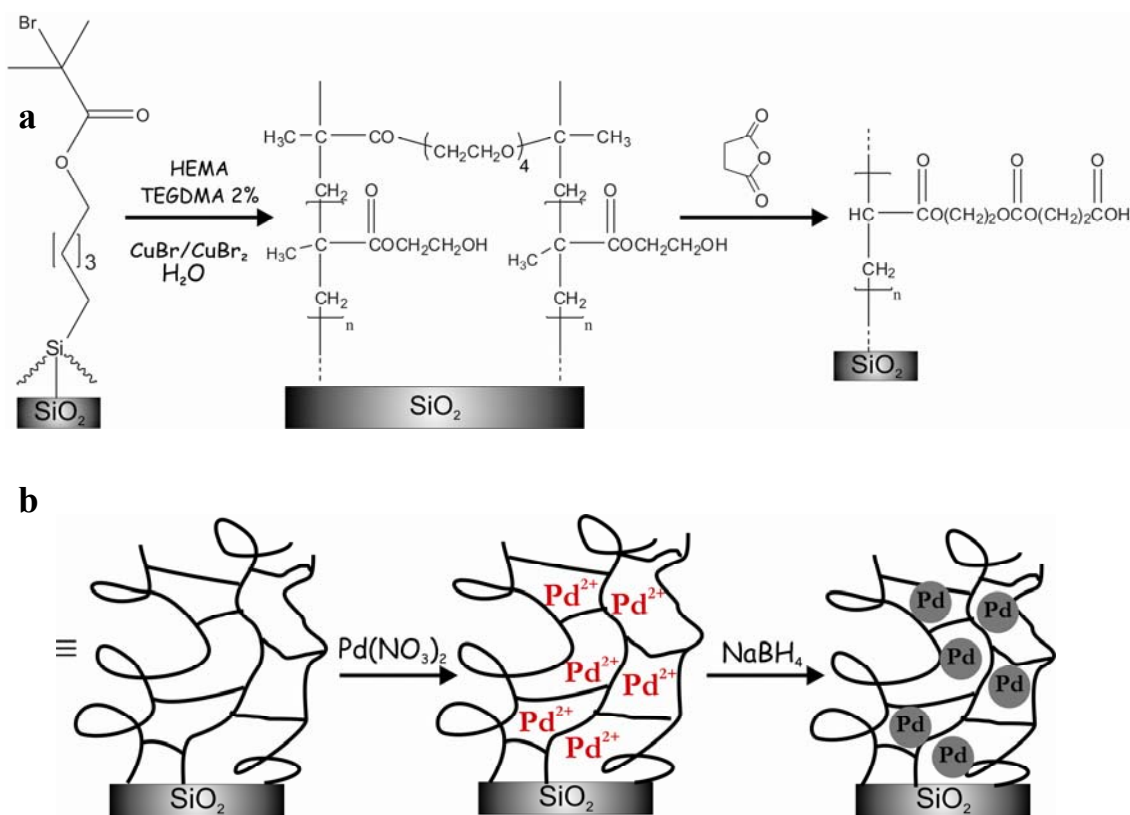


Scheme 6.2. Heck reaction between ethyl acrylate (**3**) and iodobenzene (**4**) to give *trans*-ethyl cinnamate (**5**) in DMSO at 80 °C.

6.2 Results and Discussion

6.2.1 Synthesis of the Hydrogel-Palladium Nanoparticles Hybrid Nanostructure on a Flat Surface and its Characterization

The formation of the palladium nanoparticles (Pd-NPs) was first studied on a silicon oxide surface. The brush-gel film (HEMA-PEG) and its derivatization to form carboxylic functional groups were obtained as described in Chapter 5 (Scheme 6.3a).



Scheme 6.3. a) Preparation of the brush-gel (HEMA-PEG) via ATRP and post-functionalization of the PHEMA-brush based layers by reaction with succinic anhydride, b) carboxylate-palladium complexes and palladium nanoparticles (Pd-NPs) formation.

The substrates were incubated in a 0.05 M solution of palladium nitrate in DMSO/water (3:1), over night, to form the carboxylate-palladium complexes. Then, the material was treated with a 1.3 mM solution of sodium borohydride (NaBH₄) in water for 3 minutes, to give Pd-NPs (Scheme 6.3b). Following each preparation step the samples were

characterized by atomic force microscopy (AFM), and FT-IR. From the AFM analysis (Figure 6.1a-b) of the brush-gel palladium nanoparticles hybrid layer (brush-NPs), the NPs size distribution was calculated (Figure 6.1c), showing an average diameter of 30 nm.

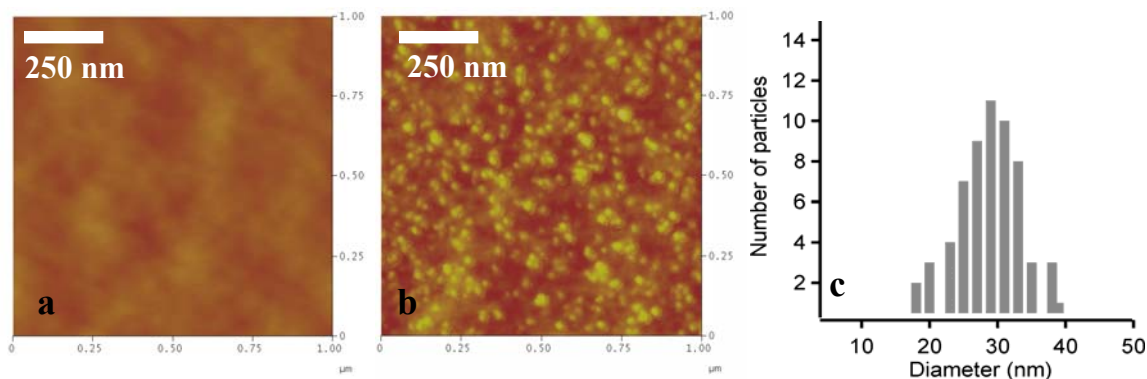


Figure 6.1. **a)** AFM image of hybrid polymer film treated with Pd(NO₃)₂. **b)** AFM image of hybrid polymer film after reduction with NaBH₄. **c)** Palladium nanoparticles size distribution.

FT-IR carried out after the treatment of the brush-gel with Pd(NO₃)₂ showed the stretching signal related to the carboxylate at 1550 cm⁻¹, indicating the formation of the carboxylate/Pd(II) complex (Figure 6.2), as observed for AgNO₃. After reaction with NaBH₄ this band disappears due to the re-protonation of the carboxylate groups and the concomitant reduction of the Pd(II) to form Pd-NPs^[12].

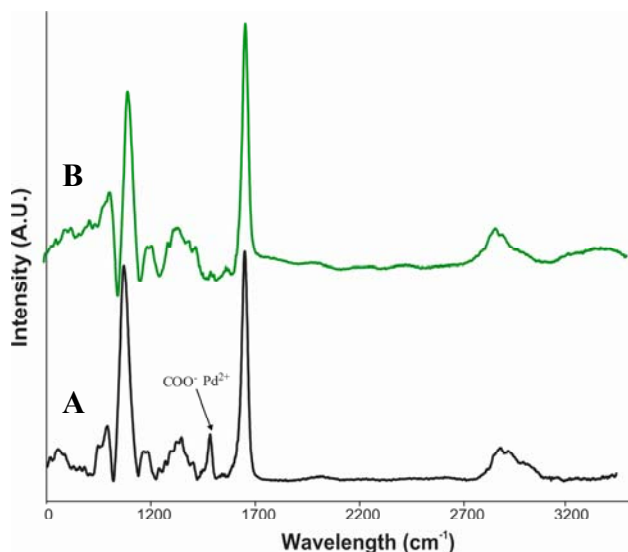


Figure 6.2. Transmission FT-IR spectra of the brush-gel layer **A**) after incubation with $\text{Pd}(\text{NO}_3)_2$, **B**) after formation of Pd-NPs.

6.2.2 Synthesis of the Hydrogel-Palladium Nanoparticles Hybrid Nanostructure on the Microreactor Interior

The procedure described for the silicon oxide surface (Scheme 6.3) was used to coat the microreactor (See Chapter 3) interior with Pd-NPs nanoparticles. The brush-NPs hybrid layer was grown on the microchannel interior in stop flow, varying the polymerization time between 3.5-20 min in order to obtain different polymer layer thicknesses, and consequently a different number of functional groups. The formation of the carboxylate-palladium complexes was achieved flowing a solution of palladium nitrate ($\text{Pd}(\text{NO}_3)_2$) in DMSO/water (3:1) through the microchannel, over night (0.1 $\mu\text{L}/\text{min}$). Upon reduction with a solution of sodium borohydride (NaBH_4) in water for 3 minutes, the microchannel turned black indicating the formation of Pd-NPs.

6.2.3 Kinetic Study of the 4-Nitrophenol Reduction Performed in the Microreactor Coated with Brush-gel Palladium Nanoparticles

Microreactors with immobilized palladium nanoparticles were used for carrying out the reduction of 4-nitrophenol (**1**) to give 4-aminophenol (**2**) (Scheme 6.1). A kinetic analysis was performed with catalytic microreactors having a 100 nm coating in pseudo-first-order conditions, using an excess of NaBH₄. The NaBH₄ concentration was varied in the range 2.5-5 mM. The pseudo-first-order rate constants were proportional to the concentration of NaBH₄, indicating a first-order dependence of NaBH₄. The second-order rate constant is $12.5 \pm 1.2 \text{ s}^{-1} \text{ M}^{-1}$.

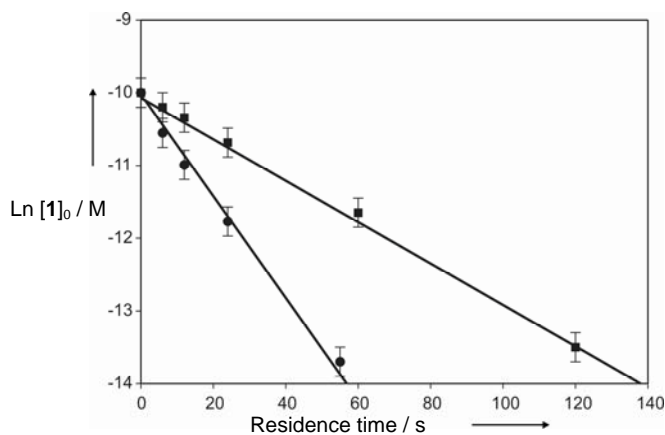


Figure 6.3. Conversion of **1** catalyzed by silver nanoparticles in microreactors coated with polymer layers: (■) = [NaBH₄] = 2.5×10^{-3} M, (●) = [NaBH₄] = 5×10^{-3} M, ([**1**]₀ = 6×10^{-5} M). Thickness 100 nm.

The thickness of the PHEMA-PEG layers, grown on the microchannel interior, varying the polymerization time between 3.5-20 min were measured by high resolution scanning electron microscopy (HR-SEM). The thicknesses were 47 nm (see Chapter 5) and 100 nm (Figure 6.4) after 10 and 20 min polymerization time, respectively^[13].

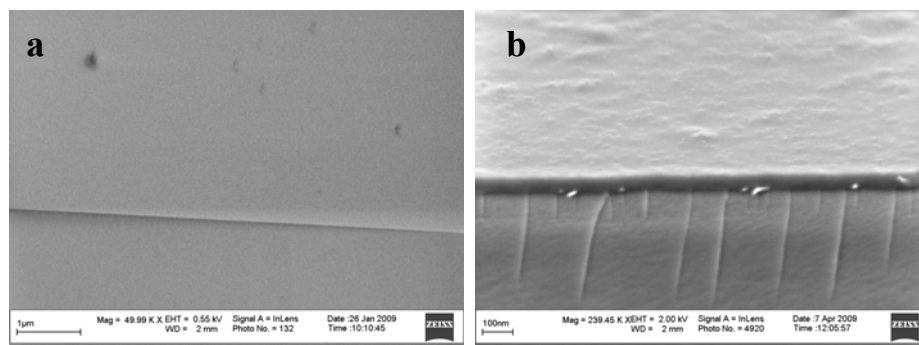


Figure 6.4. HR-SEM **a)** zoom of microchannel cross section without polymer, **b)** zoom microchannel cross section of polymer film with Pd-NPs (20 min polymerization time, thickness 100 nm).

Microreactors with different concentrations of Pd-NPs exhibited a linear dependence of the k_{obs} and the polymerization time (Figure 6.5), as also observed for the Ag-NPs in Chapter 5.

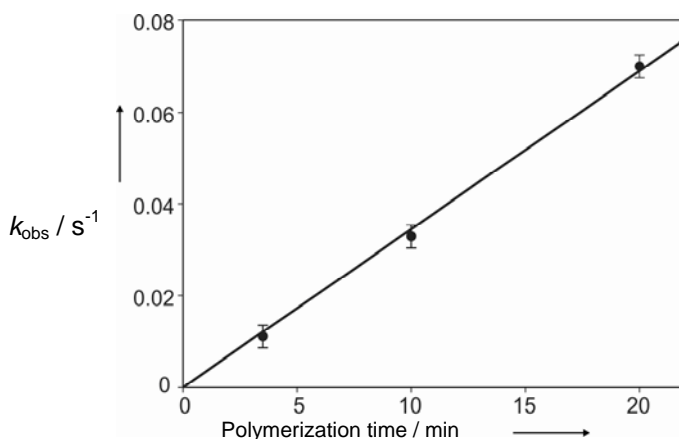


Figure 6.5. Dependence of observed pseudo first-order rate constant k_{obs} as a function of polymerization time, for the reduction of **1** catalyzed by palladium nanoparticles.

To compare the catalytic activity of the two metals, the second-order rate constants obtained for 4-nitrophenol (**1**) reduction catalyzed by silver (k_{Ag}) and palladium nanoparticles (k_{Pd}), formed in a polymer film of 47 nm thickness, were normalized to the whole nanoparticle surface area, contained in the system. From AFM analysis the number of Pd nanoparticles formed per square micrometer within the polymer film ($2.9 \times 10^2 \mu\text{m}^{-2}$) was estimated and was within the same order of magnitude as the calculated value of

$1.0 \times 10^2 \mu\text{m}^{-2}$ (see Experimental). In line with the literature data^[11], the Pd-NPs showed a higher catalytic activity than Ag-NPs, being $k_{\text{Ag}} = 0.20 \times \text{s}^{-1} \text{M}^{-1} \text{m}^{-2} \text{L}$ (see Chapter 5) and $k_{\text{Pd}} = 0.36 \times \text{s}^{-1} \text{M}^{-1} \text{m}^{-2} \text{L}$.

The palladium catalytic devices showed no leaching and could be re-used for at least 4 months, without showing a decrease of catalytic activity, when stored under nitrogen.

6.2.3 Kinetic Study of the Heck Reaction Performed in the Microreactor Coated with Brush-gel Palladium Nanoparticles

The Heck reaction^[14] between ethyl acrylate (**3**) and iodobenzene (**4**), in the presence of triethylamine, to give *trans*-ethyl cinnamate (**5**) in DMSO at 80 °C (Scheme 6.2), was carried out in microreactors coated with the brush-gel Pd-NPs .

The formation of the product, **5**, was monitored in real time using UV-vis in line detection (see Chapter 3, Figure 6.2), measuring the increase of the absorption peak at 290 nm. A 50 μL sample of the reaction product was also analyzed by ¹H-NMR spectroscopy showing the exclusive formation of **5**; no side products could be detected.

When the reaction was performed in the catalytic device only coated with PHEMA-PEG no product was formed. The reaction time was varied by changing the flow rate between 0.2-0.06 $\mu\text{L}/\text{min}$; after 26 min **4** was fully converted into **5** (Figure 6.5).

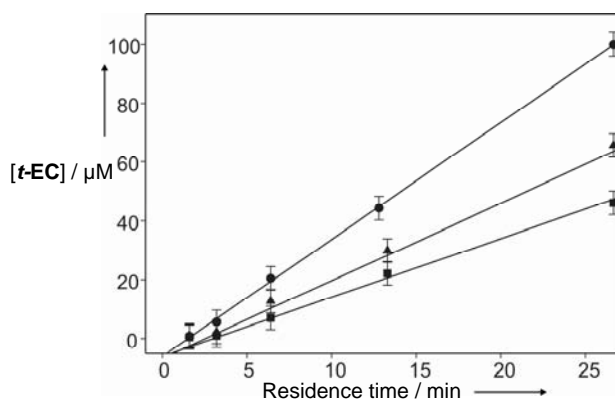


Figure 6.5. Formation of **5** catalyzed by palladium nanoparticles in a microreactor at different initial concentrations of **[4]**, (\blacksquare) = 4.5×10^{-5} M, (\blacktriangle) = 6.5×10^{-5} M, (\bullet) = 10^{-4} M, **[3]** = 0.01-0.02 M, in DMSO at 80 °C; brush-gel hybrid film thickness 100 nm.

We also conducted a kinetic study using an excess of **3**. Data obtained carrying out experiments employing different concentrations of **3** (0.01-0.02 M) and **4** ($50-100 \times 10^{-6}$ M) showed a short induction period^[14], and they were fitted to a zero-order rate equation. Nevertheless, the rate constants depend on the concentration of iodobenzene (**4**), being $(6.7 \pm 0.3) \times 10^{-8}$ M s⁻¹, $(4.3 \pm 0.2) \times 10^{-8}$ M s⁻¹, and $(3.3 \pm 0.16) \times 10^{-8}$ M s⁻¹ for iodobenzene (**4**) concentrations of 10^{-4} M, 6.5×10^{-5} M, and 4.5×10^{-5} M, respectively (Figure 6.5). This can be attributed to a leaching phenomenon. Inherent to the mechanism of the Heck reaction, Pd²⁺ ions are being generated when using Pd(0) nanoparticles, for which iodobenzene (**4**) acts as the oxidant^[15]. As a consequence leaching of catalyst takes place^[16]. Inductively Coupled Plasma-Mass Spectrometry (ICP-MS) analysis of one of the reaction samples showed the presence of 8 ppm of Pd. Our finding was also supported by the absence of leaching when only DMSO was flowed through the channel at 80 °C, and by the observed induction period. Thus, the leached palladium is the active catalyst and is dependent on the initial concentration of **4** and on the residence time applied.

Devices with a 100 nm brush-gel layer could be re-used for about 40 h before showing a decrease of activity. On the other hand devices prepared with 10 and 3.5 min

polymerization time, exhibited diminished catalytic activity after being employed for about 17 and 7 h, respectively.

6.3 Conclusions

We showed that the PHEMA-PEG films on a microchannel interior can also be used for coating the microreactor interior with Pd-NPs. The nanoparticles are stable during 4-nitrophenol (**1**) reduction, and the number can be tuned simply varying the polymerization time, as observed with the Ag-NPs. For the reduction of **1**, Pd-NPs were more efficient than Ag-NPs. In the case of the Heck reaction, due to its mechanism, the hybrid nanostructure acts as a reservoir, releasing catalytically active Pd²⁺ species into solution. This shows that our approach is versatile and can be efficiently used for conducting a variety of metal-catalyzed chemical reactions in microreactors. This system for anchoring metal nanoparticles displayed long term stability. Therefore metal-catalyzed reactions can be studied under varying conditions in a relatively fast way, giving important informations about their possible reaction mechanisms.

6.4 Experimental

Materials and Equipment, Ellipsometry, Atom Force Microscopy (AFM), FT-IR, Scanning Electron Microscopy (HR-SEM), UV-vis Spectrometer, Microreactor Fabrication, and On-line UV-Vis Detection. See Chapter 5.

Synthesis of the Catalytic Polymer Coating. PHEMA-PEG layer was synthesized as described in Chapter 5, the polymerization time was between 3.5 and 20 min.

For the preparation of palladium nanoparticles/brush film hybrid layers all samples were first incubated overnight in a 0.5 M aqueous solution of Pd(NO₃)₂. The same solutions

were flowed at a flow rate of 0.1 $\mu\text{L}/\text{min}$ through the microreactor. Subsequently, the silicon wafer and microchannel were rinsed with milliQ water. Then the material was treated with a 1.3 mM solution of sodium borohydride (NaBH_4) for 3 min to give Pd-NPs.

Kinetic Study. Reduction of **1** was performed using the same conditions described in Chapter 5.

The Heck reaction between ethyl acrylate (**3**) (0.01-0.03 M) and iodobenzene (**4**) ($100\text{-}50 \times 10^{-6}$ M) in the presence of triethylamine (0.02 M) was performed in DMSO at 80 $^\circ\text{C}$. The molar absorptivity of *trans*-ethyl cinnamate (**5**) is $\epsilon_{290} = 22560 \text{ cm}^{-1} \text{ M}^{-1}$. The k_{obs} values were calculated by fitting (least-squares method) the experimental data with the following equation: $[\mathbf{4}] = k \cdot t + q$. The experimental error in these measurements is $\pm 4\%$.

$^1\text{H-NMR}$ Experiment. The Heck reaction between ethyl acrylate (**3**) (0.2 M) and iodobenzene (**4**) (0.1 M) in the presence of triethylamine (0.2 M) in deuterated DMSO at 80 $^\circ\text{C}$ was carried out in the catalytic device. 50 μL of sample were collected overnight, dissolved in 1 mL of deuterated DMSO, and analyzed by $^1\text{H-NMR}$ spectroscopy.

Concentration of Palladium Nanoparticles in the Microreactor.

Assuming that all carboxylate protons are replaced by palladium cations in a 1:2 ratio, the concentration of palladium nanoparticles in the microreactor was calculated as follows:

The mass of one nanoparticle, m , is:

$$m = V \times d_{Pd} = 1.68 \times 10^{-16} \text{ g} \quad (1)$$

Where $V = 1.41 \times 10^{-17} \text{ cm}^3$ is the volume of one nanoparticle considering it as a sphere, having a diameter of 30 nm and $d_{Pd} = 11.9 \text{ g cm}^{-3}$ is the density of the palladium.

$$M_{mol,Pd} = \frac{m}{AW_{Pd}} = 1.58 \times 10^{-18} \text{ mol} \quad (2)$$

Where $M_{mol,Pd}$ is the number of moles of palladium atoms in one nanoparticle, and $AW_{Pd} = 106.42 \text{ g mol}^{-1}$ is the atomic weight of palladium.

$$N_{Pd} = \frac{\alpha_{mol}}{M_{mol,Pd} \times 2} = 103 \text{ nanoparticles per } \mu\text{m}^2 \quad (3)$$

Where N is the number of nanoparticles per μm^2 . Multiplying N with the internal area of the microchannel $A_I = 1.08 \times 10^8 \mu\text{m}^2$, the total number of nanoparticles N_T is:

$$N_T = N_{Pd} \times A_I = 1.11 \times 10^{10} \text{ nanoparticles} \quad (4)$$

Dividing N_T by Avogadro number, N_{AV} , and the microchannel volume, V_m , the molar concentration of nanoparticles, N_M , immobilized on the microchannel interior is:

$$N_M = \frac{N_T}{V_m \times N_{AV}} = 1.09 \times 10^{-8} M \quad (5)$$

And the active particle area is:

$$A_{Pd} = N_M \times S_{Ag} \times N_{AV} = 18.54 \text{ m}^2 \text{ L}^{-1} \quad (6)$$

Where $S_{Pd} = 28.26 \times 10^{-16} \text{ m}^2$ is the surface area of one silver nanoparticle.

AFM analysis of the hybrid film showed on average the presence of 288 nanoparticles per μm^2 , considering that the thickness after 10 min polymerization time is 47 nm and that the diameter of one nanoparticle is 30 nm. In the microreactor with an internal area of $A_I = 1.08 \times 10^8 \mu\text{m}^2$ there are 3.11×10^{10} nanoparticles.

Comparison of Ag-NPs and Pd-NPs Catalytic Activity.

To compare the catalytic activity of the two metals, the second-order rate constants, determined with devices bearing 47 nm coatings, were normalized both to the surface and to the total number of nanoparticles immobilized in the microchannel (normalized rate constants: k_{Pd} for palladium and k_{Ag} for silver). This allows to compare systems with different contents of nanoparticles.

Dividing the second-order rate constant ($k = 13 \text{ s}^{-1} \text{ M}^{-1}$), obtained for the reduction of **1**, catalyzed by silver nanoparticles entrapped in the polymer film, by the active Ag nanoparticles area, A_{Ag} , the normalized rate constant k_{Ag} is:

$$k_{Ag} = \frac{k}{A_{Ag}} = 0.204 \text{ s}^{-1} \text{ M}^{-1} \text{ m}^{-2} \text{ L} \quad (7)$$

Dividing the second-order rate constant ($k = 6.6 \text{ s}^{-1} \text{ M}^{-1}$), obtained for the reduction of **1** in microreactors catalyzed by palladium nanoparticles entrapped in the polymer film formed applying 10 min polymerization time, by the active Pd nanoparticles area, A_{Pd} , the normalized rate constant k_{Pd} is:

$$k_{Pd} = \frac{k}{A_{Pd}} = 0.356 \text{ s}^{-1} \text{ M}^{-1} \text{ m}^{-2} \text{ L} \quad (8)$$

References

- [1] I. P. Beletskaya, A. V. Cheprakov, *Chem. Rev.* **2000**, 3009.
- [2] N. T. S. Phan, M. V. D. Sluys, C. W. Jones, *Adv. Synth. Catal.* **2006**, 609.
- [3] G. M. Greenway, S. J. Haswell, D. O. Morgan, V. Skelton, P. Styring, *Sens. Actuators B* **2000**, *63*, 153.
- [4] P. He, S. J. Haswell, P. D. I. Fletcher, *Lab Chip* **2004**, *4*, 38.
- [5] J. Kobayashi, Y. Mori, K. Okamoto, R. Akiyama, M. Ueno, T. Kitamori, S. Kobayashi, *Science* **2004**, *304*, 1305.
- [6] E. V. Rebrov, A. Berenguer-Murcia, H. E. Skelton, B. F. G. Johnson, A. E. H. Wheatley, J. C. Schouten, *Lab Chip* **2009**, *9*, 503.
- [7] E. V. Rebrov, A.E. Klinger, A. Berenguer-Murcia, E.M. Sulman, J. C. Schouten, *Org. Process Res. Dev.* **2009**, *13*, 991.

- [8] G. Shore, S. Morin, M. G. Organ, *Angew. Chem.* **2006**, *17*, 2827; *Angew. Chem. Int. Ed.* **2006**, *45*, 2761.
- [9] M. Ueno, T. Suzuki, T. Naito, H. Oyamada, S. Kobayashi, *Chem. Commun.* **2008**, 1647.
- [10] N. Yoswathananont, K. Nitta, Y. Nishiuchi, M. Sato, *Chem. Commun.* **2005**, 40.
- [11] Y. Mei, Y. Lu, F. Polzer, M. Ballauff, M. Drechsler, *Chem. Mater.* **2007**, *19*, 1062.
- [12] E. M. Benetti, X. F. Sui, S. Zapotoczny, G. J. Vancso, *Submitted*.
- [13] Devices with a hydrogel thickness obtained with a polymerization time < 10 min, could not be accurately measured by HR-SEM.
- [14] K. Okamoto, R. Akiyama, H. Yoshida, T. Yoshida, S. Kobayashi, *J. Am. Chem. Soc.* **2005**, *127*, 2125.
- [15] A. Biffis, M. Zecca, M. Basato, *Eur. J. Inorg. Chem.* **2001**, 1131.
- [16] N. Nikbin, M. Ladlow, S. V. Ley, *Org. Process Res. Dev.* **2007**, *11*, 458.

CHAPTER 7

Enzyme Immobilization on a Microreactor Channel Wall Using Polymethacrylic Acid Polymer Brushes

The lipase from *Candida Rugosa* was immobilized to a polymethacrylic acid polymer brush layer, grown on the microchannel interior of silicon-glass microreactors. The hydrolysis of 4-nitrophenyl acetate to give 4-nitrophenol and acetate, was used as a model reaction to study this biocatalytic system. The amount of bound lipase could be tuned changing the polymerization time of the brushes. The Michaelis-Menten constants, calculated for immobilized and free lipase, show similar values, demonstrating that the substrate affinity for the active lipase sites remained unchanged after immobilization on the microchannel wall.

7.1 Introduction

Microreactors for performing enzymatic reactions have been shown to be advantageous compared with conventional batch systems^[1, 2]. Microreactors have been used both for homogeneous^[3] and heterogeneous biocatalysis, using free and immobilized enzymes, respectively. Several publications are focused on the development of new methodologies to conduct heterogeneous biocatalytic reactions, since they allow easy separation and recycling of enzymes.

Packed-bed microreactors with silica^[4, 5] and magnetic^[6] nanoparticles, agarose beads^[7] and zeolites^[8], all functionalized with enzymes, have been reported. These examples and a monolithic microreactor^[9], in which an enzyme is absorbed within a polymeric matrix, comprise a simple and efficient way to perform biocatalysis. However, these methods are inconvenient for large scale processing, because they may cause an increase of the pressure drop along the microchannel^[1]. In order to solve this issue, other approaches have been investigated. Enzyme immobilization on a nylon membrane in a microchip, formed by an interfacial polycondensation reaction, has been reported^[10]. Beside that, chemical modification of the microreactor surface interior was the most exploited method. For example, silica spheres have been deposited on micro-capillary inner walls as support for anchoring lipase^[11]. A mesoporous silica layer^[12] has been implemented on the channel interior for enzyme immobilization, but it resulted in low substrate association with the active enzyme sites.

A cross-linking enzyme membrane on a microchannel surface^[13] for biocatalysis has been developed. However, this technique is only limited to enzymes with low isoelectric points. Other examples of wall coating are based on silane nanostructures,^[14, 15] which provide the formation of an enzyme multilayer, offering a good biocatalytic activity. On

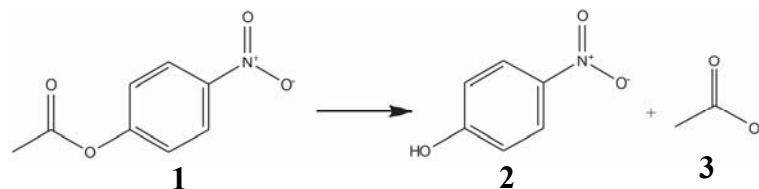
the other hand, these methods do not display control over the amount of anchored enzymes. Moreover, it is known that silanized surfaces may cause nonspecific absorption and enzyme denaturation^[16].

Polymer brushes have been widely applied for anchoring enzymes and proteins^[16-18], since they offer mechanical and chemical stability, providing a high number of reactive functional groups controllable by the selected monomer type.

We demonstrated that nanostructures based on polymer brushes, grown on a microchannel wall, can be efficiently used for anchoring an organic catalyst^[19] and metal nanoparticles in microreactors. Varying the polymer thickness, the number of catalytic sites can be easily tuned.

In this Chapter the fabrication of a polymethacrylic acid (PMAA) polymer brushes nanostructure grown by photopolymerization on the interior of silicon-glass microreactors is described, and the covalent attachment of an enzyme to the carboxylic acid groups of the polymer.

To study the behavior of the catalytic device, the lipase, *Candida Rugosa* type VII, was selected, and the hydrolysis of 4-nitrophenyl acetate (**1**) to give 4-nitrophenol (**2**) and acetate (**3**) (Scheme 7.1) was performed as a model reaction.

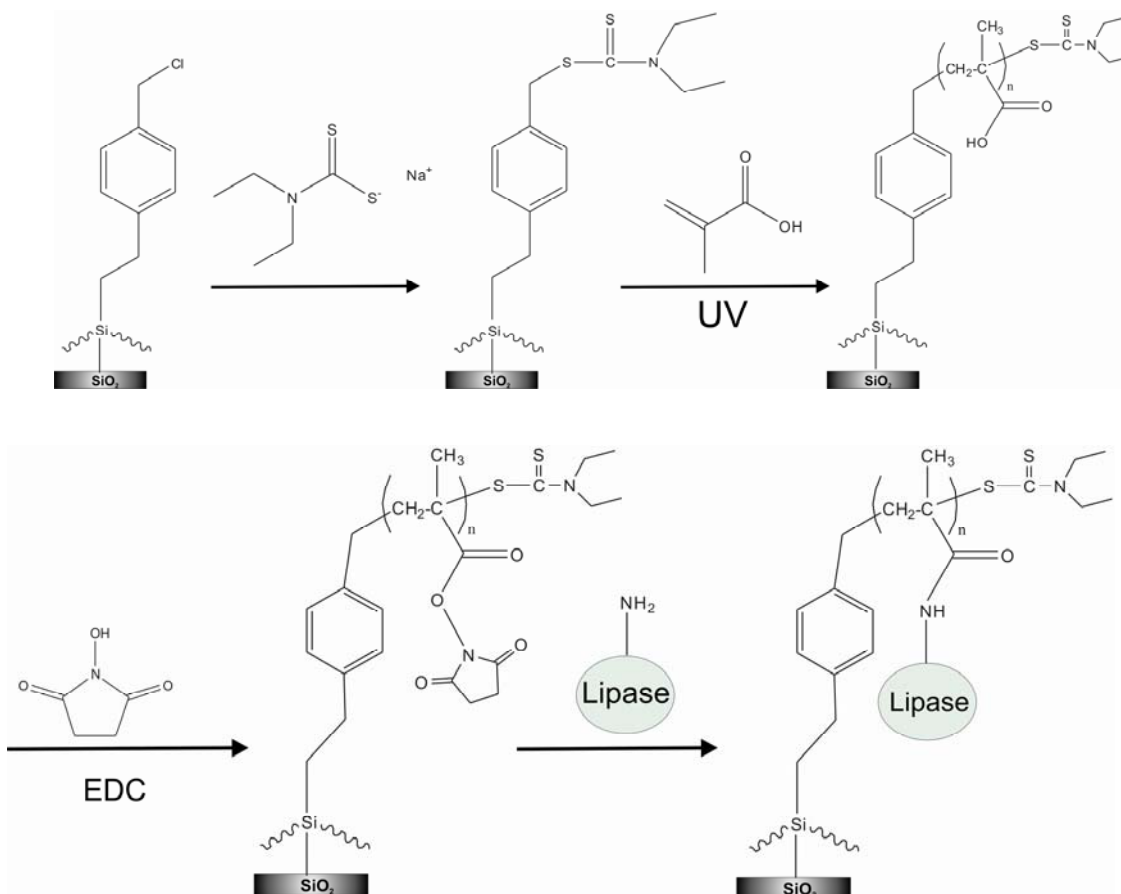


Scheme 7.1. Hydrolysis of 4-nitrophenyl acetate in PBS buffer at room temperature.

7.2 Results and Discussion

7.2.1 Synthesis of Polymethacrylic acid Polymer Brushes and Lipase Immobilization on a Flat Surface

The fabrication of the biocatalytic polymer nanostructure was first performed on a flat silicon oxide surface. Polymethacrylic (PMAA) polymer brushes^[20] were synthesized according to the procedure summarized in Scheme 7.2.



Scheme 7.2. General scheme for photo-initiator monolayer formation, surface initiated photopolymerization of MAA monomer, NHS-ester formation, and lipase immobilization.

First a monolayer of [(chloromethyl)phenylethyl]trichlorosilane (CTS) was grown on a silicon wafer. The chloromethyl-derivatized surfaces were subsequently functionalized with sodium diethyldithiocarbamate trihydrate (DTC), in order to obtain the initiator-

bearing monolayer. The samples were then placed in a glass flask containing an aqueous solution of methacrylic acid (MAA) and irradiated using a UV-lamp for 5-40 min, to give PMAA polymer brushes. The PMAA layer thicknesses were analyzed by ellipsometric thickness and Atom Force Microscopy (AFM) measurements and the data obtained were plotted versus polymerization time (Figure 7.1). The shape of the curve of the layer thicknesses versus polymerization time is typical for photopolymerization^[21].

Afterwards, the PMAA brushes, formed on the silicon oxide surface, were functionalized with *N*-hydroxysuccinimide (NHS) and the substrates immersed in a buffered solution of the lipase, over-night (Scheme 2). The enzyme-functionalized polymer films were analyzed by AFM, showing a 100% increase of the thickness compared to that measured for the PMAA film (Figure 1), proving the immobilization of the lipase.

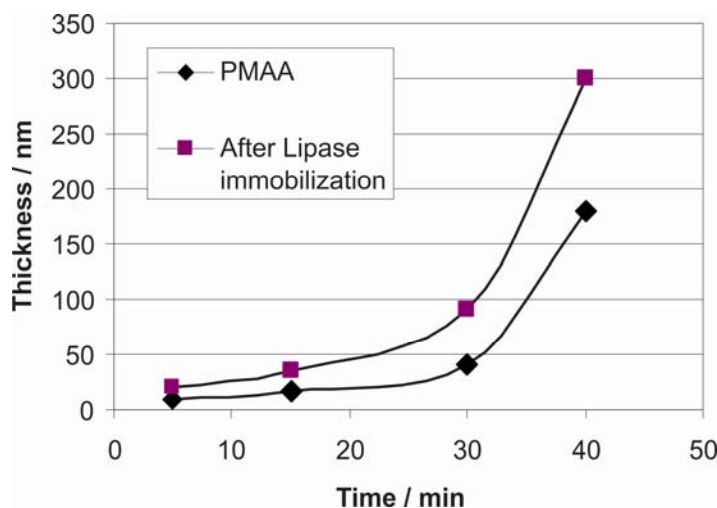


Figure 7.1. Plot of polymerization time versus PMAA polymer thickness on a flat surface: (◆) = PMAA measured by ellipsometric thickness and (■) = PMAA-lipase measured by AFM.

An additional proof was obtained by FT-IR spectroscopy, which revealed the presence of the typical NHS-ester peaks at 1744 and 1780 cm^{-1} and the subsequent amide peaks at 1550 and 1650 cm^{-1} , upon treatment with the enzyme solution (Figure 7.2).

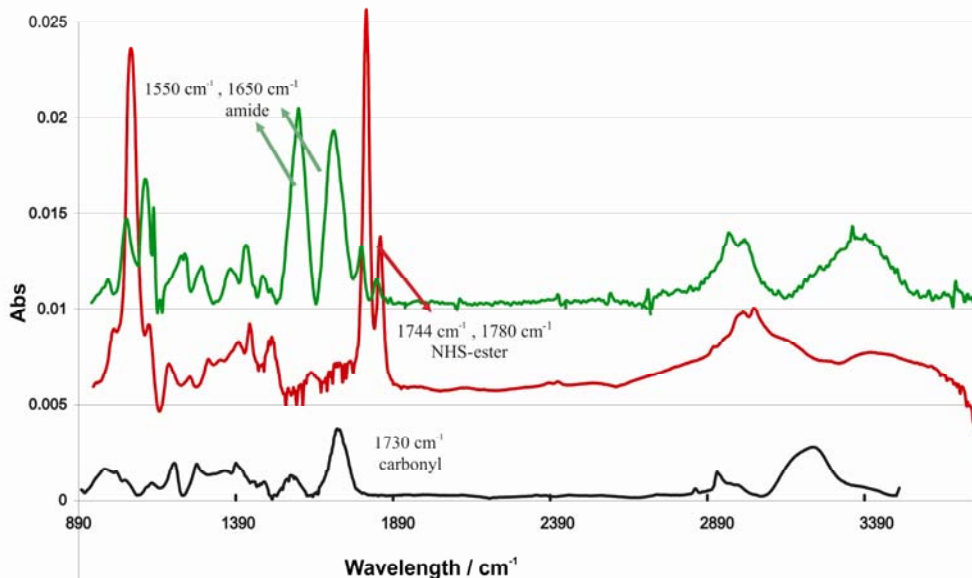


Figure 7.2. FT-IR spectra of: (a) PMAA, (b) PMAA functionalized with NHS-EDC, and (c) PMAA-lipase.

7.2.2 Synthesis of Polymethacrylic Acid Polymer Brushes and Lipase Immobilization on the Microreactor Channel Wall

The same procedure, applied to immobilize the enzyme on the silicon oxide surface, was used to obtain the biocatalytic coating on the channel wall of silicon-glass microreactors (see Chapter 4).

Successively, solutions of the monolayer initiator, CTS, and DTC were flowed through the microchannel at a flow rate of 0.1 $\mu\text{L}/\text{min}$. Afterwards an aqueous solution of MAA was flowed through the microreactor at 1 $\mu\text{L}/\text{min}$, and meanwhile irradiated by a UV lamp, varying the polymerization time between 5-20 min, in order to induce different thicknesses, and consequently different numbers of functional groups.

Once the PMAA polymer brushes were formed, the carboxylic groups were reacted with NHS. Afterwards a lipase buffer solution was flowed through the microreactor, to give the PMAA-lipase nanostructure (Scheme 2).

7.2.3 Kinetic Study of Hydrolysis of 4-Nitrophenyl acetate in the Biocatalytic Microreactor

Microreactors, bearing a PMAA-lipase nanostructure, were used to study the hydrolysis of 4-nitrophenyl acetate (**1**) (Scheme 1) in PBS buffer solution (pH = 7.4) at room temperature. The nanostructure turned out to be very efficient in the biocatalysis; 4-nitrophenol (**2**) was fully formed after a few minutes. No product could be detected when a solution of **1** was flowed through microreactors having only PMAA polymer brushes, proving that lipase was the catalytically active species.

A kinetic study was performed in microreactors bearing a PMAA-lipase nanostructure obtained after 5 min polymerization time. The reaction was followed measuring the formation of the 4-nitrophenol UV-vis absorption peak at 405 nm, using the same UV-vis on-line detection set-up described in Chapter 3. The hydrolysis was carried out with different concentrations of **1** ($0.7\text{--}2.1 \times 10^{-4}$ M). The data were fitted to a first-order rate equation (Figure 7.3). The rate constants, for different p-NPA concentrations, of $(22 \pm 1) \times 10^{-3} \text{ s}^{-1}$ are the same, within experimental error, as expected for first-order conditions.

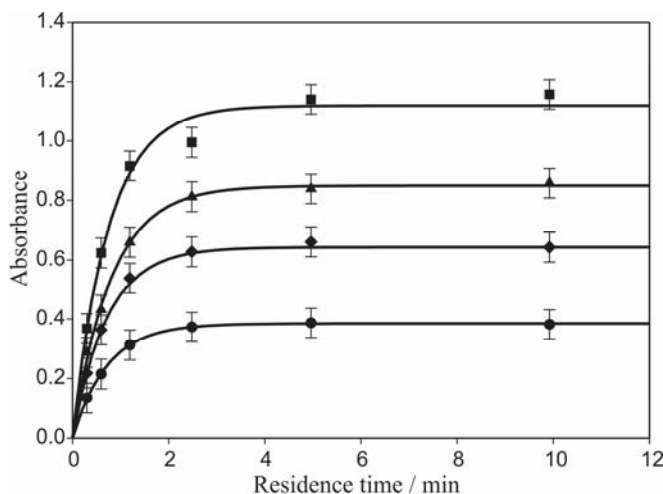


Figure 7.3. Formation of **2** catalyzed by lipase immobilized on PMAA polymer brushes at different **1** concentrations: (■) = 2.10×10^{-4} M, (▲) = 1.05×10^{-4} M, (◆) = 1.40×10^{-4} M, (●) = 0.75×10^{-4} M.

The reaction was also performed with microreactors having PMAA-lipase nanostructures fabricated applying 10 and 20 min polymerization time; the rate constants are $(26.0 \pm 1.3) \times 10^{-3} \text{ s}^{-1}$ and $(30.0 \pm 1.5) \times 10^{-3} \text{ s}^{-1}$, respectively.

The thicknesses of the polymeric coatings were determined by high resolution scanning electron microscopy (HR-SEM), after 5, 10, and 20 min polymerization time being 13.5, 23, and 30 nm, respectively. These analyses were carried out on the channel cross section after breaking the device (Figure 7.4).

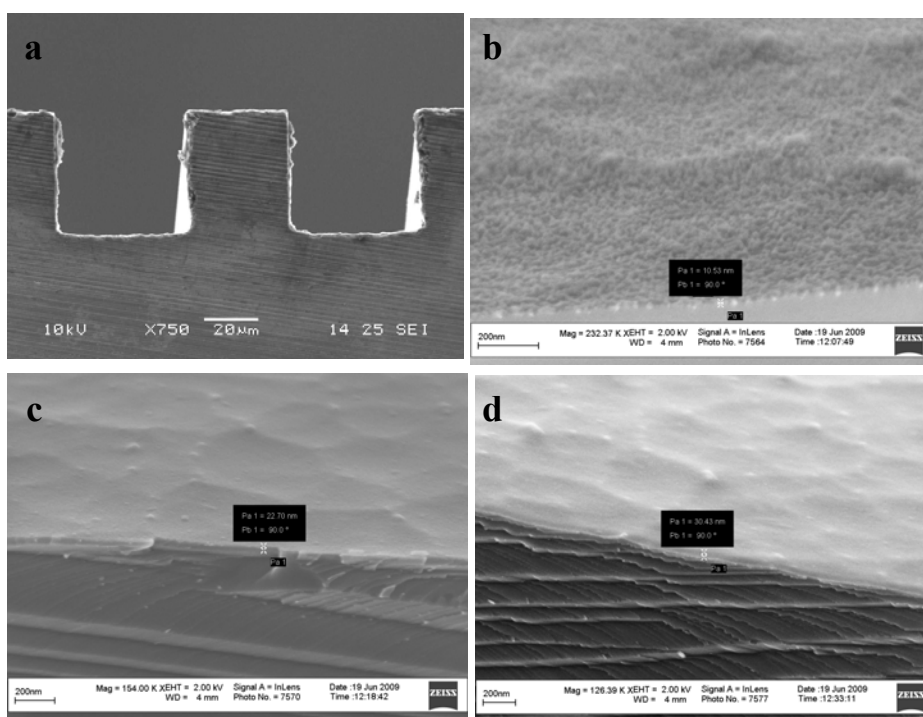


Figure 7.4. (a) HR-SEM picture of the channel cross section before polymer immobilization. The channel surface shows some roughness as a consequence of the etching procedure. Channel cross-section of a device bearing PMAA-lipase polymer brushes formed with a polymerization time of 5 min (b), 10 min (c), and 20 min (d).

The enzyme concentrations in the microreactors were measured using the BCA assay, being 1.3, 1.5, and 1.7 $\mu\text{g}/\mu\text{L}$ (micrograms of enzyme per microreactor volume), for microreactors with PMAA-lipase nanostructures having a thickness of 13.5, 23, and 30 nm, respectively. A linear dependence was found between these enzyme concentrations

and the corresponding rate constants (Figure 7.5). This result infers that, using PMAA polymer brushes, it is possible not only to form a lipase multilayer within the nanostructure, but also to control the amount of immobilized enzyme changing the polymerization time. In addition, it shows that all enzyme molecules are involved in the biocatalysis and thus that the whole layer is accessible for reagents.

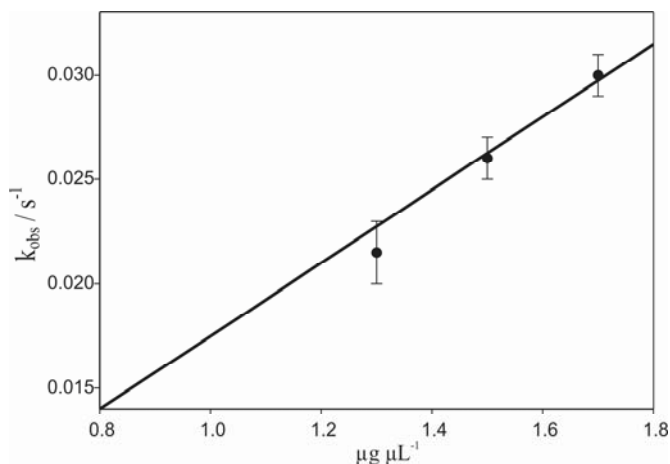


Figure 7.5. Dependence of rate constant versus lipase concentration in microreactors having a PMAA-lipase nanostructure thickness of 13.5, 23, and 30 nm.

In order to investigate the activity of the anchored lipase, the Michaelis-Menten constant (k_M) and the maximum velocity (V_{max}) were calculated for both lipase immobilized in the microreactor having a PMAA layer thickness of 13.5 nm, and free lipase in solution, for the same enzyme concentration. First, the initial rates (v_{in}) of hydrolysis of **1**, at different concentrations, were calculated fitting the experimental data with a straight line equation. Afterwards, the initial rates were plotted versus substrate concentrations and the data were fitted (Figure 7.6) with the Michaelis-Menten equation: $V = V_{\text{max}} \times [\mathbf{1}] / (K_M + [\mathbf{2}])$, from which the Michaelis-Menten constant was calculated both for the immobilized and free lipase. The K_M values are similar, being $(5.6 \pm 0.2) \times 10^{-4}$ M and $(6.7 \pm 0.3) \times 10^{-4}$ M, for immobilized and free enzyme, respectively. The maximum velocity (V_{max}) of $(10.0 \pm$

$0.5) \times 10^{-4} \text{ M s}^{-1}$ is the same for both the immobilized and the free lipase. This experiment clearly shows that the covalent immobilization of lipase on PMAA does not have a negative influence on the enzyme affinity for the substrate. The nanostructure does not limit the substrate diffusion to the enzyme active site.

The catalytic devices exhibited no leaching and could be re-used for at least 40 days when stored in a buffer solution at 4 °C.

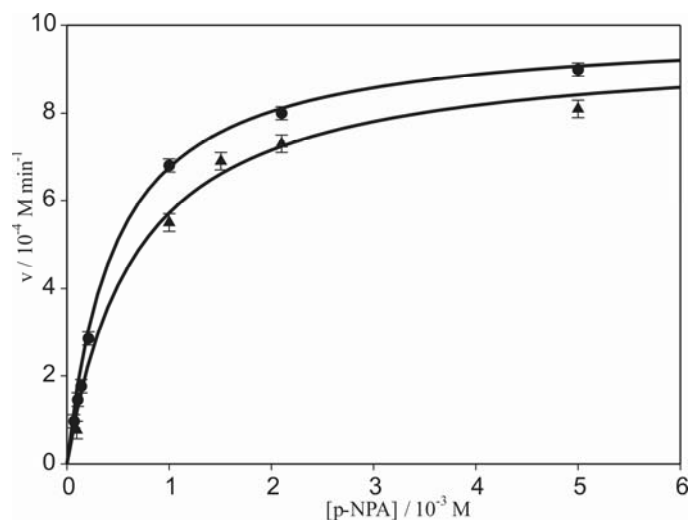


Figure 7.6. Michaelis-Menten plots for the hydrolysis of **p-NPA** mediated by: (●) = lipase anchored on PMAA-lipase nanostructure with a thickness of 13.5 nm, (▲) = free enzyme in solution.

7.3 Conclusions

In this chapter, PMAA polymer brushes, grown on a microreactor channel wall, were used to anchor the lipase *candida rugosa* type VII. The catalytic coating was very efficient in the hydrolysis of 4-nitrophenyl acetate and showed long term stability. The amount of enzyme anchored to the PMAA nanostructure was controlled varying the polymerization time. The results clearly indicated that all enzyme molecule in the nanostructure were involved in the catalysis.

The Michaelis-Menten constants, K_M , calculated for the enzyme anchored on the microreactor interior and free in solution, have similar values demonstrating that PMAA polymer brushes do not influence the affinity of the substrate for the enzyme active sites. We feel our method could be used as a general approach for anchoring enzymes on a microreactor interior, providing a new platform for studying the activity of enzymes and for performing biocatalysis.

7.4 Experimental

Materials and Equipment. All commercial reagents were purchased from Aldrich Chemicals unless specified. All chemicals were used without purification unless specified. [(Chloromethyl)phenylethyl]trichlorosilane was purchased from ABCR. Toluene (VWR, analytical reagent grade) was distilled over sodium. Methacrylic acid (MAA) was purified from inhibitors by condensation under high-vacuum. Water was purified with the Milli-Q plus (MILLIPORE, R=18.2 M Ω ·cm) ultra pure water system. 1-(3-Dimethylaminopropyl)-3-ethylcarbodiimide hydrochloride was purchased from Across Organic. PBS buffer, pH = 7.4, was purchased from Braun. 4-Nitrophenyl acetate was purchased from Fluka. Acetonitrile was purchased from Across. Ethanol, methanol, and acetone (analytical reagent grade) were purchased from VWR.

Photopolymerization was performed with a UV spot light source xenon lamp, with a cut-off filter between 280-400 nm, equipped with an optical fiber (Hamamatsu).

Ellipsometry measurements were performed with a plasmon ellipsometer ($\lambda = 632.8$ nm) assuming a refractive index of 1.5 for the polymer.

Samples were measured using an atomic force microscope (AFM) Nanoscope III (Veeco digital instrument, USA) in tapping mode, equipped with a Si₃N₄ tip with a J scanner at a

scan rate of 0.6 Hz. FT-IR spectra were recorded using a BioRad FTS-60A spectrometer. Spectra of polymer films were taken in transmission mode using a bare silicon wafer as background.

High Resolution Scanning Electron Microscopy (HR-SEM). See Chapter 4.

Microreactor Fabrication. See Chapter 4.

Setup of the Microfluidic Device. See Chapter 3.

On-line UV-Vis detection. See Chapter 3.

Photopolymerization. Microchannels and silicon wafers were first cleaned with a Piranha solution ($\text{H}_2\text{SO}_4\text{:H}_2\text{O}_2$ 3:1) and then copiously rinsed with milliQ water and dried with a stream of nitrogen. Caution: Piranha solution is a very strong oxidant and reacts violently with many organic materials. The cleaned silicon wafers were soaked in 5% solution of [(chloromethyl)phenylethyl]trichlorosilane in dry toluene for 18 h^[23]. For the synthesis in the device the same solution was flowed for 18 h at a flow rate of 0.1 μL / min. The silicon wafer and the microchannel were rinsed with dried toluene, acetone, and ethanol and finally dried with a stream of nitrogen. The so prepared surfaces were then immersed in a 0.1 M methanol solution of sodium diethyldithiocarbamate trihydrate overnight. For the device the same solution was flowed over night at a flow rate of 0.1 μL / min. The surfaces and the microchannel were rinsed with methanol and dried with a stream of nitrogen.

Silicon wafers were placed in a glass flask containing a 1 M aqueous solution of MAA. They were extensively purged with argon (30 min) and finally irradiated with a UV lamp at 18 cm distance, for 5-40 min. For the microreactors, a 1 M solution of MAA in water was purged with argon (30 min) and then flowed at 1 μL / min through the microchannel, and meanwhile irradiated with a UV lamp towards the glass side of the microreactor for

5-20 min at 18 cm distance. After photopolymerization the silicon wafer and microchannel bearing the polymer film were rinsed abundantly with milliQ water. PMAA polymer brushes, grown on the silicon oxide surface were reacted with a PBS buffer solution of 1-(3-dimethylaminopropyl)-3-ethylcarbodiimide hydrochloride/ *N*-hydroxysuccinimide (EDC/NHS) (38 mg/ mL: 6 mg/ mL) for 2 h. For the microreactor the same solution was flowed at 0.1 μL / min for 2 h. Subsequently, the so prepared surfaces were soaked in a buffer solution containing 250 μg / mL of lipase overnight. The enzyme solution was flowed through the microchannel at 0.1 μL / min for the same time. Surfaces and microchannel were rinsed with buffer in order to remove all the excess of unbound enzyme.

Kinetic Study. The hydrolysis of 4-nitrophenyl acetate (**1**) ($0.7\text{-}2.1 \times 10^{-4}$ M) to 4-nitrophenol (**2**) was performed in PBS buffer pH = 7.4 at room temperature.

Since **1** is not very soluble in water, initially a 0.14 M stock solution of **1** was prepared in acetonitrile / buffer 1:1. The formation of the product was followed using UV-vis detection, measuring the increase of the **2** peak at 405 nm. The molar absorptivity of **2** in PBS buffer is $\epsilon_{405} = 10166 \text{ cm}^{-1} \text{ M}^{-1}$. The k_{obs} values were calculated by fitting (least-squares method) the experimental data with the following equation: $[\mathbf{2}] = [\mathbf{1}]_0 * (1 - e^{(-k_{obs} \times t)})$. The experimental error in these measurements is \pm 5%.

Quantification of Lipase Immobilized in the Microreactors.

The lipase concentration in the microchannel was quantified using the BCA protein assay kit (Thermo Scientific). Several standard samples were prepared with a known concentration of BSA standard protein, from which a calibration curve was determined,

plotting the Albumin standard protein (BSA) concentrations vs. the absorbance at 562 nm measured for each individual standard sample. A working reagent solution^[24, 25] was flowed through the microchannels and kept inside for 30 min at 37 °C. Afterwards the microchannels were rinsed with buffer and the eluted solution collected in a volumetric flask. The absorbance at 562 nm was measured and the enzyme concentration determined from the calibration curve.

References:

- [1] M. Miyazaki, H. Maeda, *Trends in Biotechnology* **2006**, *24*, 463.
- [2] P. L. Urban, D. M. Goodall, N. C. Bruce, *Biotechnol. Adv.* **2006**, *24*, 42.
- [3] K. Koch, R. J. F. van den Berg, P. J. Nieuwland, R. Wijtmans, H. E. Schoemaker, J. C. M. van Hest, F.P.J.T. Rutjes, *Biotechnol. Bioeng.* **2008**, *99*, 1028.
- [4] P. He, G. Greenway, S. J. Haswell, *Nanotechnology* **2008**, 19.
- [5] H. R. Luckarift, B. S. Ku, J. S. Dordick, J. C. Spain, *Biotechnol. Bioeng.* **2007**, *98*, 701.
- [6] A. Nomura, S. Shin, O. O. Mehdi, J. M. Kauffmann, *Anal. Chem.* **2004**, *76*, 5498.
- [7] A. Srinivasan, H. Bach, D. H. Sherman, J. S. Dordick, *Biotechnol. Bioeng.* **2004**, *88*, 528.
- [8] Y. H. Zhang, Y. Liu, J. L. Kong, P. Y. Yang, Y. Tang, B. H. Liu, *Small* **2006**, *2*, 1170.
- [9] K. Sakai-Kato, M. Kato, K. Ishihara, T. Toyo'oka, *Lab Chip* **2004**, *4*, 4.
- [10] H. Hisamoto, Y. Shimizu, K. Uchiyama, M. Tokeshi, Y. Kikutani, A. Hibara, T. Kitamori, *Anal. Chem.* **2003**, *75*, 350.
- [11] H. Nakamura, X. Y. Li, H. Z. Wang, M. Uehara, M. Miyazaki, H. Shimizu, H. Maeda, *Chem. Eng. J.* **2004**, *101*, 261.
- [12] S. Kataoka, A. Endo, M. Oyama, T. Ohmori, *Appl. Catal., A* **2009**, *359*, 108.
- [13] T. Honda, M. Miyazaki, H. Nakamura, H. Maeda, *Adv. Synth. Catal.* **2006**, *348*, 2163.
- [14] J. Kaneno, R. Kohama, M. Miyazaki, M. Uehara, K. Kanno, M. Fujii, H. Shimizu, H. Maeda, *New J. Chem.* **2003**, *27*, 1765.
- [15] M. S. Thomsen, B. Nidetzky, *Biotechnol. J.* **2009**, *4*, 98.
- [16] J. H. Dai, Z. Y. Bao, L. Sun, S. U. Hong, G. L. Baker, M. L. Bruening, *Langmuir* **2006**, *22*, 4274.
- [17] S. P. Cullen, I. C. Mandel, P. Gopalan, *Langmuir* **2008**, *24*, 13701.
- [18] F. J. Xu, Q. J. Cai, Y. L. Li, E. T. Kang, K. G. Neoh, *Biomacromolecules* **2005**, *6*, 1012.
- [19] F. Costantini, W. P. Bula, R. Salvio, J. Huskens, H. J. G. E. Gardeniers, D. N. Reinhoudt, W. Verboom, *J. Am. Chem. Soc.* **2009**, *131*, 1650.
- [20] E. M. Benetti, S. Zapotoczny, G. J. Vancso, *Adv. Mater.* **2007**, *19*, 268.
- [21] E. M. Benetti, E. Reimhult, J. de Bruin, S. Zapotoczny, M. Textor, G. J. Vancso, *Macromolecules* **2009**, *42*, 1640.

- [22] W. P. Bula, W. Verboom, D. N. Reinhoudt, H. J. G. E. Gardeniers, *Lab Chip* **2007**, *7*, 1717.
- [23] T. Matsuda, S. Ohya, *Langmuir* **2005**, *21*, 9660.
- [24] P. K. Smith, R. I. Krohn, G. T. Hermanson, A. K. Mallia, F. H. Gartner, M. D. Provenzano, E. K. Fujimoto, N. M. Goeke, B. J. Olson, D. C. Klenk, *Anal. Biochem.* **1985**, *150*, 76.
- [25] K. J. Wiechelman, R. D. Braun, J. D. Fitzpatrick, *Anal. Biochem.* **1988**, *175*, 231.

Summary

The realization of catalytic microfluidic platforms for performing (bio)organic reactions is the main topic of this thesis. Organic, metallic (in the form of supported nanoparticles), and enzymatic catalysts have been immobilized on the interior of glass or glass/silicon microreactors using self-assembled monolayers (SAMs) and different types of polymer brushes. Kinetic studies of (bio)chemical reactions have been carried out in these catalytic microreactors to demonstrate the applicability of the developed catalytic systems.

The basic concepts of microreactors as well as the application of microreactors to conduct catalytic reactions have been described in Chapter 2. A literature overview is given, describing different methods to incorporate catalysts in microreactors and the (bio)catalytic organic reactions which were performed in these devices. Those examples showed the advantages of performing catalytic reactions in microreactors, however, a general and versatile procedure for anchoring and tuning catalysts in microreactors is lacking in literature.

In Chapter 3, SAMs of 1-propylamine, TBD, and PAMAM dendrimer G2, were successfully immobilized on the microchannel interior of glass microreactors. SAMs together with microreactor technology provides an easy and fast method to investigate the activity of a catalyst towards a chemical reaction. The Knoevenagel condensation reaction of benzaldehyde and malononitrile was conducted in such catalytic devices and a kinetic study was carried out. It turned out that the three catalysts had almost the same catalytic activity. This type of coating did not provide long-term stability, probably due to

the hydrolysis of the silane monolayer on the surface. In addition, the amount of catalyst that can be immobilized on the microchannel interior using SAMs is not sufficient to have full product formation.

To overcome the problems of low catalyst activity and stability, the fabrication of PGMA polymer brushes was introduced in Chapter 4 for anchoring the TBD catalyst, in order to obtain a catalytic nanostructure (PGMA-TBD) on the wall of a microreactor. The Knoevenagel condensation between benzaldehyde and malononitrile was carried out in the catalytic device. The amount of catalyst can be tuned by variation of the polymerization time and thus the thickness of the active layer, which also shows that the whole catalytic nanostructure is involved in the catalytic process. The second-order rate constant of $0.30 \pm 0.03 \text{ s}^{-1} \text{ M}^{-1}$, calculated for the device having a PGMA-TBD layer of 400 nm, shows that the reaction proceeds up to 150 times faster than in the case of a monolayer coating of TBD. This is attributed to the larger number of catalytic groups that can be anchored due to the intrinsic functional group capacity of the polymer brush layer. In addition, the hydrophobicity of PGMA endows longer stability (one month) to the catalytic structure.

In Chapter 5, the fabrication of a hydrogel-silver nanoparticles hybrid nanostructure on a microchannel interior has been described as a novel method for performing heterogeneous catalysis in microreactors. The number of nanoparticles synthesized within the nanostructure can easily be tuned by changing the polymerization time. The silver nanoparticles (Ag NPs) were formed within the complete brush-gel and the whole hybrid brush-gel nanostructure was involved in the catalysis. This procedure for immobilizing Ag-NPs allowed the efficient catalysis of the reduction of 4-nitrophenol.

In Chapter 6, the same method was employed to have palladium nanoparticles (Pd-NPs) on the microreactor interior. Microreactors bearing Pd-NPs were applied in the reduction of 4-nitrophenol. The Pd-NPs within the polymer layer were stable (three months) during the reduction, and the Pd-NP loading could be tuned simply by varying the polymerization time, as observed for the Ag-NPs. For the reduction of 4-nitrophenol, Pd-NPs were more efficient than Ag-NPs. In the case of the Heck reaction between ethyl acrylate and iodobenzene, due to its mechanism, the hybrid nanostructure acts as a reservoir, releasing catalytically active Pd²⁺ species into the solution. This was derived from the dependence of the catalytic activity on the concentration of iodobenzene which acts as the oxidant of the Pd-NPs, and from the observed limited activity of the catalytic layer under the Heck reaction conditions. In general, the results show that our approach is versatile and can be efficiently used for conducting a variety of metal-catalyzed chemical reactions in microreactors.

In Chapter 7, poly(methacrylic acid) (PMAA) polymer brushes, grown on a microreactor channel wall, were used to anchor the lipase *candida rugosa* type VII. The catalytic coating was very efficient in the hydrolysis of 4-nitrophenyl acetate and showed long-term stability. The amount of enzyme anchored to the PMAA nanostructure was controlled by varying the polymerization time which confirmed that the whole biocatalytic nanostructure was involved in the catalysis. The Michaelis-Menten constants, K_M , calculated for the enzyme anchored on the microreactor interior and free in solution, have similar values demonstrating that PMAA polymer brushes do not influence the affinity of the enzyme for the substrate.

In this thesis, the immobilization of catalysts on a microreactor interior has been investigated in order to obtain an efficient and durable catalytic microsystem to conduct

(bio)organic reactions with a supported catalyst. It was demonstrated that the use of polymer brushes for anchoring catalysts permits a wide range of application areas. In addition, polymer brushes allow the formation of a dense active functional film which can be easily tuned by varying its thickness. These features, combined with the continuous flow operation mode and the on-line monitoring of product formation, promise the possibility of high-throughput catalytic microdevices, which makes these catalytic platform a unique tool for performing and exploring catalyzed (bio)chemical reactions.

Samenvatting

Het onderwerp van dit proefschrift betreft het maken van microfluidische systemen voor (bio)organische reacties. Gebruik makend van zelfgeassembleerde monolagen (self-assembled monolayers; SAMs) van verschillende soorten polymere 'brushes', werden organische, metallische (in de vorm van nanodeeltjes) en enzymatische katalysatoren geïmmobiliseerd aan de binnenwanden van glas- of glas/silica-microreactoren. Kinetische studies van (bio)chemische reacties werden uitgevoerd in deze katalytische microreactoren om de toepasbaarheid van de ontwikkelde katalytische systemen aan te tonen.

In hoofdstuk 2 worden zowel de basisconcepten van microreactoren en hun mogelijke toepassingen voor katalytische reacties beschreven. Daarnaast wordt er een literatuuroverzicht gegeven waarin zowel de verschillende methoden voor het integreren van katalysatoren in microreactoren als de (bio)gekatalyseerde organische reacties die kunnen worden uitgevoerd in deze systemen, worden besproken. De genoemde voorbeelden laten de voordelen zien van het uitvoeren van katalytische reacties in microreactoren. Een algemene procedure voor de verankering van verschillende katalysatoren in microreactoren ontbreekt echter in de literatuur.

In hoofdstuk 3 werden, met succes, SAMs van 1-propylamine, TBD and PAMAM dendrimeer G2 geïmmobiliseerd op het inwendig oppervlak van de microkanalen van glas-microreactoren. Het gebruik van SAMs in microreactortechnologie biedt een eenvoudige, snelle methode om de activiteit van een katalysator te onderzoeken. De Knoevenagelcondensatie van benzaldehyde en malonitril werd uitgevoerd in een

dergelijke katalytische microreactor, waarin ook de kinetische aspecten van de reactie werden bestudeerd. De resultaten lieten zien dat alle drie de katalysatoren bijna dezelfde katalytische activiteit vertonen. Dit type coating is op langere termijn niet stabiel, waarschijnlijk omdat de silaanmonolaag op het oppervlak wordt gehydrolyseerd. Daarnaast is de hoeveelheid katalysator die geïmmobiliseerd kan worden (d.m.v. SAMs) in het microkanaal niet voldoende voor volledige omzetting.

Om de geringe katalytische activiteit en stabiliteit van de (bovengenoemde) SAMs te verbeteren, worden in hoofdstuk 4 polymere PGMA-‘brushes’ geïntroduceerd. Deze ‘brushes’ werden gebruikt om de TBD-katalysator te verankeren, waardoor er een katalytische nanostructuur (PGMA-TBD) aan de wanden van de microreactor ontstaat. De Knoevenagelcondensatie van benzaldehyde en malonitril werd uitgevoerd in deze katalytische microreactor. De hoeveelheid katalysator kan gestuurd worden door het variëren van de polymerisatietijd en daarmee de dikte van de actieve laag, wat ook laat zien dat de hele katalytische nanostructuur betrokken is bij het proces. De berekende tweede-orde-reactieconstante in het geval van de 400 nm PGMA-TBD-laag ($0.30 \pm 0.03 \text{ s}^{-1} \text{ M}^{-1}$) geeft aan dat de reactie 150 keer sneller is dan in het geval van een TBD-monolaag. Dit kan toegeschreven worden aan het feit dat er meer katalytische groepen verankerd kunnen worden, omdat de ‘brush’-laag meer functionele groepen bevat. Daarnaast zorgt de hydrofobiciteit van de PGMA-laag voor een hogere stabiliteit (> één maand) van de katalytische structuur.

In hoofdstuk 5 van dit proefschrift wordt het samenstellen van een hybride nanostructuur van hydrogel-zilver nanodeeltjes in een microkanaal beschreven. Het betreft een nieuwe methode voor heterogene katalyse in microreactoren. Het aantal nanodeeltjes in de nanostructuur kan gemakkelijk gestuurd worden d.m.v. de polymerisatietijd. Zilver

nanodeeltjes (silver nanoparticles, Ag-NPs) werden gevormd in de 'brush-gel' en de hele nanostructuur nam deel in de katalyse. Deze immobilisatieprocedure voor Ag-NPs is geschikt voor de efficiënte katalyse van de reductie van 4-nitrofenol.

In hoofdstuk 6 wordt de bovengenoemde methode toegepast op palladium nanodeeltjes (Pd-NPs). Microreactoren met geïmmobiliseerde Pd-NPs werden gebruikt voor de reductie van 4-nitrofenol. De Pd-NPs in de polymeerlaag waren stabiel (drie maanden) tijdens de reductie en de Pd-NP-belading kon gestuurd worden d.m.v. de polymerisatietijd, zoals eerder waargenomen voor de Ag-NPs. Wat betreft de reductie van 4-nitrofenol, waren Pd-NPs efficiënter dan Ag-NPs. Voor de Heckreactie tussen ethylacrylaat en joodbenzeen, fungeert, vanwege het mechanisme, de hybride nanostructuur als reservoir voor katalytisch actieve Pd²⁺-deeltjes die in de oplossing losgelaten worden. Dit werd afgeleid van de gevonden afhankelijkheid van de katalytische activiteit van de concentratie van joodbenzeen (dat de Pd-NPs oxideert) en de waargenomen beperkte levensduur van de activiteit van de katalytische laag onder de Heckreactieomstandigheden. In het algemeen laten de resultaten zien dat onze benadering veelzijdig en efficiënt is en gebruikt kan worden voor verschillende metaal-gekatalyseerde chemische reacties in microreactoren.

Polymere 'brushes' van poly(metacrylzuur) [poly(methacrylic acid); PMAA], gegroeid aan de wanden van een microreactor, werden gebruikt in hoofdstuk 7 om het enzym lipase *candida rugosa* type VII te verankeren. De katalytische laag was zeer efficiënt in de hydrolyse van 4-nitrofenylacetaat en vertoonde lange-termijn-stabiliteit. De hoeveelheid enzym die verankerd werd op de PMAA-nanostructuur werd gestuurd door de polymerisatietijd, hetgeen bevestigde dat de hele biokatalytische nanostructuur deel nam in de katalyse. De Michaelis-Menten constanten, K_M , die berekend werden voor

zowel het verankerde enzym als het enzym in oplossing, hebben overeenkomstige waarden. Dit laat zien dat de polymere PMAA-'brushes' geen invloed hebben op de affiniteit van het enzym voor het substraat.

In dit proefschrift werd de immobilisatie van katalysatoren aan de wanden van microreactoren bestudeerd om een efficiënt en duurzaam katalytisch microsysteem te verkrijgen voor (bio)organische reacties. Er werd aangetoond dat het gebruik van polymere 'brushes' om katalysatoren te verankeren in verschillende gebieden toegepast kan worden. Daarnaast kunnen er met polymere 'brushes' dichte, actieve, functionele lagen gevormd worden waarvan de activiteit gemakkelijk gestuurd kan worden d.m.v. het variëren van de dikte. Al deze eigenschappen, gecombineerd met het gebruik van continue doorstroming en het 'on-line' volgen van de productvorming, bieden de mogelijkheid tot "high-throughput" katalytische microsystemen. Dat maakt deze katalytische systemen tot een uniek studieobject voor gekatalyseerde (bio)chemische reacties.

Acknowledgments

Writing the acknowledgments looks the easiest part of a thesis. I can tell you that it took me some time to find the right words to thank everybody who believed in me, and supported my research in different ways.

First of all I would like to thank my first promotor, Prof. Reinhoudt, for giving me the possibility to join SMCT. I will never forget our first work-meeting, you noticed that I was not the most self confidence student you ever had and you told me “in the next four years this is going to change”. Now I can tell you that you were right, doing a Ph.D is not only a matter of doing experiments but also to overcome obstacles and therefore to make many choices which made me stronger. David, thank you for supporting and pushing me to achieve my goal.

After David retired I became a MnF member and this thesis would not have been possible without the precious supervision of my second promotor Prof. Huskens. Dear Jurriaan, it was a pleasure for me working in your group. Thank you very much for guiding me in the last part of my Ph.D, for your useful suggestions about kinetics and for the interesting discussion during the work-meetings. Thanks for being always available to talk about the outcomes of my experiments, even during lunch time.

I would like to thank my co-promotor Dr. Verboom, for giving me the possibility to enter in the microreactors world. Thanks for all the time you spent correcting my thesis and for teaching me how to write a scientific publication.

Special thanks go to Prof. Gardeniers, thanks Han for supporting me in all my ideas about microreactors and for all the useful discussions. The collaborations I had with your group were really worth for the outcome of this thesis.

I am grateful to Julius Vancso for his scientific support to my research.

Marcel and Richard, without your technical support my life in the lab would have been much more difficult. I would like to thank also Clemens for all the help with the FT-IR machine and for all the jokes during the “coffee-time”.

I would like to thank Izabel, the best secretary, for being always helpful with all the Dutch bureaucracy.

In this moment if I look back to the past 4 years I remember especially the good moments, fortunately it is very easy to forget the bad part. I can not deny that in a few moments I really thought to give up, but likely I did not do it, thanks also to the many friends who were close to me and who made me see the positive part of the situations.

One of those friends is Roald, dear Roald I will never forget how you explained me how a fluid behaves in a microreactor. Thanks for being always there, even if sometimes we did not understand each other I really appreciate you as a person and as a scientist.

Many thanks also to Wojciech for all the discussion about microfluidics.....your chips are fantastic!!!!

I am really grateful to Jealamy for all the fun we had together in the lab, at the gym and when we were hanging out together....I will never forget when you told to the body-step teacher, in Dutch, that I wanted to go on the stage with her during the lesson....I was not understanding anything but I was laughing a lot and you even more!!!! Thanks Jealamy for translating the summary in Dutch. Remember, soon or later I will come to Margarita.

Another important person is Albert, thanks Albert for all the Italian dinners we had, for the parties at your place and for all the nice discussions about the Heck reaction. Grazie per tutte le volte che sono venuta a lamentarmi alla tua cappa e tu mi dicevi di tener duro. In bocca al lupo per questo tuo ultimo anno di dottorato!!!!

Special thanks to Riccardo (the younger) and Olga for the nice night we had in Enschede when we were going out for dinner or for a beer.....a Roma ci siamo fatti i super-alcolici però.....!!!!!!!!!!

I will never forget my favorite lab-mate Ignacio, dear Ignacio I had a lot of fun with you...we were very “close” in the lab, always telling each other our adventures with chemistry and “lab on a”. I will never forget you with tortellino!!!!

Many thanks to Francesca Scaramuzzo, you came to live at my place after Riccardo left, thank you to be there when I was feeling alone, for the nice dinners we had together; thanks to Arancha for listening to me when I had to choose about my future, I can tell you: it is nice to be back in my country with all its disadvantages, it is the best place to live.

I would like to thank Denis “the Russian” for the funny evening at the tennis center....I will never forget your tennis style!!!

Other big thanks go to Raluca and Jordi, although I left just after your arrival in Twente we spent nice time together!!! Jordi come va il tuo Italiano....?

Thanks to all my former lab mates: Olga and Alessio, thanks for understanding me in some very bad moments. Alessio you were right: il quarto anno è quello buono! Thanks to Mirko, for many moments in which we were supporting each other....I will never forget the world cup final match in Berlin!!!!

I would like to thank also Monica and Emiel, the first year of my Ph.D would have been much more difficult without you.

Thanks to Victoria for sharing all the frustration about the chip... You were right, they are too small!!!!

I would like to thank all my lab mates: Kim, the English speaker... , how many times did I ask you to repeat something? Deniz.....thanks for being in the lab every Sunday, I was never feeling alone. Thanks to Srinidhi for his nice jokes about Italians habits, thanks to Pieter for checking all the time my car papers, thanks also to Shu-Han, Xuexin, Mudassir, Alberto and Melanie, Lanti, Chien-Ching, Vijay, Dae June and Nicolai for sharing with me many working days. Thanks also to Oya for the drinking parties we had and Joost for being helpful with Dutch “unemploying” papers.

I would like to thanks some Italian friends who were far during these four years: Marta e Maria grazie per la copertina della tesi, Andre, Michela e il Tommy, grazie per essere venuti a trovarmi ad Enschede. Cari Marta e Andre, anche se lontani mi siete stati sempre di aiuto nell’affrontare tutte le difficoltà, grazie, spero che ora che sono tornata in Italia ci vedremo più spesso. Grazie a Luca..... il mio amico di sempre. Un grazie enorme anche alla mia amica Silvia, anche se non ci vediamo spesso la nostra amicizia rimane sempre forte.

Dear paranimfen, I am happy you will be there with me the day of my promotion. Janet, it is very difficult to find the best words to say how much I am grateful to you for the help you gave me, not only in these last few months when I was in Italy, but for all the times you understood what I was feeling. You are a special person, I am glad to have you as a friend. I hope we will keep in contact in the future. Eddy, what to say...we arrived in Twente together and we shared work, fun and frustrations....thank you for being there when I really needed it.

Vorrei ringraziare mia madre e mio padre per avermi sempre spronato a raggiungere questo risultato, per cercare sempre di essermi di aiuto. Grazie anche a mio fratello Andrea per aver sempre cercato di farmi fare la cosa giusta anche se spesso abbiamo opinioni diverse. Grazie a zia Giuliana per i super pranzi e per la pizza quando vengo a casa, grazie a zio Diego....viva juve..ahahah, grazie a zia Mirella, per essere sempre disponibile quando ho voglia di sfogarmi. Grazie ai miei cugini Sara ed Ale e quelli acquisiti Roberta e Giacomo, per le ore spensierate che ho passato con voi quando tornavo a casa. Voglio anche ringraziare i miei nonni che quando ero bambina mi hanno insegnato tante cose che mi sono state utilissime nella vita.

In fine, ma non meno importante, un grazie enorme a Riccardo per essermi sempre vicino per condividere con me gioie ma anche delusioni. Grazie Ric per riuscire sempre ad essere obbiettivo nelle varie situazioni, questo mi ha spesso aiutata a superare molte difficoltà.

Curriculum Vitae

Francesca Costantini was born in Macerata (MC), Italy, on October 1st 1977. In July 1996 she received her diploma from the “ Liceo Scientifico” G. Galilei (Macerata, Italy).

She studied Medicinal Chemistry at University of Bologna, Italy, where she received her degree in October 2003. During her undergraduate training period she worked on fatty acid chemistry at the Biochemistry department of Bologna University, under the supervision of Prof. L. Landi. From July 2004 till December 2004 she spent a training period at Pepsam System B.V., Lelystad, The Netherlands.

Since February 2005 she joined the Supramolecular Chemistry and Technology, and Molecular Nanofabrication groups as Ph.D candidate, under the supervisions of Prof. Reinhoudt and Prof. Huskens. The results of her research are described in this thesis.

Since August 2009 she is working at the Bioimaging PET-CT department of “Policlinico A. Gemelli” at La Cattolica University, Rome, Italy, on the synthesis of radiopharmaceuticals for PET applications.